Politecnico di Torino

Politecnico di Torino

Corso di Laurea Magistrale in Ingegneria Biomedica

A.a. 2022/2023

Sessione di Laurea Ottobre 2023

MULTIFUNCTIONAL LAYER-BY-LAYER NANOCAPSULES LOADING DOCETAXEL, ENZALUTAMIDE, RESVERATROL AND DOXORUBICIN WITH ENHANCED TARGETING, IMAGING AND THERAPEUTIC EFFECTS AGAINST PROSTATE CANCER AND OSTEOSARCOMA

Supervisors

Prof.ssa Chiara Tonda Turo

Dr. Irene Carmagnola

Prof. Piergiorgio Gentile

Candidate

Mosca Daniel Andrea

S296690

DECLARATION OF WORK

I declare that this thesis is based on my own work and has not been submitted in any form or for any other degree at this university. Except where otherwise noted in the text or the acknowledgements below, this is the sole work of Daniel Andrea Mosca. I am aware of the penalties for plagiarism, fabrication, and unacknowledged syndication, and declare that this report is free of these.

ACKNOWLEDGEMENTS

In this section, I would like to express my sincere gratitude to those who have played a pivotal role in my journey towards completing this master's thesis.

First and foremost, I extend my heartfelt appreciation to my primary supervisor, Professor Piergiorgio Gentile. He not only directed my research, but also instilled in me the right mindset to reach this significant milestone. His remarkable ability to simplify complex concepts and make them more affordable has left a lasting impact on my approach. Moreover, his passion for our field has ignited a similar enthusiasm within me, which I intend to carry forward in all my future new experiences.

I would also like to express my profound gratitude to Professor Chiara Tonda Turo and Doctor Irene Carmagnola for affording me the opportunity to embark on this academic journey.

Additionally, I wish to dedicate a special portion of my acknowledgments to my family. My parents have been unwavering in their support, providing not only the resources but also the encouragement needed to embark on this chapter of my life. They have consistently inspired me and pushed me beyond my limits, instilling in me a determination to surmount any obstacles that came my way. My brother has grown alongside me, becoming not only a sibling but also a steadfast companion, always ready for new adventures together. I extend my appreciation to every member of my family for their enduring support and encouragement, which has allowed me to flourish and express myself fully.

Furthermore, I owe a debt of gratitude to my girlfriend, Marta. Her unwavering support, understanding, and commitment have been a pillar of strength throughout this journey. She has been my rock, sharing in both the challenges and the triumphs, all while ensuring our relationship remained unshaken. Marta, your presence in my life has been a source of immeasurable strength, and I thank you for being by my side.

Finally, I would like to express my gratitude to all my friends, both longstanding and newfound, who have made this path not only more enjoyable but also less daunting. Your camaraderie, willingness to lend a helping hand, and shared cups of coffee have lightened the load during the arduous process of writing this thesis. Your unwavering support and friendship have been invaluable, and I am grateful to have you in my life. To all those mentioned and to anyone else who has contributed to my academic and personal growth, I offer my heartfelt thanks. Your influence and support have been indispensable, and I am deeply appreciative of your roles in shaping my journey.

TABLE OF CONTENTS

LIST OF FIGURES

LIST OF TABLES

ABSTRACT

The calcium phosphate (CaP) nanoparticles (NPs) have taken interest as one of the most promising inorganic nanocarriers in the scientific research against cancer. They are mostly used due to the low toxicity paired with a high biocompatibility inside the human body. The initial compounds are easily retrievable, in addition they can be processed with several methods and most of them do not require aggressive condition. Therefore, these NPS have been widely exploited as drug delivery system to encapsulate biomolecules of different nature, avoiding a reduction in their therapeutic activities. Furthermore, calcium and phosphate can be functionalized to acquire properties tuned on the specific disease they are exploited for.
Multilayered CaP nanotheranostic particles have been deeply studied to confirm that this promising technology can be adapted to a wide range of applications in tumour research. The goal of the project was to create a base medication that acts as a carrier for the specific drug already used in medicine, to enhance their efficiency and administration as well as the targeting and imaging of overall formulation.

In this thesis, novel therapies have been developed to be applied to both prostate cancer (PCa) and osteosarcoma (OSa).
Prostate cancer stands as the second most prevalent cause of cancer-related mortality worldwide. This is largely attributed to the aggressive progression of high-grade tumours and the challenging nature of metastasis, which presents formidable obstacles for conventional treatment approaches. Besides the conventional treatments like surgery and radiotherapy, androgen deprivation therapy is a common approach for managing PCa. However, it tends to promote the development of castration-resistant tumour forms, which worsen the prognosis for patients. Thereafter, the common drugs used in PCa treatment include docetaxel as chemotherapy and enzalutamide (ENZ) as a hormonal antagonist. Much of the ongoing research in this field focuses on designing specialized drug delivery systems to enhance pharmacokinetics and improve tumour targeting.

In contrast, OSa distinguishes itself as one of the most prevalent bone tumours affecting both younger and older individuals. It originates from mesenchymal cells that undergo differentiation to form bone cells. In younger individuals, it often presents as a primary tumour, frequently associated with congenital conditions, making early diagnosis challenging. Conversely, in older individuals, OSa tends to manifest as a secondary tumour resulting from treatments for other medical conditions. This type of cancer remains particularly challenging to treat, with conventional therapies often leading to various complications, including the drastic measure of limb amputation. Nanoparticles have emerged as a promising nanoplatform for both smart disease diagnosis and localized delivery of chemotherapeutic agents. This approach aims to minimize the drawbacks associated with common treatments such as surgery and radiotherapy while enhancing the effectiveness of OSa treatment.

Therefore, PSMA-targeted, DTX, ENZ and RESV and HA, DOXO and RESV co-loaded NPs containing Quantum carbon dots respectively for PCa and OSa were designed for both imaging and therapy and then validated. The nanocore of all system was made up of calcium and phosphate encapsulating RESV or DOXO and stabilized by PAH deposition via a pumping method. Sequentially, layer-by-layer assembly technique has been performed for depositing two oppositely charged natural polysaccharides, chitosan and alginic acid, containing the drugs mentioned.

For each tumour two formulations have been developed to confirm the high adaptability of CaP with different drugs and in addition to assess the efficiency of the complex combination of chemotherapeutic agents with antioxidants and active targeting molecules. For PCa, the group of formulations was characterized by the presence of a gradient of DTX and ENZ inside nanolayers, while RESV was encapsulated only in one of the two samples in the core and nanolayers. Moreover, the outermost layer of both encapsulated CQD and grafted PSMA, a targeting agent to specifically interact with tumour cells of prostate that overexpress the small molecule. On the other hand, for OSa, the group of formulations was characterized by the encapsulation of DOXO both in the cores and in layers, while RESV was inserted only into the shell. The last layer was added of CQD, and a deposition of HA could allow to target CD44 receptor widely expressed on cancer cells.

The final systems have been in-depth characterized through chemical-physical and morphological analyses. Presto Blue and Live/Dead assays the efficacy and cytotoxicity of the proposed treatments were evaluated. In particular, cellular tests were conducted on four different lines, especially Lncap and Vcap for PCa and U2os and Saos for OSa. The results revealed that the combination of drugs and materials yielded a complex formulation with notably high effectiveness, although varying degrees of cytotoxicity observed across the different cell lines. Furthermore, Vcap and U2os cell lines were employed to conduct 3D tests using spheroid structures. These tests served to affirm the ability of formulations to penetrate cells for treatment while simultaneously aiming to restore the overall cellular microenvironment.
In conclusion, our study highlights the considerable potential of CaP NPs in the treatment of a range of cancer types, particularly with regard to PCa and OSa.

1 INTRODUCTION

1.1 Prostate Gland

1.1.1 Anatomy of the Prostate

The prostate is a gland comprised in the men reproductive systems. It has a size and morphology similar to chestnut with a weight around 30 grams. Prostate gland is directly involved in the production of seminal fluid which is the liquid component of semen that is produced in combination with sperm cells and other liquids from other glands. The prostate is located beneath the bladder and the urethra cross through it, especially the urethra mainly passes through the transition zone with a part in the peripheral zone, meanwhile in the central zone the ejaculatory ducts join with the urethra where the peripheral zone starts. Those ducts are located directly after the seminal vesicles which represent the connection point between vas deferens from testis and urethra.

Overall, the prostate is a fibromuscular gland and is surrounded by a capsule of connective tissue containing plenty smooth muscle fibres which gives it an elastic conformation at touch.

In Figure 1, it is clear to notice how the prostate tissue can be divided into 3 different zones which are the following from innermost to outermost:

- **Transition zone.** The transition zone is the smallest part of the gland, and it makes up the innermost tissue. This zone is directly in contact with the urethra and surrounds it.
- **Central zone.** The middle part called central zone encases the transition zone and makes up around one quarter of the total mass of the gland. It is the part where the different components can be found such as seminal ducts and seminal vesicles.
- **Peripheral zone.** The peripheral zone comprises the higher percentage of prostate's tissue and act as a shell around the other two zones.

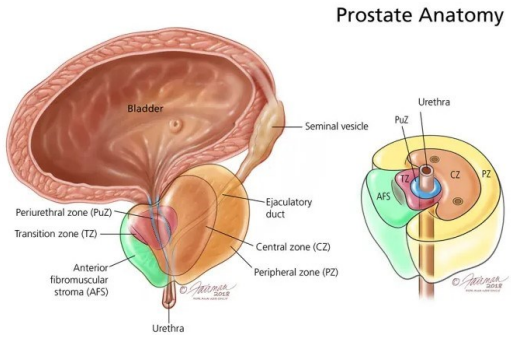

Figure 1 - Anatomy of prostate and zones division
(Urological Illustrations by Fairman Studios for American Urological Association patient education materials)

The different tissues which compose the prostate gland are crucial to distinguish, since both benign and malignant growth have specific common areas where they could arise. For example, non-cancerous growths, even called benign prostatic hyperplasia, commonly emerge in the innermost tissue, the transition zone. On the other hand, cancerous growths originate the majority of the time in the outermost zone, the peripheral zone[1].

1.1.2 Function of the Prostate

The prostate has a variety of different roles, most of them are connected to the sexual male reproductive system. Firstly, prostate gland with its fibromuscular cells acts as biological pump that pushes the sperm through the urethra in order to reach the female reproductive system. Secondly, this peculiar gland also produces some components of the semen through the ejaculatory duct are mixed with some other compounds from the bulbourethral glands and the ones from the testis. This compost is combined during the contraction leaded from ejaculation stimulus, after the prostate reach the right pressure.
Furthermore, this gland also regulates urine flow and semen ejaculation by contracting and relaxing its muscles, since it is located around the proximal part of the urethra[1].

1.1.3 Prostate - cells

The prostate tissue comprised different cell types and in the following lines they are quickly described.

Secretory epithelial cells. These cells represent the major type of cells in the prostate, specifically they make up acini which are the basic structure of the prostate and ducts that allow the fluids produced by them to reach the prostatic urethra. On the other hand, these kinds of cells are important to produce prostate specific antigen (PSA) and prostatic acid phosphatase.[2]

Basal cells. The cells of the basement are important to synthesize and secrete components of the basement for the support of acini and to separate them form the fibromuscular tissue. With the contribute of some studies it has been understood that a subset of basal stem cells is able to replace epithelial cells.[3]

Scattered neuroendocrine cells. These cells have some hybrid characteristics such as epithelial, neural, and endocrine. Thanks to several neurosecretory granules these cells can secrete several different biochemical products, for example the most important are serotonin, a variety of peptides, such as the ones from chromogranin family, the calcitonin family and some hormone-like peptides and hormone-related proteins with an important role in signalling.[4]

Stroma cells. Stroma cells which comprised a variety of cells like fibroblasts, smooth muscle, nerves, and lymphatics. The interactions between stroma and epithelial cells suggest that stroma have an important role in the production of multiple growth factors related either in the development of normal prostate or prostate cancer.[5]

1.1.4 Prostate – signalling

Androgens

Androgens make up one of the most important groups of sex hormones in men. In particular, they are directly involved in the development of the male body since they help starting puberty as well as maintaining the overall health of the reproductive system. This group contains different molecules the most important is the testosterone, while the other androgens are the androstenedione, dehydroepiandrosterone (DHEA), DHEA sulphate (DHEA-s), dihydrotestosterone (DHT).

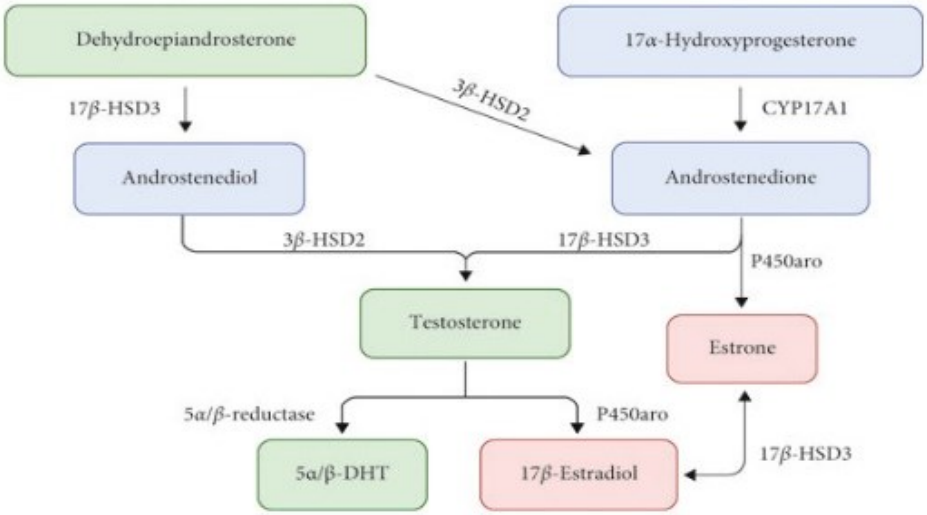

Figure 2 - Schematic illustration of the androgen synthesis[6]

As **Error! Reference source not found.** shows, the androgens are only one part of the hormonal pathways in the human body. DHEA could be considered as the precursor of all of them, it is mainly produced in adrenal glands, the gonads and the brain in both males and females but in different quantity[7]. DHEA as a major precursor enter in different pathway such as an androgen, an oestrogen and a neurosteroid. Focusing on the androgen part it can weakly interact with androgen receptors, even so its involvement is strictly related to the conversion into testosterone[8]. The androstenedione is the nearest chemical structure to testosterone (Figure 3). They share the same structure except for ono of the oxygen connected with a double bond, indeed the work of 17β-HSD3 (Figure 2) is to transform the carbonyl group into a hydroxyl group.

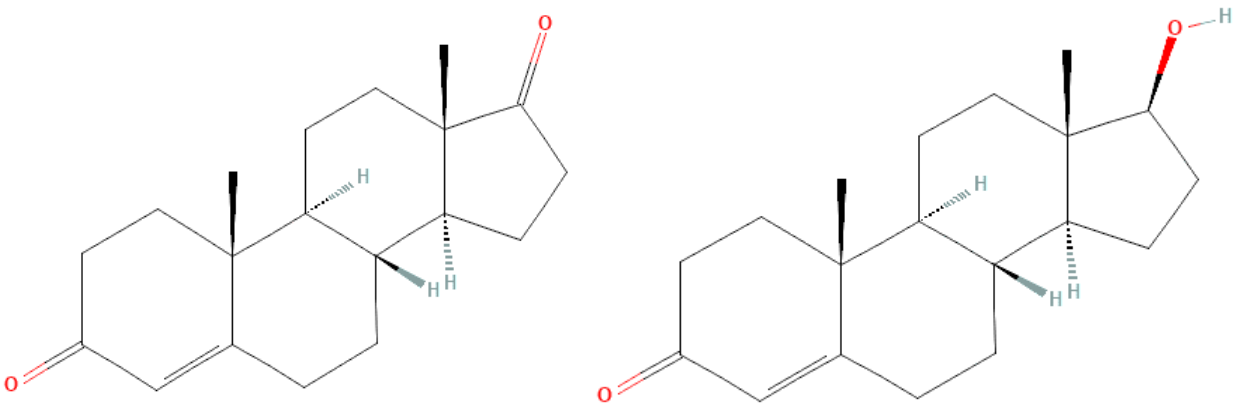

Figure 3 - Chemical structure of androstenedione (left) and testosterone (right)
PubChem, National Library of Medicine

Considering all the androgens, testosterone remains the most important one. It has a direct involvement in the development of the male characteristics such as the growth of the testis and prostate as primary sexual characteristics as well as the secondary such as the development of muscles and bone mass, the growth of body hair and the deep voice[9]. In addition, testosterone in both sexes is involved in health and well-being, where it has a significant effect on overall mood, cognition, social and sexual behaviour, metabolism and energy output, the cardiovascular system, and in the prevention of osteoporosis[10]. Focusing on a cellular level testosterone can increase the cellular activity by promoting the protein synthesis, meanwhile it can increase the growth of the tissue binding with androgens receptors[11]. Moreover, testosterone could be converted in other hormonal form, even to some oestrogens, the dihydrotestosterone is considered the pure one (Figure 2). DHT is the results of the action of a reductase enzyme and is more proficient than testosterone at binding itself to the androgen receptors[12]. Furthermore, the DHT is majorly involved in the differentiation of the male genitals during embryogenesis, and during development it helps developing outer tissue such as scrotum and penis, while testosterone focuses mainly on the innermost part such as prostate and testicles[13].

Androgen receptors

Prostate growth and functionality are due to the communication between the different types of cells. In more details different receptors are exploited from prostate cells, the most important are the androgen receptors that let cells grow by the presence in the environment of androgens. The principal male sex hormone is testosterone that among prostate cellular population, mainly interacts with epithelial cells[14]. However basal cells do not use androgens to grow, and neuroendocrine cells have mainly calcitonin receptors [15].

PCa emerges more commonly in cells that use androgen receptors and for this reason researcher concentrate their focus on these ones.

Androgen receptors use androgens to activate and leading to the transcriptions of some genes inside prostate cells. These receptors are included in the subfamily of steroid receptors which in turn are part of the nuclear receptor family and due to this reason 3 different sites and the relative linker can be detected[16]:

- **N-terminal domain** which is the most variable.
- **DNA-binding domain (DBD)** which is less variable than the N-terminal one, as part of a steroid nuclear receptor this site consists of two zinc fingers that recognise specific DNA.
- **An interdomain linker**
- **C-terminal ligand-binding domain**. This last part can be divided into other sub-sites: the ligand-binding pocket and two solvent-exposed surfaces important for interacting with coregulators which are the activation function 2 and binding function 3.

It is important to mention that as nuclear receptors, androgens ones are located inside cells in their monomer form in complex with heat-stock proteins such as chaperones and cochaperones[17]. These proteins have the aim to protect the receptors against stressful condition and covered their pocket. Inside the human body cells the pathway of androgens is very complex since it needs to be carefully managed because they regulate the proliferation of cells.

Due to the complexity of these receptors, they use two types of signalling[16]:

- **DNA binding-Dependent.** This path typically involves the receptor in complex with heat-shock and chaperone proteins. In this state different coregulators can interact with the receptor, these ones are for example coactivator and corepressor, and they can modulate the ability to transactivate the target gene.
- **Non-DNA binding-Dependent.** When androgens enter cells they can bind to the receptors, this event leads to some conformational changes that allow the dissociation of chaperone proteins and exposure of the nuclear localisation signal (NLS). In this way NLS is exposed and permitted the transferring of the complex androgen receptor/androgen into nucleus. Here the complex can dimerize and start its transcription modulating in bond with androgen response elements which allow specific activation of androgens receptors.

1.1.5 Prostate-specific antigen (PSA) and Prostate-specific membrane antigen (PSMA)

Prostate-specific membrane antigen (PSMA) is a type II membrane protein located upon the surface of all forms of prostate tissue, including carcinoma. As type II membrane protein the prostate's one has an internal portion with a length of 19 amino acids, 24 amino acids comprise the transmembrane portion which cross the membrane only once, and the longest part, the external, counts 707 amino acids. Another specific mark of this kind of proteins is the presence of a C-terminus in the external part and cytoplasmatic N-terminus[18]. This membrane protein seems to have a negative correlation with healthy cells. Normal cells together with hyperplastic ones express a low concentration of this antigen and it is usually truncated, the scientific community refers to it as PSM' [19]. In contrast, tumour masses expose on their surface a higher level of whole

PSMA[20], and as it can be seen, the ratio between these two antigens could be used as an index of tumour growth as well as its aggressivity.

Prostate-specific antigen is an androgen-regulated protease of the family of tissue kallikrein. It is mainly produced by prostate ductal and acinar epithelium which are the closest cells toward ducts and is secreted into the lumen. Its major aim is to maintain a right viscosity of the seminal liquid by interacting and cleaving the two proteins involved in in the seminal coagulum: semenogelin I and II[17].
PSA is a major protein in seminal fluid, doctors refer to it for an initial screening for PCa. An average value is around 4ng/mL, and it is statistical true that lower level indicates a normal prostate tissue. In contrast higher level may indicate the presence of PCa. Although it is possible that men with a lower PSA level may develop cancer while men with higher level not[21].

1.2 Prostate cancer (PCa)

Regrettably, PCa represents one of the most common and challenging disease which targets men. PCa is the second tumour more frequent and the fifth death cause in men[22], and for this reason a lot of researchers are focusing on treating this disease. In accord to the database of PubMed, around twelve thousand papers are shared in the scientific community each year and the trend is still increasing. This kind of tumour by the opinion of different research centres has a good survival rate if early diagnosed. Among the most common ways to diagnose this cancer are PSA assay and biopsy (1.2.6).
For this reason, nanoparticles (NPs) have taken interest in their ability to both treat and diagnose tumours using a right design and in addition they are more suitable in the case of initial growth to assess the presence of the tumour as well as in well-established masses which are more challenging to treat only with common strategies. Moreover, NPs are able to specifically interact with the pathological cells and delivery them a higher dose of drugs than with the common ways of administration delivered avoiding side effects and as it is reported below in following chapters, the PCa is defined as a hormonal cancer due to its dependence to androgens to grow. For this reason, antagonists of androgen receptors are used together with the common therapeutic molecules, and thus inserted inside NPs. Furthermore, the use of generic treatments may lead tumour to become more aggressive and in addition to develop specific resistance and independence from androgens. This state is defined as castration-resistant form of tumour and lead to a very low prognosis for the patients, also due to the presence of widespread metastasis around the body.

1.2.1 Prostate cancer epidemiology

Prostate cancer is one of the most diagnosed cancers among men in the 60% of the countries in the world. This specific type of non-cutaneous tumour is the second most widespread tumour after the lung cancer. It is estimated that around the world about 1.4 million of new cases arose only in 2020, especially in Figure 4 is showed that the aged-standardized incidence rates (ASIR) exceeded 59 per 100,00 males in Northern and

Western Europe, the Caribbean, Australia/New Zealand, North and South America, and Southern Africa. Of that 1.4 million, over 0.375 million of death have been observed in the same year, confirming PCa as the first death cause by cancer in a quarter of the world's countries[23]. In accord with the Global Cancer Observatory the crude incidence rate was 36.0 per 100,000 in males with a mortality rate of 9.5 and regarding the age-standardized incidence rate (ASIR) was 30.7 per 100,00 males with a mortality rate of 7.7. It is important to consider that the incidence rate is strictly related to the screening strategy, especially during years the incidence rate has had drops as well as rises and it depended on the increase of prostate-specific antigen (PSA) testing.

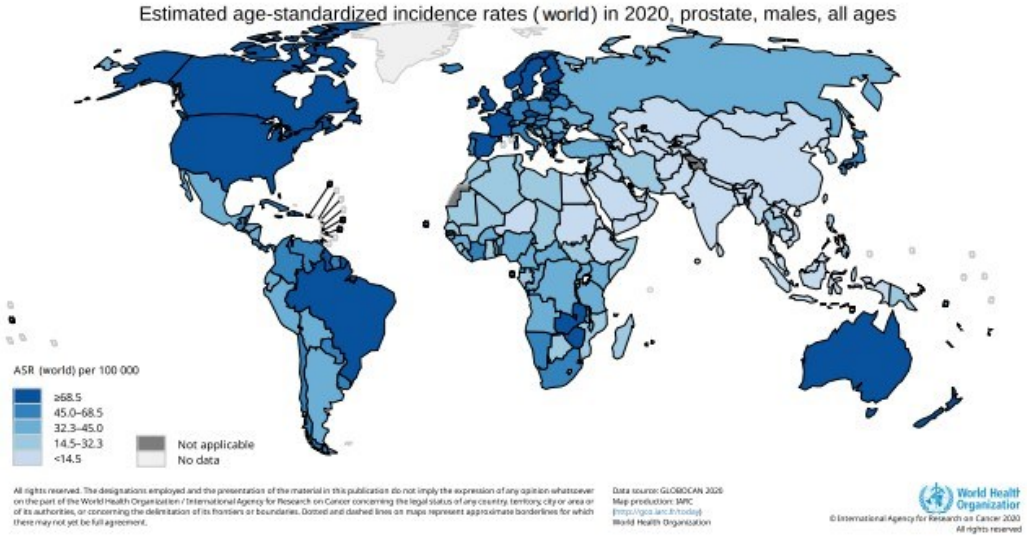

Figure 4 - Estimated age-standardized prostate cancer incidence (world). ASR = age-standardized incidence rate. Global Cancer Observatory (GCO) (https://gco.iarc.fr)

Throughout the data from United States summarized by the American Society of Clinical Oncology (ASCO), the incidence rate is high, and the mortality rate still confirm a problem that needs to be solved. Although the rates are very high, the 5-year relative survival rate for PCa is 97%, while at 10 years it is 98%. Anyway, the survival rate strictly depends on the stages and grade of the PCa, whether it is metastatic or not, however approximately 83% of PCa are found when the disease is in only the prostate and nearby organs.

That was the present, in the future the number of cases is estimated to increase. Figure 5 shows that from 2020 to 2040 the number of cases could almost duplicate in Asia and Africa, for the first it may be related to the higher proliferation rate of the eastern countries, while for Africa it is well know that Black men are more likely to develop such tumour. In contrast, western countries will not increase more than around 28%, except for Latin America and Caribbean. Lastly, Oceania may have three over second patients more than 2020.

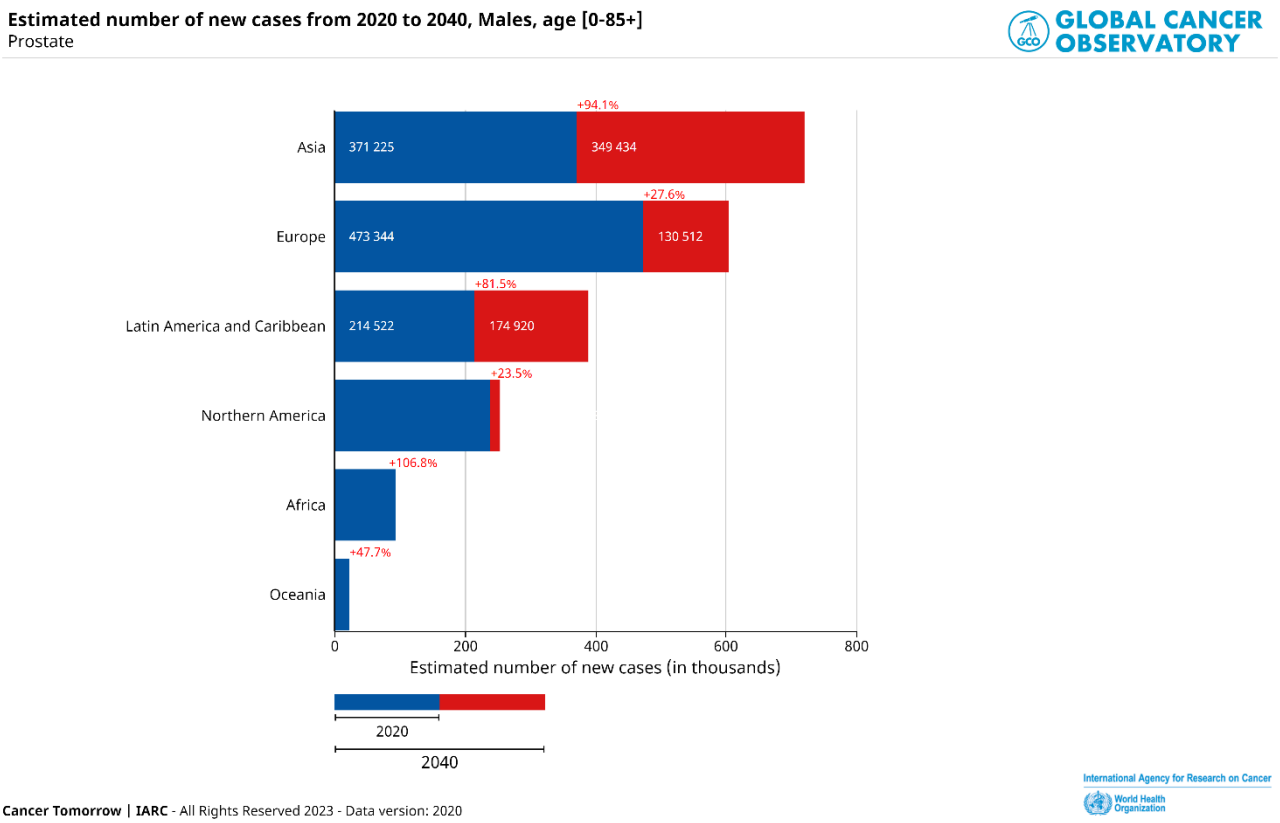

Figure 5 - Estimated number of new cases from 2020 to 2040 in males
Global Cancer Observatory (GCO) (https://gco.iarc.fr)

1.2.2 Prostate cancer aetiology

The aetiology of PCa comprises several risk factors, during years they have been largely analysed. In the paragraphs below are summarized the factors written directly by the America cancer society and delved in the chapter of Keng Lim Ng's book[24]. Among these factors are present age, ethnicity, family history, genetics, obesity, diet, hormones, smoking, alcohol, and certain medications. Although all these have been investigated in their ability to influence the PCa arising or the prevention from that, only ethnicity and age are known to be etiological factor in these tumours arising. This is mainly due to specific investigations in which the percentage of tumour case increased in a positive correlation with age and in men of black African ancestry. Following there are the major risk factors analysed.

- **Age.** Age has a positive relationship with the tumour arising percentage, especially the percentage started with a 0.005% of probability to develop before 39 years of age while it went up to 13.7% in the range of 60-79 years.
- **Family history and genetic predisposition.** Prostate cancer is well-considered one of the most heritable cancers. Men with some relatives diagnosed with cancer of prostate have an increased percentage of developing the disease, up to two to four-fold times rather than people without affected family members.

Some studies have explained this correlation investigating the problem at gene level and they found a possible involvement in the BRCA gene mutation due to its presence also in the breast cancer by correlating PCa patients whit their relatives with breast cancer.

- **Ethnicity.** Different studies have carried out to understand the incidence of PCa in relation with ethnicity and geography, especially a result from USA population analysis demonstrated that mortality rates are 2.4 times higher in black men with African descendent when compared to white man. In specific research on this topic, a group of scientists explain how ethnicity could be related on mutation, especially the problem is related to a methylation of specific genes that lead to and up-regulation of MNX1 in men of African descent promoting oncogenesis, by reducing the ability of its protective tumour suppressor roles.
- **Smoking and alcohol.** Smoking is a well-known risk factory of different cancerous disease due to the insertion of cancerous molecules in the body. In this, smoking has showed association also with PCa. Although, the results of a specific study explained that there are correlations in the amount of smoked rather than between smoker and not.

  On the other hand, for the alcohol it was evaluated a rising of the risk with increased volume of alcohol intake when compared to non-drinkers.
- **Obesity and metabolic syndrome.** Obesity and high body mass index are well-known risk for cancer development, including PCa, meanwhile adiposity level leads to more aggressive form of tumour affecting a positive prognosis of patients. In a study was evaluated that a value of around 5kg/m2 in body mass index could lead the mortality percentage to 20%. Among the reason of this value three possible reason related to obesity have been considered: insulin like growth factor 1 (IGF-1), sex hormones, and adipokines.

  On the other hand, metabolic syndrome has been associated with the incidence of the PCa. This group of disease includes such problems as hypertension, hyperglycaemia, hypercholesterolemia/ high triglycerides, and excess body fat. In particular this syndrome has low association with the risk of PCa, while has a higher association with more aggressive form of the later.
- **Physical activity.** An interesting study revealed that vigorous exercise with a duration of at least 3 hours a week leads to a reduction of the PCa mortality of about 60% demonstrating an inverse relationship among the activity and the disease and a same time it could also affect the progression and the mortality. Although this value is promising there is not real evidence about decreasing the risk to develop PCa with physical activity.
- **Diet and nutrition.** Several foods and their nutrients have been investigated in order to understand some kind of correlation with prostate, if it were positive or negative. High processed foods could increase the risk of PCa, while on the other and unprocessed foods seems to limit the possibility to develop that kind of tumour.

  Lycopene is an organic pigment present in vegetables and fruits and acts as powerful antioxidant which may protect cells from damages. A high level of lycopene as well as isoflavone from soy in the blood can drastically reduce the risk of PCa.

- **Hormones.** Although it is known that androgens, and in particular testosterone, have an impact on the prostate growth, feedback controls exist in the cells of prostate. Indeed, even when the physiological testosterone level is overcome, all intraprostatic androgen receptor sites are saturated avoiding a bad effect of an increased of the hormone. At the end, also 5 alpha reductase inhibitors which is a way to treat lower urinary tract symptoms have some correlations with PCa, especially its delivery is able to decrease the possibility to develop PCa, but there is an increased risk of high-grade PCa at diagnosis.

1.2.3 Precursors of Prostate cancer

The prostate could undergo different changes during aging. Androgens have a fundamental role in the growth of the prostate from the young age to the adult. The testosterone and dihydrotestosterone are the molecules that manage the development and maintenance of prostate structure and functional integrity, just considering that from 2 g in childhood prostate becomes 20 g after the complete development[25]. After prostate reaches the maximum size, a balance between new cells and death ones is appreciable throughout androgen receptors signalling in both endothelial and stromal cells. In adult prostate androgen receptors are mainly expressed in the prostate luminal epithelial cells rather than in the stromal ones, indeed, a depletion of them could directly lead to a reduction on the mass of prostate. However, the prostate tissue has an enhanced self-renewal potential that allows to rapidly re-establish the original size, and this confirms why prostate is so likely to grow in a wrong way also considering the role of stem cells located in the basement of basal cells[26]. In the following will be cleared ow tissue change in years and the possible involvement in the PCa arising.

Benign prostatic hyperplasia. This disease involves an abnormal growth in prostate tissue. BPH is extremely common and disease risk increases linearly with age, beginning at about age 40, and almost all men who live until 90 years of age are favourable to develop microscopic BPH [27]. Hyperplasia is an umbrella-term to explain an enlargement of a tissue due to either natural aging or pathological condition, in the specific case of the prostate it could be due to an increase of cells number as well as the presence of hypertrophy on them with an increment of their size. Usually, this phenomenon is located in the transition zone in a little zone beneath the bladder that contains periurethral glands [28]. This kind of disease is split in two different level of progression: pathological and clinical. The first one involves an abnormal proliferation of cells and an abnormal enlargement of the tissue, while in the second other symptoms appear for the enlargement extent, such as symptomatic dysuria and the development of lower urinary tract symptoms [29]. An important index to consider is the PSA level which seems to have a correlation with the prostate size, indeed, in accord with the National Cancer institute free PSA level is more related with benign hyperplasia against bound PSA which is mainly related with cancerous growing.

Prostatitis. This disease is a common urinary tract condition which its treatment remains a challenge. It is one of the most found urinary tract disease, the third after benign prostate hyperplasia and PCa [30], even so these

kinds of disease are different in targeting, in contrast prostatitis affects men of all ages, mainly in the middle age group. In accord with the National Institutes of Health (NIH) the prostatitis is furthermore classified into 4 different categories. These categories change in symptoms and treatments well as in the original cause. The first two are characterized by the presence of a systemic infection[31], especially the first category remains acute while the second one is classified for being chronical. On the other hand, the last two categories do not present an infection and whether the first one is the most common[32] and rises with pelvic pain[33], the second one is almost painless. They are overall treatable but not curable and if for the first one anti-inflammatory are used to treat the pain, the second one is untreated until the appearance of pain[34].

It is well known that an inflammatory state usually has correlation with the cancer. The amount of immune system cells and inflammatory agents such as cytokines can lead to some changes in the tissue, especially chronic disease that constraints cells into a stressful environment. All molecules and agents present in the microenvironment are likely to induce cells to regenerate with higher ratio in order to re-establish the correct physiology of the tissue, meanwhile oxidative stress may interact negatively with the DNA, mutating its structure during cellular division. Therefore, there are different complications during a chronic inflammation state which may convert the normal tissue in neoplastic one, in addition with the immune system in the microenvironment is compromised and the normal defence is corrupted. The prostatitis for definition is the inflammatory state of the prostate and with time can lead to a neoplastic growing.

Proliferative inflammatory atrophy. In the case of a spread inflammation state in the prostate by different agents as cytokine and immune system cells, epithelial prostate cells could undergo atrophy. Weirdly, contrary to the expected quiescence, prostate cells exhibit an increased proliferation index and a reduced apoptotic rate compared to normal epithelium[35]. For this phenomenon this kind of lesions have been defined as proliferative inflammatory atrophy and usually they target basal cell layer and some secretory cells. A hallmark of this disturb is the presence of some cells with a phenotype intermediate between basal and secretory prostate epithelium, this is due to the presence of a stem cell population located into the basement[36]. Since the inflammation leads to a repeated episode of injury, the normal balance between new and death cells fails in favour of a higher proliferation rate leading to cell instability and emergence of a premalignant cell phenotype. These findings sustain the hypothesis of PIA as a benign lesion with certain genetic instability, which can degenerate into PIN or carcinoma, provided that the balance between anti-carcinogens and carcinogens is perturbed[37].

Prostatic Intraepithelial Neoplasia. As the name says this disease occurs when the epithelial cells start becoming neoplastic**.** Prostatic intraepithelial neoplasia (PIN) is a condition, by the words of Kim H and al. "defined by neoplastic growth of epithelial cells within pre-existing benign prostatic acini or ducts."[38]**.** This neoplasia formation affects commonly the peripheral part where there is the highest concentration of epithelial cells. Differences between normal tissue and neoplastic tissue are appreciable with a histological comparison, at high magnification it is possible to see luminal cells with amphophilic cytoplasm, nuclear crowding, and

stratification, irregular spacing and chromatin hyperchromasia, and clumping, and prominent nucleoli. At the same time nuclear and nucleolar space undergo enlargement. Studies are in accord to classify the prostate intraepithelial neoplasia in four different categories by their architectural patterns: flat, tufting, micropapillary, and cribriform[39]. The flat pattern consists in a single layer of cells with atypical nuclei, tufted pattern expresses different area with different degree of stratification with neoplastic cells near hyperplastic areas, in the case micropapillary an elongation from the epithelium lacking fibrovascular cores is evident, lastly the cribriform in which more benign nuclei appearing toward the centre of the gland[40]. PIN could be classified into in low-grade and high grade.

Low-grade. In low-grade PIN there still are some common features with a benign growth, it expresses a minimal nuclear enlargement and stratification, even though prominent nucleoli are not evident, even so a study reported a correlation of 30% between the presence of low-grade PIN and cancer[41].

High-grade. It is considered as the most important precursor of the PCa[42], even so High-grade PIN cannot be used alone to predict the cancer, since it is discovered with a first biopsy a second one is required to determine the presence of PCa. Unfortunately, the percentage risk to follow to a cancer state after a High grad PIN is found to be the 25%, while the ninety percent of diagnosticated PCa are found after the first or second biopsy. The extent of high-grade PIN is a strong predictor in subsequent biopsies[43].

1.2.4 Prostate cancer pathology

Different types of cancer can be diagnosticated in the prostate. As the prostate could be divided in 3 different comparts, each type of cancer can arise in different of those parts and can affect different types of cells.

Adenocarcinoma. From the National Cancer Institute own definition Adenocarcinoma is a “Cancer that forms in the glandular tissue, which lines certain internal organs and makes and releases substances in the body, such as mucus, digestive juices, and other fluids. Most cancers of the breast, lung, oesophagus, stomach, colon, rectum, pancreas, prostate, and uterus are adenocarcinomas.”. The prostate adenocarcinoma is the most common cancer found in the prostate gland and represents the 99 % of cases of PCa. Specifically in the Prostate, this cancer affects the secretory epithelial cells mainly located in the peripheral zone of the gland. Considering prostate adenocarcinoma two different disease could be noticed: acinar adenocarcinoma and ducts adenocarcinoma. Both show some common features and some differences. They equally express some specifical prostate markers, such as prostate specific antigen (PSA), prostatic acid phosphatase (PAP), alpha-methylacyl coenzyme A (CoA)-reductase (AMACR), androgen receptor (AR), and cytokeratin 7 (CK7), meanwhile in the cellular part there is a partial or total lack of the basal cell layer with an abnormal proliferation rate of cells[44]. At the same time the diagnosis of one type of prostate adenocarcinoma rather than the other is challenging and this is due to the facts that the two tumour types could coexist. Both acinar and ductal carcinoma overexpress the PSA[44].

- **Acinar.** Considering only the acinar adenocarcinoma, the spread of this peculiar cancer form covers around the 90-95% of cases of adenocarcinoma. Usually, acinar tumours are located in the ducts in the second part of the urethra rather than the first where ductal one is more common. From and histological perspective the disposition of cells in this carcinoma commonly follows a glandular and acinar pattern [45].
- **Ductal.** It is comprised in the class of rare histologic subtypes of prostate carcinoma. Usually, ductal tumours arise in peripheral prostate ducts which join urethra in the first part [46]. Speaking about the geometrical disposition of cells they are commonly seen arranging in column in either papillary or cribriform pattern, especially the first one shows a variable degree of nuclear pleomorphism and hyperchromasia in cells while the second one consists in back-to-back cribriform glands with central necrosis. Both in the first and second pattern mentioned, the surrounding stroma is fibrotic or altered [45].

Transitional cell carcinoma of the prostate. This carcinoma is also known as urothelial carcinoma. It involves the cells that line the urethra in the transition zone. This type of cancer usually starts in the bladder and spreads into the prostate. In this case it could be thought that urothelial carcinoma is a metastatic component form the bladder, but researchers are in accord to classify it as prostatic due to the cellular component[47]. The spreading of this type of cancer is in the range of 0.2-3.5% of all prostatic carcinomas. The common hallmarks of this type of carcinoma mainly are the presence of some plugs of solid tumour present in ducts together with elongated cylinders, meanwhile necrosis could occur and undergo dystrophic calcification and pagetoid spread can also be found, lastly rarely an intraductal papillary pattern can be detected. Spread of prostatic urothelial carcinoma within ducts and acini can be extensive, without stromal invasion. Speaking about the conformation of the inner part of cells, in this carcinoma they express a high nuclear grade, with substantial nucleomegaly, nuclear pleomorphism, and nuclear hyperchromasia, and sometimes the cytoplasm can appear as eosinophilic squamous. Rather than the others, urethral carcinoma is negative for PSA and PSAP out-boundaries level and is usually positive for CK7, CK20, high molecular weight CKs bound by 34bE12 (CK903), p63, and thrombomodulin[44].

Squamous cell carcinoma of the prostate. This carcinoma takes part in the group of rare cancer growths which affect the prostate. These cancers may develop from cells that cover the prostate. They tend to grow and spread more quickly than adenocarcinoma of the prostate. This specific form of cancer comprises only the 0.5-1% of all carcinoma cases[44]. In contrast of the common adenocarcinomas, this malignant growth does not espouse an increase on PSA and PAP levels and this makes researcher think that this carcinoma affects cells that produce the two proteins. Among the histological features are a large mass which usually replace the physiological tissue of the prostate and small tissue pieces show a solid, firm, unphysiological coloured mass meanwhile other problems could occur such as the compression of the prostatic tract of the urethra, local invasion into the bladder, rectum, and seminal vesicles[44].

Small-cell prostate cancer. In contrast with others, this disease is categorized inside the neuroendocrine cancer family, in addition it comprises only the 0.3-1% of the cases, meanwhile it represents one of the most aggressive PCa that can easily spread around the body, even though visceral metastasis is more common in this rather than others[44]. At cellular level this cancer expresses some unique features, for example the proliferation of small-cell occurred and they express scant cytoplasm, undefined border, chromatin dispersed in granular "salt and pepper" pattern together with the absence or inconspicuousness of nucleoli and frequent nuclear molding[48]. In contrast with adenocarcinoma, this cancer typology is resistant against hormonal therapy, expresses a rapid progression which reach the maximum with spreading in viscera, and in addition the PSA level remains overall in the limits.

Carcinosarcoma. This cancerous mass is one of the rarest, it makes up less than 1% of all cancer formations, and less than 5% of them occurs in the genitourinary tract, among the primary prostate malignancies less than 0.1% are sarcomas[49]. This cancer, also known as sarcomatous carcinoma, is a biphasic malignancy which could arise in the prostate, and in addition it is possible to recognize a high-grade epithelial component (carcinomatous) and a malignant mesenchymal or mesenchymal-like component (sarcomatous)[44]. Due to the composition, carcinosarcoma may develop either in a homologous or heterologous pattern. In the first one the mesenchymal-like areas express a population with undifferentiated sarcoma cells, while in the second one a grade of differentiation is appreciable along the specific lines of mesenchymal cells. This cancer can origin in mesenchymal non epithelial components of the prostate stroma[50]. It is worth noticing that this cancer is recognised to be castration resistant due to the lack of androgen receptors occurred, in addition due to the presence of some undifferentiated and differentiated cells, the level of PSA is useless, even so GSTP1 could be a good diagnostic marker for sarcoma as a substitute for PSA [49]. At tissue level masses containing haemorrhagic, necrotic tissue extended to surrounding structure with a grey whitish to pinkish colour can be recognized, while pathologically speaking the common symptoms of this disease are tract obstruction and symptoms of frequency, urgency, and nocturia[44].

1.2.5 Kind of cancer: castration sensitive and castration resistant

Throughout the previous chapters was possible to understand the importance of the androgens in the signalling between the cells of the prostate. The mainly used are the testosterone and dihydrotestosterone which are able to recognize and interact with androgens receptor managing the proliferation rate and other fundamental functions of the cells.

Figure 6 shows the trend of the acquired resistance of PCa along treatments. The presence or the absence of androgens could have a crucial impact on the disease healing. In more details the PCa can undergo different changes and through different steps of development.

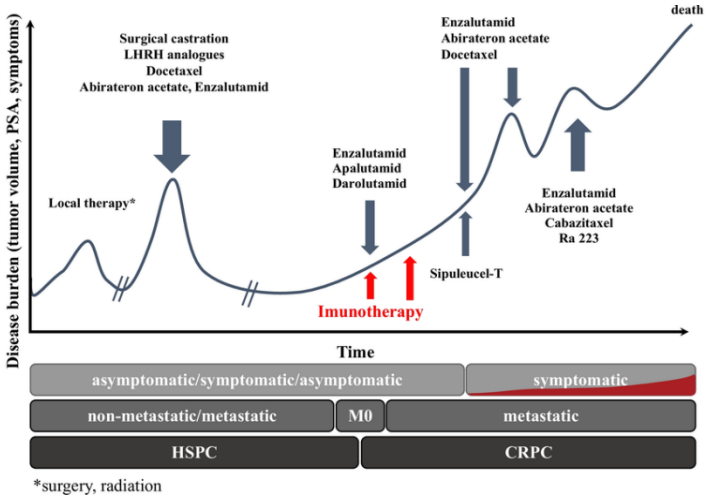

Figure 6 - Curve of prostate cancer resistance development[51]

In the early stage after some cells proliferate with some aberration and changes in their life cycle the mass slowly grow without notable symptoms which in some way could have alerted the future patient. In this step it is difficult to diagnose the cancer due to the absence markers such as a higher level of PSA and a similar structure to the pathological tissue pattern, in addition a biopsy can be confused to a benign growth or a prostate interepithelial neoplasia. In the last two cases a surgery or a radiation ablation could be used to remove the mass and avoid future development and the reduction of the mass can be explained from the first peak in the figure.

Consequently, if cells were not all removed or some other in the neigh place are undergoing mutation the cancer could start growing again with more aggressivity. If the situation gets aggravated in this way, the proliferation is usually slowed down by the deprivation of androgens, the use of some antagonists which interact with androgen receptors rather than androgens or some molecule which may bind free androgens to avoid the interaction with the real receptor, or in the worst scenario the castration. In the chart is possible to see this trend after the second peak, after castration a big decrease of the cancer mass is shown, since the major pathway which manages the proliferation has been interrupted.

Unfortunately, PCa cells could change pathways to survive and/or mutate the DNA affecting change the conformation and the length of their androgen receptors, especially a lack of the outer part of the protein may occur and the singling is established again by the auto paracrine communication. If this event happens the cancer moves from a castration-sensitive to a castration-resistant behaviour in which the use of hormonal therapies or similar do not affect the proliferation anymore and PCa becomes more likely to spread around the body with metastasis, mainly in near bones. At this point the majority of therapies are not equally useful as initially against the primary tumour and possible metastasis, one of the last choices is the use of stronger chemotherapeutic agents, a possible response of the disease against this kind of therapy is shown after the last

peak, with a very low decreasing of the mass size. Unfortunately, in this condition, the survival hopes are very low because it is almost impossible remove the primary tumour and all metastasis which at that point may have reached lymph nodes and different bone compartments.

1.2.6 Diagnosis of prostate cancer

As mentioned before, most of the times in the early stage, the disease develops without symptoms. Different cancer research centres, such as Cancer research UK, Centres for Disease control and prevention (.gov), American cancer society, are in accord that usually the first signs that can be alarmed doctors are: trouble starting the flow of urine, frequent urination, trouble emptying the bladder completely, and weak or interrupted flow of urine, while in the advanced state they usually comprise: pain in the back, hips, or pelvis that doesn't go away, and shortness of breath, feeling very tired, fast heartbeat, dizziness, or pale skin caused by anaemia. Some of these symptoms may be caused from other prostate disease and some other diagnostic tests are needed while the second one most of times are strictly related with the cancer.
The guidelines for diagnosing cancer are summarized below from the National Institute for Health and Care Excellence (NICE) in combination with the centres cited above. For assessing the real presence of the cancer, doctors can choose among different tests:

- **Physical exam and health history.** The aim is to discover the overall health history of patients and to check the family patient that have been positive at PCa.
- **Digital rectal exam (DRE).** In this exam doctors inserts and use a gloved finger inside the rectum to directly feel the prostate tissue and searching for some lumps or abnormal areas.
- **Prostate-specific antigen (PSA) test.** PSA has a strict relationship with the cancer, especially PSA could increase during tumour arising or growing. This test measures the PSA level inside a blood sample. Usually, this test can confirm the prognosis, but alone it could give some false results, because other disease can increase the PSA level.
- **PSMA-PET scan.** A probing molecule is exploited to find out prostate cells which have left the prostate tissue. To do so, a radioactive substance is combined with the PSMA which is a protein able to bind specific membrane proteins upon the cells of the prostate overexpressed in PCa. In this case the PET instruments detect the position in which the labelled molecules interact with prostate cells. It is important to consider that this kind of diagnosis scan is helpful to look for metastasis rather than determine the presence of primary tumour.
- **Transrectal ultrasound and magnetic resonance imaging (MRI).** An ultrasound probe is inserted into the rectum to acquire images of the prostate and surrounding soft tissue, throughout echoes and the sonogram is possible to watch the health state of the prostate tissue. Usually, this test is used to acquire images during a biopsy procedure. On the other hand, MRI is very similar to the previous scan but with radio waves, especially a probe is inserted into the rectum, meanwhile a strong magnet can detach waves,

and these are converted into a human-appreciable images. This technology is commonly used to see the surrounding tissue and if some prostate cells spread in those areas.

- **Transrectal biopsy.** This test is the one that can confirm the presence of the cancer. A needle is inserted in rectum to reach the prostate from the rectal wall, by that a small piece of tissue is collected. After fixation of the tissue different markers can be searched to confirm or not the presence of the cancer.

1.2.7 Treatment of prostate cancer

In the years different types of treatment have been developed. In accordance with the National Cancer institute, the PCa has both chemical and physical treatment which can be exploited, each one with its pros and cons.
After the cancer is found in the patient the doctor gives a grade at the disease, and this is related to the abnormalities that the tissue expresses and about how quickly the cancer is likely to grow and spread. The grade of the cancer is well-known as Gleason score from the pathologist who first used it Donald F. Gleason and it has been used to understand the aggressivity of the cancer and to plan the best treatment.
By the guidelines of different cancer research centres cited in the previous section, doctors have a quantity of different treatments against the cancer, especially some of them are common in different cancer form, while other are specific for PCa and for its own nature.

- **Surgery.** The aim of the surgery is to remove either the whole the prostate or specific part of prostate tissue affected by the tumour. First one is done by the radical prostatectomy in which in addition to prostate most of the times even surrounding tissues, seminal vesicles and lymph node are removed. This surgical procedure can be done either in open way or in laparoscopic way, through robot-assisted or by-hand procedure.

  Instead, the second procedure can be done by the pelvic lymphadenectomy in which only lymph nodes are removed and by transurethral resection of the prostate (TURP) in which through the urethra a resectoscope allows to resect parts of prostate tissue. These procedures have some consequences like impotence, leakage of urine from the bladder or stool from the rectum, shortening of the penis, inguinal.
- **Radiation therapy and radiopharmaceutical therapy.** This family of treatments uses energy to remove the tumour mass, as x-rays or other ones, among the common are external radiation therapy that from outside focuses a ray in a drawn area of the cancerous growth, while the internal radiation uses radioactive substance that is directly placed into or near the cancer. The treatment could be also fractionated with higher does for shorter periods. Among the consequences are impotence and urinary problems as well as increased risk to develop other cancer form such as to the bladder and /or to gastrointestinal system.
- **Hormone therapy.** Hormones such as androgens have a direct involvement in the cancer proliferation and spreading as well as in the maintenance of the prostate tissue. The main aim of these treatments is to block the signalling of cancer cells and let them undergo death. To reduce the presence of hormones around the body is possible to use antagonist molecules or surgery. The family of these treatments is known as androgen deprivation therapy and this includes drugs able to prevent PCa cells from producing androgens,

orchiectomy to remove testis as most important source of male hormones, or stopping them by exploiting, and lastly anti-androgens that occupy the binding domain of the androgen receptors prevent them from interacting with real androgens.

- **Chemotherapy.** This treatment is one of the most common for several tumours. In particular, some chemotherapeutic agents are delivered in the body by oral or vein administration. Trough the blood stream, the molecules can reach cancer cells and start to block their proliferation or kill them. One of the most important side effects is the low specificity of such molecules that requires drug delivery system to avoid as much as possible it.
- **Targeted therapy.** This peculiar treatment targets directly cancer cells to limit useless damages to surrounding safe cells. Targeted therapy uses all things that can strongly interact with the specific tumour environment and its cells. In the case of PCa, it is commonly used PARP inhibitors which could block some enzymes involved in cell function including the tumoral ones, these enzymes help repairing DNA and blocking them prevent cancer cells from continue with their life cycle and died. Usually, this treatment is used to treat metastatic PCa.
- **Immunotherapy.** Immune system is the protagonist of this therapy. Indeed, human immune system is able to eliminate mutated and harmful cells, unfortunately some kind of cancers can mutate and quickly acquire specific capabilities to hide their condition, sometimes they may influence the surrounding environment to help their growth. The aim of immunotherapy is to enhance immune system cells in recognizing and fighting cancer, cells are modified in lab to express specific protein receptors and antigen to bind and kill cancer cells, at the same time the therapy is promising for metastatic PCa due to the circulation of modified cells without hitting normal cell.
- **Bisphosphonate therapy.** Since PCa can easily spread in nearby bones and makes them frailer, and in addition this is enhanced in cases of hormonal therapy exploiting, bisphosphate drugs have been studied as agents which can prevent or slow the growth of bone metastasis.

1.3 Skeletal system

1.3.1 Anatomy of bones

Skeletal system is one of the most interesting systems in human body as well as in all animals provided. Although its aim inside the human body is complex and fundamental, it make up less than the 20% of the whole weight. Below it is summarized the composition of this apparatus delving into the cellular population and structure[52].

Cortical bone. This hard tissue has the highest density among all tissue in the body, it is around 1.6-2 g/cm^{-3}. This is mainly due to the long-term disposition of cells and extracellular matrix, as well as the presence of some inorganic crystals entrapped inside the matrix. In more details the bone tissue owes its properties to the

specific disposition of collagen fibres, indeed, collagens type I fibre are located in oblique sheet and are wrapped around the osteoid, the hole in which vessels can pass through to irrorate the cellular components of bones. In order to increase the mechanical strength, the different fascicles are overlapped orthogonally with an angle of almost 90°, this allows cortical bone to achieve traction, compression and bending resistance. The hydroxyapatite represents the inorganic part and act as a second phase between fibres. This kind of tissue is mainly present in the epiphysis which are the extremes of long bones and as tiny layer of diaphysis, especially it is formed by the alignment of different osteons following the weight line, it is thought that bone cell can follow the mechanical stimuli in their dynamic repairing of the bone allowing to adapt and reach the maximum resistance against them.

Cancellous bone. On the other hand, the cancellous bone represents the part of the bone with the lower density, this is due to the presence of different holes and a sponge conformation, and as it was mentioned in previous chapter, it contains the bone marrow as storage for the blood cells. In this specific tissue the osteons are no aligned along a specific direction and this let them grow in a trabecular casual structure. It is important to specific that even if the presence of sponge bone seems to be unproductive for the mechanical strength of bones, it has a specific role. Indeed, since the cortical bone is very strength, but frail, the cancellous bone can withstand higher stress due to it toughness.

For more focusing into at cellular level, in the case of bones there are different cells with different roles in the maintenance of the latter. It is important to specify that contrary to people belief bone tissue undergoes different changes, it is a dynamic tissue which continuously is broken and remade in order to maintain the calcium and other ions balance in the body and to restore any crack during human days. Therefore, it is possible to understand as it has to have some cells involved in the construction of the tissue and other in the destruction of the one, indeed, these are respectively the osteoblasts and osteoclasts, especially osteoblast could be found in a quiescent form in which they are called bone lining cells rather than in active form in which they are considered osteoblast. Before going into the description, it is also important to mention the osteocytes which represent another form of osteoblasts which have been buried inside the bone.

1.3.2 Bone types

In all vertebrate animals, skeletal system plays a fundamental role to allow the life. Among the bone roles are firstly protection for example of skull box and ribcage which protect all important organs secondly bones allow muscles to find a scaffold which can be pulled during contraction and moved. Since bones have different roles in the body, following the description of the National Cancer Institute it is possible to recognize a subset of types: flat, long, short bones.

Flat bones. From the name is easy to understand their geometry, in this case the cortical part of the bone is widely distributed while cancellous one counts a low percentage in the middle part. Usually, these bones are mainly focused on the protection role as in the skull or in specific compartments where a specific joint

movement is required as for shoulder blades. In flat bones the presence of bone marrow is very low considering that the latter is set inside the cancellous bone.

Short bones. While in flat bones the width is the bigger dimension, in short bones almost each dimension is equal to the others. Short bones are no widespread in the body since they are only present in the carpals of the wrists and the tarsals of the ankles. As the previous, in these bones diaphysis is not present, so there is a lack of the part which should contain bone marrow, for this reason their most important aim is to provide stability and support as well as some limited motion.

Long bones. These among all bones represent the most complex in human body, they cover a quantity of different roles. Firstly, these bones have one bigger dimension, usually the length, and for this reason limbs mainly carry on them. Long bones provide the larger set of movements. Indeed, they gather in several joint which allow a quantity of movement, among them is possible to find ball and socket joint, saddle joint, hinge joint, condyloid joint, pivot joint, gliding joint. For the structure and the dimension of long bones two different part can be appreciated: epiphysis and diaphysis. The first one is located at the beginning and at the end of the bone, it is manly made up of cortical bone and contains the bone parts which interact with the other bones, the second one is located in the middle part and since there the cancellous bone is more extent, it is possible to see the presence of bone marrow which as the aim to provide new blood cells to the blood flow.
All three types of bones have in common the presence of cortical bone, while cancellous bone is mainly present into the middle part of the long bones called diaphysis.

1.3.3 Bone cells

The skeletal apparatus is a dynamic system that relies on various specialized cell types to maintain a delicate balance between bone formation and resorption. These cells play pivotal roles in ensuring the structural integrity of bones while also serving as a reservoir for essential hematopoietic stem cells, thereby highlighting the multifaceted nature of bones in supporting both structural and biological functions. The most important cells are summarily described below from the analyses of Florencio-Silvia et al.[53].

Bone lining cells. Thinking ideally to a snapshot of the bone, the surface is intact and no activities from different cells are appreciable. In this case the osteoblasts stay in a dormient state laying upon the external surface of the bone. They create a covering around the bone waiting for the activity of the osteoclast in order to deliver signals and activate osteoblast in response of them. It has been discovered that these cells can bind with hematopoietic stem cells to maintain them in an undifferentiated state behaving as a niche, while some jap junctions with superficial osteocytes allow to start the differentiation in osteoclast from stem cells in order to continue the bone life cycle. A particular is that they have a flat shape to cover and spread around the bone, while the active osteoblasts have a rounded shape[53].

Osteoblast. These specific cells have as the main role to form new bone starting from the external part of the bone, in particular when some chemical and/or chemical signals are delivered in the bone environment, hematopoietic cells can differentiate in osteoblast, these are able to attach on the bone surface and start the deposition of new matrix, in particular they can synthetize collagen type I and secrete in the environment, this is easily to demonstrate by the presence of a "large number of nucleosomes and rough endoplasmic reticulum in the cytoplasm of osteoblasts"[52]. In more details, the formation of new matrix from osteoblast occurs in two main steps: the first one involves the deposition of collagens and other non-collagen proteins, while the second involves the mineralization of the new matrix with hydroxyapatite crystals. The first phase comprises the secretion of collagen proteins together with proteoglycans and other linking proteins, the second one starts with the delivery of some vesicles which bind with the proteoglycans. After that, some enzymes can degrade proteoglycans and calcium ions are released to cross the calcium channels upon the vesicle membranes, meanwhile other enzymes can degrade some compounds which contains phosphate groups and these can enter in the vesicles[53]. Lastly after the supersaturation of vesicles carried form the hydroxyapatite formation leads to the membrane rupture allowing crystals to spread to the surrounding matrix. In this way the new bone is formed. Osteoblast can be spotted in different form, usually at the start of the process the have a spherical shape, which undergoes ovalization until obtaining a flat conformation before becoming bone lining cells, or remaining oval if they were buried into the matrix becoming osteocytes[53].

Osteocytes. These cells are like a storage of bone cells, in particular these specific cells are entrapped inside the bone matrix during the bone formation and there they remain quiescent. These kinds of cells originate from osteoblast, especially from osteoblasts that during the deposition of the molecules remain entrapped beneath the surface. Inside the matrix, osteocytes preserve their work, especially they secrete and delivery protein for making to fill the bone lacunae. Moreover, they can act as mechanic sensors communication the well-being of the bone and allow osteoblast to be differentiated and started restoring the bone[54]. Although osteocytes are buried, some channels called canaliculi which have been deposited within the collagen matrix allow the exchange of nutrients and waste materials. Another important role of the osteocytes is the regulation of calcium, indeed, they are able to acquire signals form the environment and understand if the environment requires more calcium or less, and so they can restock the calcium degrading the matrix.

Osteoclasts. Lastly there are the osteoclasts. In contrast with the other bone cells, these ones are polynucleate cells, they are made up by the fusion of different monocytes and due to this they descend again from hematopoietic stem cells[53]. The most important role of the osteoclast is to degrade the bone matrix, especially the need of this could be to restore the bone after a break to allow osteoblasts starting their work or to release some ions as calcium in the blood flow[55]. Usually, osteoclasts reaching the complete aggregation and activated form after bind the RANK receptor which is located upon the membrane of superficial bone cells, this also provide osteoclast from still moving and allow to attach on the bone surface.

Lastly, after osteoclast finish their work because the calcium level in the environment increases, osteoclasts detach from the surface and undergo apoptosis.

1.4 Osteosarcoma (OSa)

With the information form the National Cancer institute, OSa is a kind of cancer that affects bone cells. The most common affected people are adolescent and young adult, it exhibits a bimodal distribution with peaks occurring between the ages of 0-14 years and after 65 years of age. In the case of adolescent, it is considered as primary paediatric bone malignancy due to the involvement of bone-forming mesenchymal cells, meanwhile in older patients it is considered as secondary form such as consequence of other pathologies that can lead to a degeneration or conversion to a malignant state. Starting with the age difference, a lot of other subcategories can be used to classify this type of cancer, especially by the histological abnormalities, the type of bone and its location and also the degree of differentiation[56]. The consequence is that bone cancers can differ for morphological appearance, demographics, and biological behaviour. This solid tumour which affects the bones usually is found around the knee and the proximal humerus[57]. Therefore, it can target any kind of bones, even so long bones are more affected than others since the major activity of bone cells and the presence of bone marrow. The first appearance of the tumour can be histologically spotted by the presence of abnormal masses probably related to the malignant transformation of cells from the mesenchymal lineage during the differentiation into osteoblasts[58]. Since the bone tumours are strict related with the type of matrix deposited, they can be furtherly classified into chondroblastic, fibroblastic, osteoblastic and telangiectatic OSa, meanwhile it confirms that cancer cells could maintain some undifferentiating properties from the mesenchymal precursors[59].

1.4.1 Osteosarcoma epidemiology

Osteosarcoma is the most common primary bone malignancy. Although, in comparison with different types of tumours, OSa is not so common. From America cancer society it has been estimated that around 1000 new cases are diagnosed each year in the United States. This type of bone cancer can affect each age, even so the children are the most affected. Indeed, of the 1000 new cases in USA, about half of those are children. In Figure 7 is reported a map of the world with the higher number of children affected in the range of 10-19 years old, all the value are expressed as age-standardized incidence rate (ASRs). It is important to consider, as it will be said in the next chapter, that for children OSa arise as primary tumour, while for older patients it is likely to be a secondary tumour develop by already present conditions. As Rojas et all reported [60], Northern Africa, Southeastern Asia and South America present the highest incidence rate with respectively 9.4, 9.2, 9.2 cases per million. In contrast the lowest incidence rates are reported in Southern Asia (4.9), Eastern Europe (6.1) and Western Asia (6.6). For OSa there are big differences in incidence between males and females. For example, for the range 10-19 the highest rate was seen in Southeastern Asia for females and in South America for males.

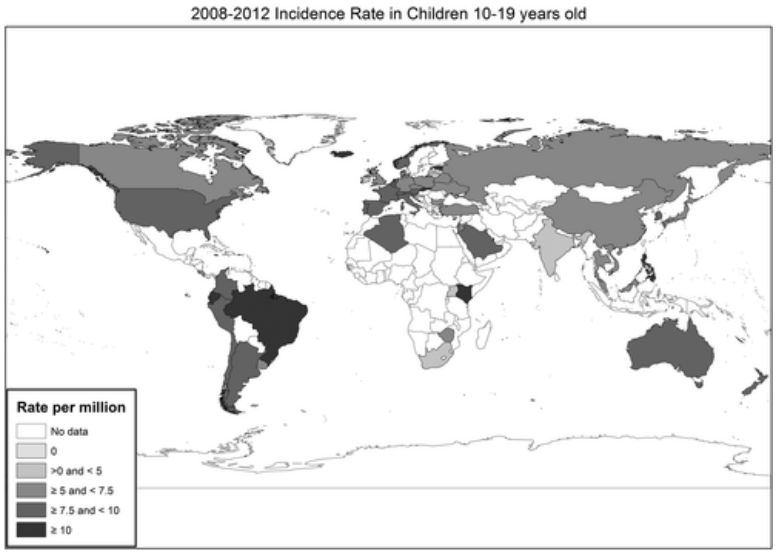

Figure 7 - World incidence rate in children 10-19 years old
Cancer Incidence in Five Continents (CI5) in 2008-2012

A second worrying rate is in the group between 60 and 79, although that range did not overcome the 6 cases per million. The highest values are reported to be in the Sub-Saharan Africa with 4.9 cases per million and in Southeastern Asia with 4.4 cases per million. Also, in this case there are disparities between males and females with the highest male incidence in Eastern Europe and in Sub-Saharan Africa for females.
As said at the start, OSa affect each age range, although these two specific ranges are the most hit by this cancer, moreover this data could not include reliable results about African countries, which are studied apart[61].
Osteosarcoma, in its malignancy could spread around the body, especially the survival rate strictly depends on that condition. Following the reports of the American Cancer Society, the percentage of 5-year survived patients is around 76% for localized tumour, while drop down for distant tumour with a percentage of 24%.

1.4.2 Osteosarcoma aetiology

Osteosarcoma has an aetiology well-defined, with causes related both to the environment and genetic. Different risk factors involve the association with other pathological condition, such as Paget's disease, hereditary retinoblastoma, the Li–Fraumeni familial cancer syndrome, and other chromosomal abnormalities, as well as other problems relation to specific kind of treatment like ionizing radiation and alkylating agents. The following paragraph are summarized from a chapter of the book "Pediatric and Adolescent OSa"[62].

Host Factors

Among host factors is possible to notice the presence of common risk factors as well as other specific for the disease.

- **Age.** Already mentioned, age play a major role in the incidence of the disease. In particular, this disease has a bimodal distribution in which peaks are locate in adolescent age and in adults older than 65 years. It is worth noticing that in youngers the prevalence of OSa is as a primary tumour while in older adults it arises as secondary tumour.
- **Gender.** It has been seen that male people has a higher prevalence than female to develop OSa, even so the cause is not very understood. However, from statistical analysis girls could develop the tumour at younger age than male.
- **Growth.** Mainly focusing on the primary tumour, they seem to have a higher impact on the extremis of the long bones and to have some relationships with the bone growth, especially the femur is well-known to be the most affected bone. Considering the distribution, the first peak perfectly corresponds to the adolescent growth spurt, demonstrating the relation with bone growth. At the same time the peak for female is at lower age because the growth spurt could occur earlier than male. The motif could be related to the recruitment of rapidly proliferating cells which may be more likely to undergo malignant transformation or to be sensitive to oncogenic agent and mitotic errors. At the same time taller individuals are more likely to develop OSa and it is related to the more impressive growth spurt required.
- **Genetic and familial factors.** As already mentioned previously, genetic aberration has a strict association with OSa as aetiological factor. In some studies which have exploited comparative genomic hybridization it has come out the presence of different chromosomal abnormalities finding that chromosome 21 regions have an important role in the OSa intercourse. The genetic role seems to have as molecular result the inactivation of tumour suppressor genes, especially p53 and the retinoblastoma susceptibility genes. Among some diseases which lead to mutation in genes and have a relation with OSa arise it is possible to find:
  - Li-Fraumeni syndrome that is mainly related to a mutation on p53 gene that codifies the relative onco-suppressor protein and due to this it has a higher risk of developing OSa.
  - The Rothmund–Thomson syndrome has the major problem related the mutation of the RECQL4 gene which encode some DNA helicase, especially the wrong working of them has been highly correlated with OSa.
  - Bloom and Werner syndromes have been discovered to have similarity with Rothmund–Thomson syndrome involvement in OSa.
- **Preexisting bone abnormalities.** Among abnormalities which affect bones are Paget's disease and Ollier disease. The first one is better explained in the following chapter, but summarizing OSa is more likely to arise from patient with the disease in a high-grade way with poor prognosis and OSa in older patient is frequently associated with Paget's disease. On the other hand, Ollier disease leads to multiple enchondromatosis increase the risk of an establishment of OSa.

Environmental Factors

On the other hand, in the environmental factors are present radiation, external agents, viruses, trauma.

- **Ionizing radiation.** Since it is analysed then, rapidly patients who have been either treated with radiation if it were external or internal with radioactive drugs, or interacted inadvertently with them could undergo this complication.
- **Alkylating agents.** Different studies have reported a relation between the use of alkylating agents and the emerging of OSa. This have been noticed since Ewing sarcoma survivors are more likely to develop a secondary OSa, meanwhile with the specific use of anthracyclines the interval for the development of secondary OSa tends to decrease.
- **Perinatal factors.** In this filed, results are conflicting in different manners. However, it seems that prenatal exposure to x-rays may be associated with an increased risk for OSa and in addition there have been reports indicating a potential link between shorter birth length and higher birth weight with an increased risk of OSa, although the findings have not been consistent or conclusive.

1.4.3 Osteosarcoma precursors

For doctors and researchers, OSa is likely to develop mainly as de novo disease. Nevertheless, some cases are recognized to have some relationships with benign precursors. In order to understand the origin and the best way to treat a tumour, OSa have been classified, according to in-depth research[63], in different categories: diseases with documented predisposition to malignant bone tumours, sporadic benign tumours with a known risk for secondary malignancy, and post-radiation malignant tumours.

Congenital syndromes. Through the age range in which humans are affected by this disease between 0-14, it makes easy to understand that inherited condition, such as congenital syndromes, can play an important role to identify the predispose conditions of patients. Among them are familial retinoblastoma, Rothmund-Thompson syndrome, and Bloom syndrome. Although the occurrence of OSa after in these diseases is rare, specific molecular mechanisms, as well as genetic hallmark of these syndromes, could led thinking about some correlation[63].

Sporadic premalignant lesions. It involves different conditions with some relationships in some cases of OSa. Paget's disease is a condition in which the balance of the bone remodelling is lost leading to an enhanced abnormal bone fabrication. The incidence of sarcoma has been estimated at around 1%. Usually, Paget's disease which affects pelvis, femur, humerus, and tibia has been reported to mainly induce an OSa growth. At the same time the strength of OSa which originate from this disease is recognized to be higher than primary tumours[64]. From a histological point of view, OSa arisen from Paget's disease are high-grade ones with striking nuclear pleomorphism or bizarre giant cells[63].

Giant cell tumour. In Giant Cell tumour, various malignant characteristics have been identified, including a high mitotic rate, necrosis, high cell density, and vascular invasion. However, the overall behaviour of this tumour tends to resemble a benign condition. This particular tissue condition can be categorized as primary or secondary[65]. The primary form is characterized by the presence of areas where giant cell tumour is in contact with a high-grade spindle cell sarcoma, while the secondary form is primarily associated with the long-term effects of radiotherapy. From a histological perspective, there is a gradual transition between areas with giant cell tumour characteristics and those resembling OSa, although with an overall presence of abnormal cells and integration into the malignant component[63].

Chronic osteomyelitis. Chronic osteomyelitis is a long-lasting bone infection that is extremely challenging to treat. It has been associated with OSa development due to symptoms such as the emergence of a growing mass, intensified pain, bleeding, or the presence of a pus-filled discharge from a long-standing sinus[63]. Upon histological examination, most cases have shown characteristics consistent with well-differentiated squamous cell carcinoma (17), rather than OSa, which has been observed in fewer instances.

Fibrous dysplasia. Fibrous dysplasia is a prevalent condition that impacts bones and occurs when abnormal fibrous tissue replaces normal bone tissue[66]. This pathological condition is considered a benign anomaly in which fibrous tissue replaces bone tissue, altering the arrangement of trabeculae[63]. From a histological standpoint, the characteristics of this particular condition might suggest a potential connection to low-grade central OSa[67], whereas conventional OSa is typically characterized as high-grade, based on histological examinations.

Post-radiation sarcoma. In contemporary understanding, sarcoma is recognized to be associated with certain risk factors, including exposure to radiation during treatment[68]. Typically, when diagnosing sarcoma, several criteria must be met to determine its origins. Specifically, the bone should have been within the radiation treatment field, there should be a period of latency, and histological confirmation of sarcoma is required[63]. Generally, radiation is known to result in benign lesions, but in some cases, malignancies can be considered[69]. Furthermore, there are other form of premalignant state, even so they have a rate drastically lower than the previous, among them are osteoblastoma, osteochondroma, chondrosarcoma and enchondroma.

1.4.4 Osteosarcoma pathology

The OSa is classified into classes which characterize the location of the origin, especially they are central, intramedullary, and surface tumours in accord with the World Health Organization.

Conventional osteosarcoma. This is the most common type of OSa and represents the 80% of cases. The cells of the tumour have specific peculiarities, for example the nuclei are pleomorphic and hyperchromatic. In the specific case of conventional OSa, the production of osteoid as well as the deposition of osseous matrix is increased, for this specific behaviour cells remain hide inside the bone matrix[70], and at the same time a portion of them undergo necrosis[71]. The conventional OSa is usually assigned to the grade 3 or 4 in accord with the classification of the Mayo Clinic. It is worth noting that the grade is determined by the cytologic atypia of tumour cells, and for this, anaplasia represents itself the grade 4[72]. Lastly, this form of tumour is the most likely to spread around the body starting from the soft tissue around the origin zone.

Telangiectatic osteosarcoma. It comprises the 4% of the whole OSa cases[73]. From a histological perspective, the hallmarks of this form of tumours are dilated blood-filled cavities and high-grade sarcomatous cells on the septa and peripheral rim. On the hit bone is possible to notice the presence of wide zone of transition with extended patterns of bone destruction. Lastly, it is commonly diagnosed in the metaphysis of long bones[74].

Small-cell osteosarcoma. In all cases of OSa, the small-cell type is only the 1-2%. In this specific tumour form, cells are small with round hypochromatic nuclei with polymorphism[75]. Similarly, to the previous cited, also in this case tumour areas are destructed with sclerotic zones, indeed, in contrast with conventional OSa, in this one osteoid production is not an important sign[70].

Low-grade osteosarcoma. This form of tumour is in a middle zone between OSa and precursor of it. Indeed, the symptoms are general and can be confused with other forms of diseases. Although it is likely to be a precursor, if not treated, it could transform in a conventional OSa[76]. Anyway, the number of cases is around 1-2%.

Parosteal osteosarcoma. This tumour form is one of the most common surface OSa with 4-6% of cases. It is a low-grade OSa that arises as the name said from the periosteum. From a histological point of view, the trabeculae of the zone hit are mainly arranged in parallel orientation[70], while from radiography usually shows a densely ossified and lobulated mass with spared cavities[77].

Periosteal osteosarcoma. The structure of this tumour is very similar to the previous one barring lower cases and a matrix mainly made up of cartilage with areas of calcification[70]. The zone between the cortex and the cambium layer is the most likely to be hit from this form of tumour[78].

High-grade surface osteosarcoma. This type of OSa is one of the rarest. A high-grade OSa the local growth is speeded up rather than in other surface tumours. In the bone that contains the mass could be noticed surface lesion at the level of the cortex and endosteum with mineralization. At the same time this form of OSa is more likely to spread in the surrounding soft tissue than others[70].

1.4.5 Diagnosis of osteosarcoma

Osteosarcoma remains one of the most challenging diseases, especially this is due to side effects of the treatment used. This specific tumour growth is usually treated in conventional ways, even so they can have a real impact on patient life both in mental and physical way, indeed, OSa commonly affects young children in the range of 0-14 years and the implications of some treatment are very severe, such as in the worst cases the loss of a limb. At the early stage some symptoms can warn patients and it can help to diagnose it quickly. In accord with the guidelines of the American Cancer Society, the tumours which affect bone usually start with generic pain in the local site of the mass growth, especially in the young patients the most common place are the surrounding area of the knee and the upper arm. At the beginning the pain can be sporadic with worsening during night, the pain could increase with activity and some difficulties in the movement can appear if they involve affected bone. At the same time redness and swelling in the specific location of the tumour can occur, this is more common in the site where bones are near the surface while in other location the selling and redness can be difficult to see. On the other hand, these symptoms are less common in adults in which early diagnosis could be more tough to do. When pain increases and a medical visit is required, different exams could be made to assess the disease state. The majority of diagnostic tests involve different types of imaging, among them it is possible to find:

- **Bone x-ray**. X-ray are used to scan the painful area, especially it is well exploited since it works very well with very dense tissues. It is worth noticing that bone cancer may affect the density of the malignant bone matrix which could help to see differences with the normal tissue. Although useful this test is not enough to establish the presence of the tumour and other confirming tests, such as biopsy, must be done.
- **Magnetic resonance imaging (MRI).** This test uses a different type of source, radio waves. This imaging test using gadolinium as contrast agent is mainly used to acquire more details about the bone mass allowing to understand the behave of tissue, meanwhile with this technique is possible to evaluate the extension of the tumour analysing the marrow inside and soft tissue around the bone. Lastly, MRI is also useful to analysis nearer tissue to spot possible small bone tumours which are spreading.
- **Computed tomography scan.** this technique exploits x-rays taking different pictures with slightly change in the position in order to create a 3d model of the site. CT is mainly used to see cancer in the surrounding tissue of the original hit bone.
- **Positron emission tomography (PET) scan.** this peculiar scan allows to test the entire skeleton by the injection of a radioactive sugar that can interact with tumour cells. A bone scan with this technique can help to recognize if cancer has spread in the other bones or tissues. Usually with this technique metastasis to the lungs and other bones are searched.

- **Biopsy.** Among all the previous, this is the only one that confirm the disease state. Due to the pain this procedure is done with local anaesthesia, and it is taken a small cylinder of bone by a hollow needle, moreover the procedure can also be done in open an open way exposing the bone and cutting a piece of the tumour.

1.4.6 Treatment of osteosarcoma

If the diagnosis is positive to the tumour usually 3 ways are mainly exploited: surgery, chemotherapy and radiation.

- **Surgery.** With this procedure it is tried to remove manually as much as possible of the tumour mass. It has to be done carefully because even a small cancer tissue left could start again to grow and becomes stronger. In this procedure doctors may try saving limb or in the worst scenario amputate the bone. One of the most difficult parts of this treatment is the rehabilitation since the healing process in the case of limb-salvage could lead to different complications and required further surgery in the growth time of the children while in the case of the amputation it required to learn to live without a limb and at the same time during the development of the young men different protests are required. The surgery could also be used for metastasis, even so a deep analysis is required to understand the spreading rate and the extent of the mass to understand the best procedure, or to understand if the tumour cannot be treated with the surgery or at all.
- **Chemotherapy.** this kind of treatments are used together with others since it cannot remove the tumour as itself but can work helping to avoid that cancer coming back after surgery or radiation treatment. In combination with surgery the drugs are delivered before as well as after to slow down the proliferation of cells and have detailed borders to cut as possible. The most common drugs are methotrexate (given in high doses, along with leucovorin to help limit side effects), doxorubicin, cisplatin or carboplatin, and others less common. Chemotherapeutic treatment leads to different side effects, even so it is recognized for having less impact on children that in adults. Among the most common initial side effects are hair loss, nausea, and vomiting, diarrhoea, loss of appetite and mouth sores.
- **Radiation.** In contrast with other tumours, OSa does not response very well against radiation therapy. Indeed, this kind of approach is mainly exploited in the case surgery is not able to remove all the tumour mass in order to remove the remaining cells. Another case in which radiation is used is for pain and swelling treatment and treating cancer that come back. After the classical way, also others have been created with different types of sources. Considering side effects, they have a dependence in the dose delivered. Firstly, among the short-term problems are problems mainly related to the heating from the radiation, therefore skin problems and burns in the local area of treatment or problems at the level of urinary system if the targeted areas are the abdomen and pelvis. On the other hand, other long-term effects that could arise are slow bone growth in children since skeleton is still forming and damage against surrounding organs regarding the location of the tumour. However, the most important problem is that a new cancer can emerge due to the radiation.

2 NANOTHERANOSTIC

2.1 Introduction

2.1.1 Nanomedicines

More than 100 years are passed when a men called Paul Erlich spoke about the idea of "magic bullet" which represents a therapy, a drug, or everything that can be used to heal people, able to specifically target the disease with the higher level of efficacy and with lower, as possible, side effects in the body. Researcher started to embrace the idea and more efforts were focused on nanomedicines. In Figure 8 is possible to look at the history of nanomedicines.

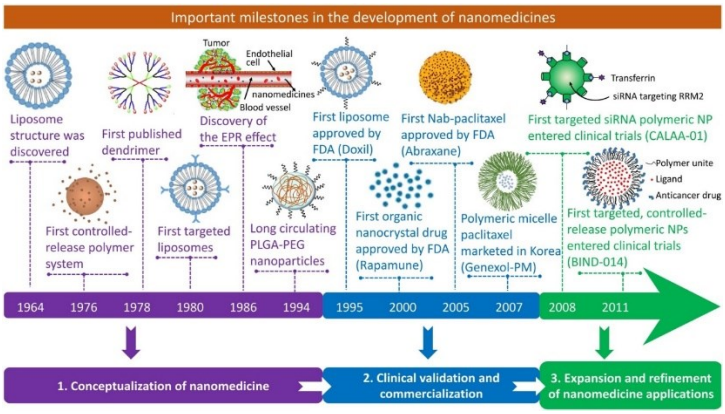

Figure 8 - History of nanomedicines[79]

Due to their scale nanomedicines include several advantages. Before the exploiting of nanomedicines, treatment mainly involved general therapies that microtargeting the organ or the site, after that a lot of different specific treatments for specific tissue or cells arose. The application of nanomedicine in treatment of disease leaded to new approaches never seen before. By the use of this newfound science, it has been and still is possible to select a little group of people, or a specific type of disease, and allow personalized medicine which also helps avoiding side effects. Biomarkers such as specific antigens or receptor are widely studied to find the best way to reach and attack only the specific disease state. This point is strictly related to drugs and anti-disease molecules selection and delivery.

In tumour research, chemotherapeutic molecules are extensively exploited. However, chemotherapeutic agents are extremely toxic for the human body, they can induce apoptosis in cancer cells as well as in normal cells and the border of toxicity between them is strictly related to the concentration of the drug. Many times, in classical therapies different treatment approaches are used, for example cancers are treated with a combination of surgery, radiotherapy, chemotherapy and immunotherapy. On the other hand, nanomedicine formulation can

combine different kind of drugs, for example different chemotherapeutic agents can be mixed with specific drug and the release can be modulate by different stimuli and with different timing. Therefore, nanomedicines are the best candidate to encapsule drugs and therapeutic agents, and they can be designed for specific site delivery to avoid the circulation of the molecules in cells that are not the original target and could undergoing death. For this reason, many times small molecules are employed for aiming to interact with specific and/or overexpressed receptors upon the cells.

2.1.2 Nanotheranostic

The term theranostic was born from the combination of the two words "therapeutics" and "diagnostics". The term represents whatever combine a diagnostic ability and at the same time the ability to treat a specific disease. It was used for the first time by John Funkhouser during personal research about anticoagulant drugs in 2002. During years the theranostic approach was many times joint with nanomedicine approaches, that was mainly to the versatility nanoparticles (NPs) have in their fabrication. Therefore, the "nanotheranostic" term indicates whatever device or formulation which contain both therapeutic and diagnostic agents, with at least one dimension at the nanoscale in accord with the standard of nanomedicines, ISO/TS 80004-1:2015, 2.1.

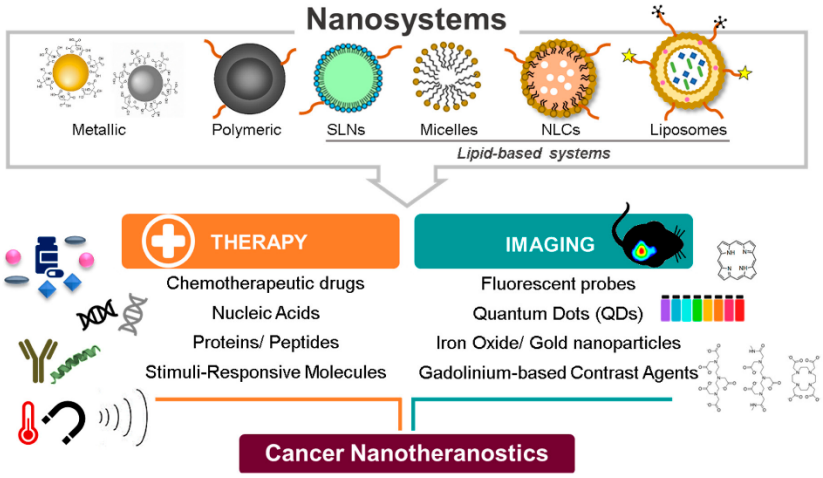

Figure 9 - Different nanotheranostic approaches[80]

In Figure 9 is shown a list of strategies to achieve nanotheranostic in cancer treatment. Each type of nanocarriers could be exploited, as it will be showed in the next paragraphs there are a lot of different materials and strategy to achieve them, to reach the aim to develop a personalized treatment with diagnostic properties the design protocols must be further delved. In particular, the main goal could be to monitor the drug delivery, drug release, and drug efficiency. This usually requires inserting specific molecules that can only be revealed if the drug was released properly, for example in a study researchers use a probe that could evaluate the change in temperature of the iron particles and sequentially control the release[81]. In other cases, the goal could be to reveal the presence of specific kind of cells, for example tumour cells, to assess their presence and their location, even for metastasis around the body which are more difficult to find with classic approaches. Usually,

for detecting the disease location, specific materials are used at nanoscale to give them specific properties, for example gold, and in general metal NPs, are largely used for that aim, or radiomolecules may be added upon or inside the carriers to be detected from outside the body.

2.2 Physiochemical properties of an ideal drug delivery system (DDS)

Nanocarriers, especially NPs, are the perfect example of drug delivery systems (DDS). The main important idea about DDS is to enhance the power of the combination of drugs selected for a specific disease. In particular, NPs are specifically designed to increase the stability, adsorption, and therapeutic action of the specific agents, in order to reach the disease location and release with their specific kinetics each drug. Therefore, the highly functionalization properties allow to target the specific location and maintain the delivery system as good as possible[82].

As one of the best drug delivery systems, NPs must follow and have specific design and physicochemical properties. Among them are sizes, shapes, surface properties. In the Table 1 are summarized the important properties and their overall effect[83].

Physiochemical characteristics	**Influence**	**Parameters**	**Outcomes**
Size	Cellular uptake, elimination, intracellular trafficking, cytotoxicity, tumour penetration, and blood circulation half-time.	<10 nm	Elevation of cellular uptake, but rapid elimination by kidneys. Higher toxicity.
		100-200 nm	Highest cellular uptake and enhanced drug release in cells.
		> 200 nm	They are likely to activate the whole immune system, rapid accumulation and elimination by liver and spleen.
Shape	Cellular uptake, blood circulation, anti-tumour activity, biodistribution, cytotoxicity, functionalization.	Sphere	Easier and faster endocytosis, less toxic than other shapes
		Rod	Slower uptake than spheres.
		Star	High surface area on volume ratio, higher drug loading and encapsulation capacity.
		Fibers	If not degradable, high accumulation and toxicity in lungs, almost impossible to eliminate.

Surface properties	Cellular surface interaction, functionalization, biomimetic properties.	Anionic	lower ability to bind with cell surfaces, smaller rates of endocytic uptake.
		Cationic	Better interaction with cellular surface, but higher harmful effect than anionic NPs due to haemolytic activity.
		Hydrophilic	Lower interaction with cellular components.
		Hydrophobic	Higher interaction with cell due to favoured surface membrane uptake.

Table 1 - Physicochemical properties of nanoparticles

In the table above different tunable properties are shown. It is important to take into account that each disease, in particular tumours, may require different combination of properties to match the requirement of drug and the specific delivery strategy to reach the right biodistribution and tumour uptake. Moreover, it is mandatory to decide the right combination also considering the possible harmful effects of NPs on whole patient body, for this a lot of efforts are still used to improve the parameters shown and to find new ways to increase therapeutic effect and reduce side effects.

2.3 Mechanism of nanoparticles targeting

Nanoparticles have mainly taken interest against cancer for different reasons which allow a better treatment related to their scale. Nanoparticles sizes are comprised between 100-1000 nm, while cells averagely have a size between 1 um – 100 um which means NPs can go through cell membranes and be internalized. This is true especially for cancer cells, and two major strategies can be exploited to reach and penetrate inside tumour masses.

2.3.1 Passive targeting

Passive targeting of NPs means every kind of property that allows the carries to reach and stay into the microenvironment of the tumour without actively acts on compounds or present molecules. Figure 10 schematically summarizes this aspect, especially NPs due to their nanoscale size are more likely to go through the membrane of the tumour and accumulate into it without crossing the endothelium of normal cells[84]. In more details, the vasculature in human body is characterized by different barriers that keep unwanted substances far from cells, in tumours this is not always true. Indeed, to quickly find a supply way, tumour cells develop an unregular vasculature which does not follow the principle of physiological barriers, this growing vasculature in the earlier step shows a lot of lacks called fenestration and an absent short-term order. In

summary this property of cancer is also known as Enhanced permeability and retention effect (EPR). Therefore, it has been demonstrated that NPs with an average of 40 kDa are more likely to penetrate inside tumour and reach the innermost part of it for their size, and due to the high requirement of nutrients, they are less likely to be eliminated[85].

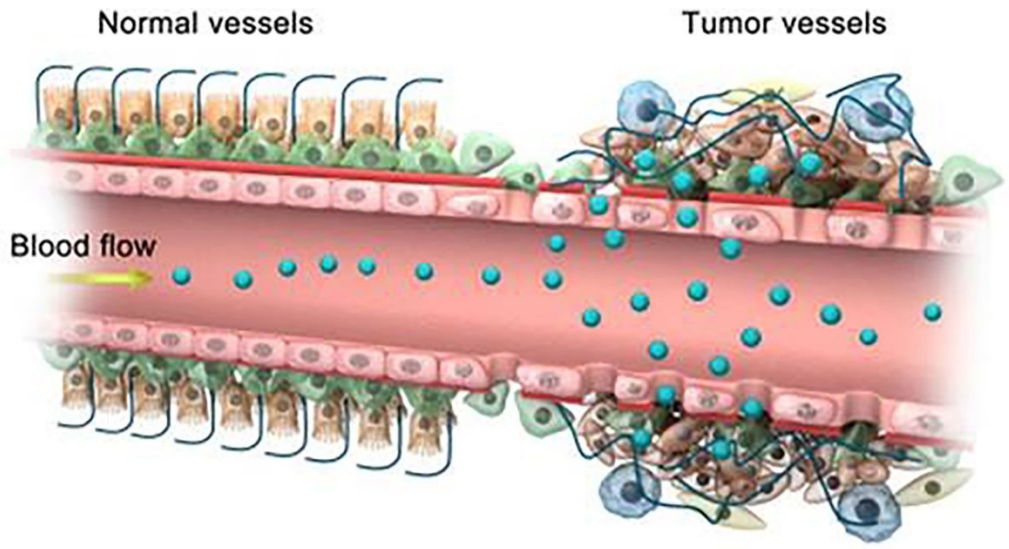

Figure 10 - Schematic illustration of passive targeting and EPR effect[86]

2.3.2 Active targeting

EPR effect and passive targeting in general are not enough to target tumours. This effect has some drawbacks which must be overcome. For example, EPR effect is mainly present in in vivo models such as xenografts which do not mimic all the reality and in patients where the tumour is in the early stage. This effect expires after the mass has established and a better vasculature has been created. Therefore, another way to target tumours must be included.

From Figure 11 can be understood that active targeting involves each kind of strategy that leads to a unique interaction with tumours. In this sense different ligands, such as antibodies, peptides, biomolecules have been exploited during time, especially for their feature to bind almost equivocally some cellular components[87]. Many times, cancer cells overexpress or mutate some types of membrane receptors in order to enhance the communication cell to cell, and environment to cells and thus survive in the body. Therefore, if nanomedicines contain desired ligands specific for tumour receptors, they could actively target tumour binding receptor on cancerous cells surface. For this reason, the use of active targeting is as much promising as the molecules are able to bind tumour avoiding interacting with normal cells and thus avoiding side effects[88].

It is possible to speak about active targeting also in different cases in which the best interaction with tumour is fit by designing specific properties or using specific materials. For example, nanocarriers may need to have a positive charge to interact with the negative charge of cellular membrane and due to use the endosomal escape to release the content inside the cytoplasm of the cell (Figure 11). Or in some therapies it is necessary to release the specific therapeutic agent inside the nucleus and additional genetic material is added. Lastly, in recent years, smart NPs have become established by carrying on molecules sensitive to external changes. This thing helped to reach specific body sites and specific cancerous tissue without a degradation or a retention of the nanoparticle around the body[89].

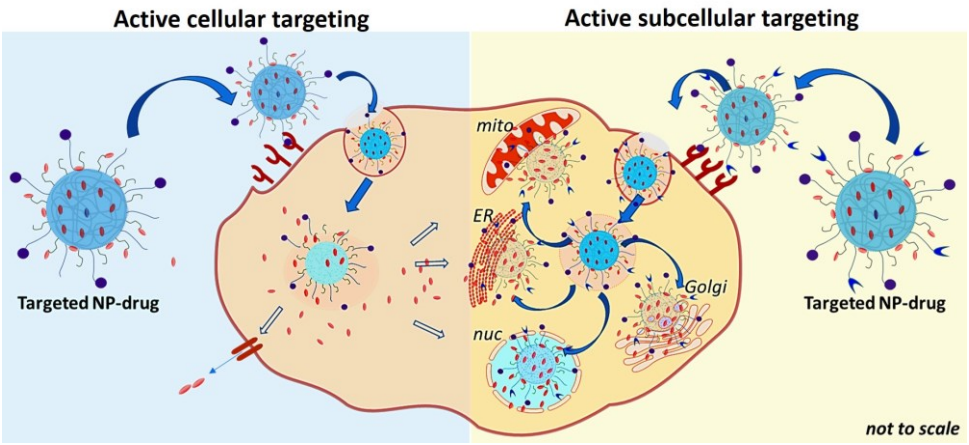

Figure 11 - Schematic illustration of active targeting strategies[90]

2.4 Common type of nanoparticle for treating cancer

Nanotechnologies has taken an important part in medicine and in the treatment process. In particular, the fundamental part of this field are the NPs that have demonstrate a crucial role in the fight against cancer. Nanoparticles are nanostructured carriers which have at least dimension at the nanoscale, considering nanoscale a length lower than 100 nm in accord with the ISO: ISO/TS 80004-1:2015, 2.1. Several materials have been exploited since the idea of nanomedicine was born, therefore NPs are mainly classified by material which makes them up: carbon, metal, metal oxides or other organic matters as well as by their shape: spherical, cylindrical, tubular, conical, hollow core, spiral, or flat.

2.4.1 Organic nanoparticles

The group of materials which makes up these NPs mainly involves lipids, genetic material, polymers and chemical species obtained from carbon chemistry. Starting from these materials different structures can be obtained.

- **Dendrimers.** They are built by strong interaction between chemical or genetic species, usually these involve the combination of single strains of DNA which interact together by the pairing of bases. Their structure is symmetric radially drawing a tree-like arms or branches[91]. They have gained particular interest for their architecture that can be exploited to let structure easily grow or to add desired physicochemical and/or biological properties by the presence of reactive end-groups [92].
- **Micelles.** They are due to the aggregations of species which interact in their hydrophobic part for avoiding interaction with aqueous solutions, while with the external exposure of the hydrophilic part create as much interactions as possible, this is true even in the opposite case with the use of lipophilic solutions. They are solid NPs and are likely to include one type of therapeutic agent dependent on which part is inside and the opposite type in the shell[93].
- **Liposomes.** Even these ones are composed by amphipathic molecules which interact together, except for their capacity to connect two layers and to enclose one of them. The two different compartments could be used to encapsule both hydrophilic and hydrophobic therapeutic agents[94].
- **Polymeric nanoparticles.** Overall, each kind of polymers can be used whether it is natural or synthetic, as long as they maintain biocompatibility and the designed properties. Among all NPs, polymeric ones are the most versatile and adaptable due to the access to the chemical nature of the polymer and the secondary modification of the formed delivery devices. Also, for this class a subdivision exists, nanospheres and nanocapsules[95]. In Table 2 below are reported examples about some formulations used in treating prostate cancer and osteosarcoma.

	Disease	**Material**	**Drugs**	**Targeting**	**Outcomes**	**Ref.**
Liposomes	PCa		Docetaxel, Resveratrol		Minimal toxicity in Pc-3 bearing nude mice	[96]
	OSa		Doxorubicin	Hyaluronic acid	Uptake linking CD44 receptors, reduction of cardiotoxicity and toxicity against cancer cells	[97]
Polymeric NPs	PCa	PEG	Docetaxel	Quercetin, LHRH hormone	In vitro and in vivo demonstrated antitumour activity	[98]
	OSa	PEA	Apatinib		Accumulation in cancer site and induced apoptosis	[99]

Micelles	PCa	PEG, cholesterol, enzyme responsive peptide, targeting ligand (DUPA)	Cabazitaxel		Higher cellular uptake, high drug loading, smart release by cleavage of particles	[100]
	OSa	Amphiphilic alendronate-HA-Octadecanoic acid	Curcumin	Composition, hyaluronic acid (HA)	Micelles adhere to bone due to the composition and curcumin treat cancer cells	[101]
Dendrimers	PCa	PAMAM		PSMA, 64Cu-label	High accumulation in PSMA+ PC3 cells	[102]
	OSa	PEG-PMAN	Zinc phthalocyanine		ROS levels are increased after the irradiation of the photosensitizer	[103]

Table 2 - Examples of organic nanomedicines used in prostate cancer and osteosarcoma treatment.

2.4.2 Inorganic nanoparticles

- **Magnetic/Metallic nanoparticles.** As the name said, these NPs share metallic materials with the ability to interact with an external magnetic field. This kind of particles have gained high interest due to their high index of functionalization, although it is more difficult to insert drugs molecules inside, the surface is most of the times high reactive. This allows to create tailored therapies that in combination with magnetic properties can release drug in a smart and more controlled way, after already guarantee a better follow up[104].
- **Gold nanoparticles.** In contrast with other types of NPs, gold, when its chemical structure is constrained at the nanoscale, can be used for the surface plasmon resonance (SPR). The ability could improve the revelation of the NPs and allow to quickly let them heat. For this reason, this peculiar material has gained high interest as drug delivery system either alone or in combination with other molecules[105].
- **Mesoporous silica nanoparticles.** These NPs are included in the family of ceramic NPs. They contain different pores in the range of 2-50 nm that let them be suitable for loading drugs inside as well as outside. For their material, these NPs are inert and highly stable inside human body and due to this are the best candidate for complex formulations with powerful drugs against a variety of tumours[106]. In Table 3 below are reported examples about some formulations used in treating prostate cancer and osteosarcoma.

	Disease	Material	Drugs	Targeting	Outcomes	Ref.
Magnetic/Metallic NPs	PCA	Bionized nanoferrite		PSMA	Thermotherapy, follow up by MRI	[107]
	OSA	Titanium dioxide		Folic acid	High cancer cells apoptosis, high infiltration in OSA cells, producing of ROS	[108]
Gold NPs	PCA	Gold	Gadolinium	PSMA-targeting ligands	Enhanced uptake, higher MRI contrast, combination with radiotherapy	[109]
	OSA	Gold	Tat peptide and Doxorubicin		100% cytotoxicity compared to non-functionalized NPs	[110]
Mesoporous Silica NPs	PCA	Manganese oxide-mesoporous silica NPs		PSA, PSA fluorescent labelled	Accumulation in prostate cancer, in vivo and in vitro imaging to detect cancer	[111]
	OSA	Mesoporous silica NPs		Concanavalin A	Highly toxicity and targeting of OSA overexpressed glycan	[112]

Table 3 - Examples of inorganic nanomedicines used in prostate cancer and osteosarcoma treatment.

2.5 Calcium phosphate nanoparticles (CaP NPs)

For the thesis projects two kinds of NPs were exploited, calcium phosphate (CaP) NPs and carbon quantum dots. In particular, CaP represented the core and the capsule for the therapeutic agents, meanwhile carbon quantum dots were chosen for their diagnostic properties and for their lower toxicity than original quantum dots.

2.5.1 Introduction

These NPs are included in the inorganic family. As the name said, this kind of NPs are made up by calcium and phosphate. Calcium and phosphate are ions well-known from the body, calcium is involved in a lot of biological pathways such as muscular signalling in skeletal muscles as well as cardiac muscles. In the same time CaP is almost ubiquitous in the body due to its presence in bone, teeth, saliva, and blood, leading to a high biocompatibility and an intrinsic non-toxicity, meanwhile it is one of the most important materials of

bones in the form of hydroxyapatite[113]. It is worth noticing, CaP powders in body could be dissolved inside endosomes or phagosomes after cellular uptake, while they are stable at neutral or basic pH like in the blood, this allows NPs to reach the specific target and makes them very good candidates for the delivery of specific therapeutic agents inside human body[113]. On the other hand, they need a well-done functionalization in order to target specifically the disease and to be internalized inside cells for releasing their uptake. They can incorporate a lot of different drugs or biomolecules both inside and upon the surface, either with physical or covalent bound[114].
So, CaP NPs are promising nanocarriers with several benefits related to their nature, but they required a good design to contain both therapist agents and targeting molecules to avoid the circulation of them around the body without the ability to degrade or with the risk they interact with unwanted site of the body.

2.5.2 Process to build calcium phosphate nanoparticles

In years of study different process to produce CaP NPs are developed. In general, the methods could be wet-chemical precipitation, sol-gel chemistry, flame spray pyrolysis and solid-state reactions[113]. Here there is an in-depth focus on wet-chemical reactions that is the same used in the experiments of this project.

As reported in Figure 12, the wet-chemical reaction uses the property of CaP to be low soluble in neutral and basic water and for that NPs tend to precipitate in easily from supersaturated solutions. For this reason, the CaP NPs manufacturing is one of the most suitable processes to develop loaded nanocarriers due to the use of aqueous and not-aggressive solvents. Moreover, the procedure can be performed at room temperature, and this demonstrates the high compatibility for inserting drugs and biomolecules that require specific conditions to maintain their effects. Furthermore, the molecules can be combined with the materials both in a chemical way or physical one and this allows to design complex formulations and pharmacokinetics.
The production of these NPs follows a straightforward process, although additional steps are taken to enhance the efficiency of the process. For instance, the solution is typically purified to eliminate secondary un-wanted products, and the resulting solution is then left to mature for a period to enable the ongoing growth of CaP particles[115].

Figure 12 - Schematic illustration of wet-chemical precipitation to produce calcium phosphate nanoparticles[116]

Most of the times, the wet precipitation leads aggregates instead of singular particles, this is mainly due to the nucleation that could enclose smaller particles[117]. Indeed, drugs and molecules could be furtherly entrapped during this process and in addition aggregates may increase the release time allowing for a more controlled administration. Moreover, the behaviour cited is also enhanced by the charge of CaP NPs. Usually, these materials combined present a negative charge, even so to increase their stability and maintain them isolated as much as possible, they are usually combined with a cationic polyelectrolyte.

Speaking about the functionalization, CaP NPs have two ways that can be exploited: electrostatic and covalent. The electrostatic way usually involves different multi-layered techniques, especially one or more layers are deposited by the attraction of opposite charged polyelectrolytes. Usually, these NPs are fabricated directly with a net charge that can be exploited to add other layers with different molecules to achieve specific requirements. These molecules could be drugs, DNA, biomolecules which can either be directly a layer or an improvement in the polyelectrolyte solution[118]. Meanwhile the CaP core can be maintained or removed, in the last case an acidic dissolution is possible with the foresight of including cargo molecules into the core[119].

2.5.3 Pathways involved in calcium phosphate internalization

Lastly, it is important to understand the pathway which allow NPs to be internalized inside cells. Two most prominent routes are exploited by CaP NPs: the endocytosis and phagocytosis[120]. In turn endocytosis can be divided into 3 other routes.

- **Clathrin-mediated.** it can occur by receptor-specific or non-specific adsorptive uptake. In the case of receptor-specific uptake, the protein clathrin mediates the process in which a clathrin-rich cavity is formed after the particle recognition, followed by an invagination of the cell membrane. With the help of adaptors and other accessory proteins, the membrane internalization is stabilized[121].

- **Caveolin-mediated.** it usually occurs via caveolae membrane invaginations with a size around 50nm. As soon as the particle is recognized, secondary proteins help with membrane stabilization and vesicle encapsulation. This kind of endocytosis favours a lysosomal escape that prevents degradation[122].
- **Clathrin/caveolae-independent endocytosis.**

After endosomes enter inside cells, they could fuse with lysosomes forming endolysosomes. These cellular organelles can encapsulate NPs before they could be released in cytoplasm. Inside the body of these organelles is present a low pH which is able to dissolve CaP NPs, this is due to the flux of protons allowing the decreasing of the pH and meanwhile the increased osmotic pressure leads to the rupture of the organelles and to the endosomal escape[123]. This effect has an important role in the delivery of cargo molecules into the cytosol, since circulating lysosomes and enzymes could degrade respectively by the low pH and by their nature. After therapeutic agents is released calcium and phosphate ions remain inside cells, even so, under a reasonable level, their presence is irrilevant[120], while with higher concentration could negatively interact with cellular balance and cells underwent apoptosis.[124]

2.6 Nanoparticles in molecular imaging

2.6.1 Quantum dot/carbon dots

These dots are the results of trying to assemble semiconductor at the nanoscale. At nanoscale as well as at the micro scale different shapes can be considered, in the case of quantum dots they are categorized as zero-dimensional and relatively to the bulk form the number of electrons is limited resulting in discrete quantized energies[125]. As the name says these nanocrystals exhibit specific features enabled for their tiny diameter, and this allows them to have quantum size effects in their optical and electronic properties[126]. In particular, changing the diameter and the material of dots is possible tuning the photoluminescence, with narrow emission and photochemical stability, even a core-shell structure is achievable in order to obtain the perfect quantum dot for each field[127]. In more details quantum dots are closer to the atomic level rather than the bulk structure, this is due to the range of 100-1000 atoms which makes them up and this allows them to have distinct narrows peaks very similar to the ones from isolated atoms[128].
It is easy now to understand why quantum dots have acquired a huge interest during time, but how they can show this behaviour needs to be declared. The tiny size of these dots allows to figure out two different related properties:

- **The quantum confinement effects.** It is due to the energy level spacing of a nanocrystal which can exceed the constraint of the Boltzmann constant allowing electrons and holes to move in the crystal. This mobility is strictly related to the size since it can tune the energy gap between states and for that shift the emission spectra[129]. The shift of the spectra can be explained figuring that smaller dots have less atoms which can stand further apart, since this happens the energy gap is bigger due to more energy requirement to let

electrons to move from bands, the consequence is to have quantum dots with an emission spectrum toward blue. In contrast bigger dots have more atoms which are more confined, and the low distance allows to have a smaller energy gap with an emission spectrum toward red. This important feature is also due to the more quantity of states with small gap in big dots.

- **Electronic states.** In structures with a low quantity of atoms discrete and well separated energy states could be observed, in this way each energy level exhibits a function that is more atomic-like and due to this atomic-like sharp emission peaks are possible.[129]

Quantum dots are very promising in fields which require the emission from a source that can be dispersed or bound at the nanoscale. It easy to understand why they has been exploited in biomedical field as diagnostic probe. The high photosensitivity and narrow emission spectra make them a perfect candidate for bioimaging, diagnostics, and biosensing application. An example of exploiting could be the fibrous phosphorous quantum dot to fluorescently label for human adenocarcinoma bioimaging[130]. Quantum dots have expressed since now several benefits in biomedical imaging and have leaded to specific functionalization to give a diagnostic property upon NPs surface, this helped in diagnostic, in following the uptake of formulation inside cells, moreover thanks to the narrow emission more quantum dots could be followed to value different pathways at the same time. Unfortunately, quantum dots as semiconductor at the nanoscale bring with them some limitation, as well they were considered so promising as different studies tried attesting their cytocompatibility and level of toxicity. Some of the latest papers about the topic demonstrated some limitations, one in particular listed[131]: the bioconjugation of quantum dots cause difficult delivery in target cell, aggregation of quantum dots can kill live cell, some material used for preparation of quantum dots leads to cytotoxicity, metabolism and excretion of quantum dots which leads to toxicity in body remain still not clear, the need of a coating of the core material with shell leads to poor control over size, the blinking property and surface of quantum dots cause their deterioration[131]. On other papers the toxicity of quantum dots due to the release of metal ions were tested on different organs, organs tested were liver, lung, kidney, brain, and some dysfunctions at the level of the immune system[132]. These aspects have required constraints on the use of quantum dots for in vivo tests.

2.6.2 Carbon quantum dots

In the years, several efforts have been dedicated to overcoming the disadvantages and limitation in the use of quantum dots in medicine. Carbon-base nanostructures bring with them the major features in confront of quantum dots. They exhibit abundant photoluminescence and photochemical properties. In the case one of these nanostructures has a size lower than 10 nm and a spherical shape, it is likely considerable a carbon quantum dot. The C-Dots, as carbon-based fluorescent NPs, can be roughly divided into several sub-groups, such as graphene dots, graphite dots, amorphous carbon dots, polymer-like dots, and so on[133]. Nowadays the process for obtaining them has been refined and C-dots are produced in definite chemical structures and controller morphologies, such as polymer-carbonized dots, chiral C-dots, triangular C-dots and crystalline C3N

C-dots[133]. Therefore, there are some motives for the exploiting of carbon structures as quantum dots, such as tunable PL, dispersibility, but other properties are present by the nature of the carbon material and these are low toxicity, biocompatibility, biodegradation, wide source of raw materials and low cost[134]. Moreover, it has been established that C-dots grew in interest by research for the abundant cheap raw materials, facile synthetic methods, and feasibility of large-scale fabrication[133].

2.6.3 Fabrication of carbon dots

Carbon dots have two ways to be fabricated: top-down and bottom-up using carbon materials and organic ones[133]. The good point of these nanocrystals is that they can be obtained from organic wastes, from sources as carbohydrates, organic acids, and polymers.

Top-down. The techniques start from carbon in bulk forms to consecutively cut them in smaller structures until reaching the scale of carbon dots. Among all the methods, the electrochemical technique represents the simplest one, also due to the presence of available appropriate equipment and for a wide range of starting raw materials. In this reaction a voltage is applied to a carbon electrode leading to an electrochemical exfoliating of the one, as electrode structures of graphite are commonly inserted in a bath of electrolytes to capture and react unwanted atoms. Overall, the other techniques use different strategies to obtain at the end carbon dots with a different cutting method[135].

Bottom-up. In this case small molecules are used to make up carbon dots from a wide range of materials starting from organic wastes and carbon polymers precursor. For this reason, in the green economy this has drawn attention to obtain the maximal yield with low-cost materials. The different processes have in common to heat with different sources the original materials and use the new products to assemble carbon dots. In the development of these methods, pyrolysis acquired more interest than other combustions due to milder working conditions. On the other hand, hydrothermal synthesis has been the most indagate as an economic, convenient, environment-friendly method[135].

2.6.4 Carbon dots from organic wastes

The previous chapter indagates why carbon dots are so promising and that they can be synthesized from different raw materials. In these lines it is explained why biomasses meet the requirements for being a valid source for carbon dots. As the European Directive 2009/28/CE,2009 cites the umbrella-term of biomass refers to the biodegradable fraction of products, wastes, and residues of biological origin from agriculture, forestry and related industries, the quantity of raw materials is huge, in this class of materials also algae keep parts. Algae family presents a very promising biomaterial its composition and worldwide diffusions. On the other hand, algae pollution is a problem that still need to be solved and a common way is to remove the plant from contaminated water and destroy them. However, biomasses from algae store a high energy and material content

and can be exploited to extract, for example, alginic acid, antioxidants and material convertible in carbon dots. Different studies have tried to convert algae biomass in bio-oil from which it is possible to extract several other secondary products.

Hydrothermal liquefaction (HTL). This technique exploits the high energy content of algae that can be converted into bio-oil, researcher agree to the fact that algae for their nature can store alternative energy through the photosynthesis[136]. Hydrothermal liquefaction can be effectively exploited to convert algal biomass into crude oil, usually a discrete quantity of nitrogen may be found after this technique, thus if from a point of view this quantity could be removed, for another nitrogen removal is time-consuming and labour-intensive[137]. This content of nitrogen if it is too high could limit the usage of the biocrude. However, it provides an excellent environment to prepare nitrogen-doped carbon dots, and this could have effect on reducing the pollution of algal blooms. The most important benefits of the HTL are related to the possibility of using directly wet biomass and converting it into a liquid biocrude oil even without a catalyst, carrying out the reaction in a closed reactor at 200-350 °C and 5-15 MPa, avoiding expensive drying processes to remove excess of moisture. After the achievement of the bio-oil studies have demonstrated the ability of the Maillard reaction to use the nitrogen bio-oil and obtain finally carbon dots.

Pyrolysis. This thermo-chemical conversion takes place at mild temperatures in an inert atmosphere without use of a catalyst, thus being faster and simpler than the process to produce biodiesel from algae. Pyrolysis decom-poses organic structures to various vapor phases and gas compounds, leaving a carbon-rich solid residue. The vapor phase compounds are condensed into liquid (bio-oil) downstream of the process. It uses high temperature in plain atmosphere without volatile molecules and atoms. This is a promising technique which can convert algal biomass into biofuel. This kind of products are named biochar and it contains a discrete quantity of activation energy and meanwhile a lot of aromatic hydrocarbons groups and many minerals. In some studies, researchers reported that fast pyrolysis presents high-yield and high purity conversion with a total or partial absence of oxygen[138], even so pyrolysis may result in the loss of functional groups initially present in biochar, including oxygen and nitrogen-containing functional groups[139]. On the other hand, that as well faster heating rates at a temperature of about 500°C maximize the yield of bio-oil as slower heating rates favour the formation of char [140].

3 LAYER-BY-LAYER (LbL)

3.1 Introduction

Layer-by-layer is an umbrella term to group all the techniques that start from a template and one-by-one deposit layers on them. These techniques are used with different aims. At a macroscale they are used for example as optimized way to paint large surfaces. However, these techniques owe their fame at medical field. Indeed, LbL is nowadays largely used to design novel therapies or to optimize classical one. Major times in biomedical field, the devices must interact with body, although for specific requirement it is not always possible to use different type of bulk materials and at the same time put them in contact with body cells. Layer-by-layer was born as a technique to overcome these limitations, its versatility allows to start from a wide range of material and cover them to give specific properties at the surfaces in contact with the body. On the other hand, with different development in the years, the shape of the template become not anymore only planar, but also spherical.

In the specific field of nanomedicines, these group of techniques have allowed to lead more complex the design of the latter and at the same time split the process, by focusing with the specific combination of drug and materials during template development, and whether necessary, adding layers in a second time to hit the requirements for the initial target. A further development of the technique was achieved by inserting the molecules of interest directly inside the newformed layer or upon them. This allowed to develop more specialized formulation and at the same time managing in a more precise way the different releasing or interaction. For example, in an ideal formulation produced using LbL, the outermost layers could graft by the desired molecules designed to interact with cells or the layers themselves could be done by bioactive materials that induce a positive response inside the body. At the same time the deepest layers could encapsulate one or more drugs and the depth in which they are inserted also lead their releasing profile.

From these considerations is possible to understand how LbL has become a fundamental designing step in the overall process of a new formulation fabrication, if not one of the most important, because it allow to control a lot of desired parameters to lead the pharmacokinetics and pharmacodynamic. Lastly, speaking from a theranostic point of view, the deposition of layers containing or attaching molecules easily allow to manage the combination of the therapeutic part and the diagnostic part by inserting both of them into the same fabrication, mostly in different layers.

3.2 How it works

As seen in the previous paragraph, the LbL technique is included in a group of techniques which have been exploited in years to change the chemistry and biological nature of groups present upon surface. Overall, this technique is an electrostatic assembly exploited to cover different types of surfaces using different

polyelectrolytes with opposite charges. It is a versatile strategy to change the superficial properties of plane surfaces as well as rounded ones without affecting the chemical composition of the material beneath which may change the bulk properties originally desired.
In the Figure 13 is shown how the process to deposit layers works. Focusing on the process (Figure 13.a), the assembly is made by iteratively dipping the initial material inside the solution of opposite charge polyelectrolytes. In more details, the process is schematized in this way: firstly, the substrate is dipped in the first solution, by moving the surface it possible to increment the percentage of covering, secondly the substrate is immersed in the washing solution one or more times, then the procedure starts again changing the polyelectrolyte solution in which the neo-covered substrate is going to be dipped.

In Figure 13.a is showed the ideal procedure for LbL, in years different procedure have been developed, but they are more discussed in the next chapters (3.5). In Figure 13.b is shown the scheme of layers growth, especially the major requirement is revealed, indeed this group of techniques share the mandatory presence of an initial charge on the substrates which behave as first point of attachment.

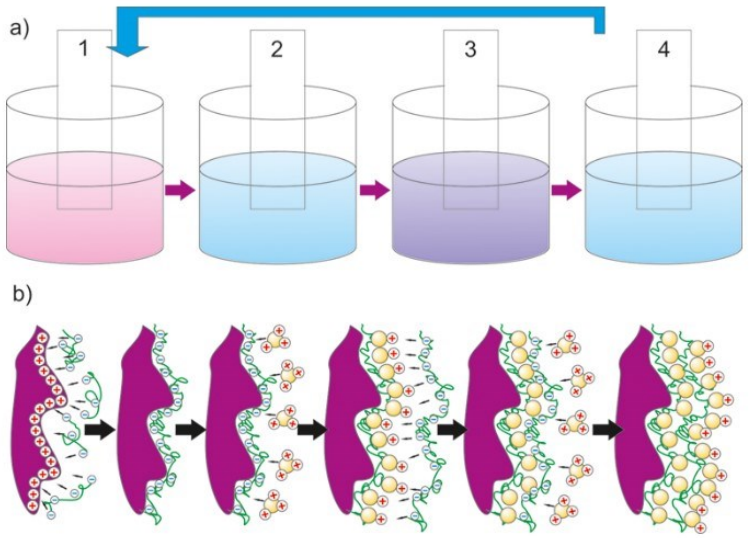

Figure 13 - Scheme of layer-by-layer assembly.
a) Deeping procedure for layers deposition. b) Illustration about deposition of opposite charged polyelectrolytes[141]

3.3 Layer-by-layer characteristics

3.3.1 Advantages

This technique does not affect the property of the material due to the exploiting of only secondary electrostatic bonds instead of covalent bonds. At the same time the range of materials as polyelectrolytes is huge since several molecules own either positive or negative charges, especially biomolecules like proteins, DNA or RNA strands own charges in specific conditions. Considering the conditions, for the technique as itself no specific

conditions are required in term of pH, temperature, pressure, and energy, meanwhile this allows to set the specific requirements of pH and temperature to use biomolecules which usually stay better at room temperature or 37° and under specific pH values to better mimic natural folding state for protein or either double or single strands for DNA and RNA. Layer by layer does not require the use of specific solvent, it lets this approach to be a green technique since many times the solvent is water both for the assembly and the washing steps. Layer-by-layer approach could be used to design a multi-layer covering since different polyelectrolytes could be used together, and in particular that give access to specific formulation in which different layer can be functionalized in different ways to encapsulate other agents. In particular, this specific functionalization allows to insert in layers different agents such as therapeutic agents, probes, targeting molecules allowing to acquire the best formulation for a specific disease, especially these agents can be encapsulated in different ways if it were covalent or secondary bonds in order to modulate the release or the adhesion on the specific carriers. At the end this technique is very promising since it possible with that to coat any type of materials, any type of shape, any type of size.

3.3.2 Disadvantages

As mentioned before this technique is largely versatile, although there are few requirements not too difficult to satisfy. Firstly, the initial surface must be opposite charged to the first polyelectrolyte since it has to have an initial electrostatic bond with something attached on the surface. Another thing related to biomolecules is that in soe case the pH must be fixed at specific level in order to let bio-polyelectrolytes to have a specific charge and the pH should be remained the same along the process to avoid ruptures. If the technique is not followed from an automatic machine the process is time-consuming and up to hours could be required to produce on layer, this is due to the requirement to add for each layer some washing step in order to remove all the polyelectrolyte remaining which have not interacted with the surface, avoiding free interaction in the solution with the new polyelectrolyte.

3.4 Parameters

For this specific technique there are some parameters to fit in the best way in the initial design, especially there are some solution and template parameters. The following list of parameters is taken by an in-depth review paper[142], especially the list that is going to be analysed comprises physico-chemical properties of the template, concentration of polyelectrolyte solutions, nature of building blocks, methodological aspects, solvent polarity, pH, temperature.

Physico-chemical properties of the template. The template has an importance mainly related to its surface properties, especially chemical features like hydrophilicity/phobicity characteristics of the substrate surface, chemical nature and density of the different charged group exposed outside, together with physical properties

as roughness, porosity and the presence of impurities are all the important details for this technique[143]. All of those can lead the LbL process in a stable and homogenic covering or unstable and heterogenic one[144].

Concentration of the solutions of polyelectrolytes. The deposition of layer relay on the concentration of polyelectrolyte inside the depositing solution. The concentration must exceed a minimum to guarantee the deposition of stable layers and the charge inversion required for the next deposition[145]. That minimum mainly depends on the solubility and charge density. The concentrations and their impacts on the process follow a bimodal trend with a minimum cited before, but also a maximum threshold over of the increase of polyelectrolytes does not affect anymore the layer growth. Until that point the thickness per bilayer increase linearly with the concentration[142]. In a study researchers demonstrate that above the threshold value layers are able to form, even so in non-linear trend[146].

Nature of the building blocks

- **Chemistry.** As the chemical composition of template, even the chemical composition of polyelectrolytes plays a role in the formation of layer. Hydrophilic/hydrophobic characteristics can influence the interaction between polyelectrolytes of the same nature and the swelling degree of the layers, especially hydrophobicity of polyelectrolytes increases the thickness of the covering[147]. Lastly, also the flexibility of the polymers can affect the final result, modifying the conformation of the layers.
- **Charge density.** Also, in this case it is thought to be present a minimum threshold. If the charge density is too low, the layer could be to weak and unstable, moreover inside the solution of the opposite layer it would be unable to stay attached to the surface and keep the new polyelectrolyte, instead it would be release forming a secondary complex[148]. Although the charge density is a fundamental parameter to take into account, the minimum threshold does not depend only on the specific molecules, but it can be shifted by adding salt inside the polyelectrolyte solution, then this strategy also improves the hydrophobic interactions.
- **Molecular weight.** It is possible to understand the influence of the molecular weight thinking about heavy and light powders inside a solution, obviously a heavier particle is more about to fall at the bottom. In the same way low molecular weight polyelectrolytes (around 10^3 Da) cannot stay well attached on the surfaces and easily can strip off upon them, affecting the overall layers growth. On the other hand, heavier polyelectrolytes are known to assemble in a better way, avoiding at the same time process off adsorption-desorption that could happen with smaller molecules in favour of bigger ones[149].

Methodological aspects

- **Contact time.** To understand the influence of the dipping time the parameter used is the diffusion of chemical species. The contact time is inversely proportional to lamellar structure organization. Indeed, shorter contact time allows to quickly stop the interdiffusion of the polyelectrolytes upon the surface and it guarantee a certain degree of lamellar structure[150].

- **Rinsing.** This step it is the more important the more optimization it is desired to achieve. Usually, after the exposure of the substrate, together with the attached molecules could remain others with a lower electrostatic attraction which remain on the surface until the substrate is removed and inserted into a second solution. Therefore, when the substrate is dipped in the opposite charge solution, two event could happen. Firstly, the new polyelectrolytes interact with a weak layer that is more likely to detach from the surface, secondly the formation of secondary complexes lead to have less molecules to cover the surface due to their occupation in such complexes which, at last, could also ruin the surface of substrate precipitating upon that[151].
- **Drying.** Overall, the LbL technique is a wet methodology, therefore drying or not the substrate with the new layers can affect their hydration and swelling index and thus affect their structural organization. In some studies researcher wrote that is almost mandatory a drying step for guaranteeing a right growth of the multilayers covering[152].

Solvent polarity. Overall, the solutions used for LbL commonly are aqueous. This carries several advantages, with low toxicity as the best one. On the other hand, the use of organic solvents is not prohibited, and indeed they are used to decrease the role of electrostatic interactions leaving space to other ones, for example dispersion forces and hydrogen bonds[153]. It is worth noting that it is possible also combine water solution with organic ones, especially the addition of ethanol reduces the solubility of polyelectrolyte resulting in an enhanced deposition[154].

Ionic strength. The ionic strength has a direct involvement in the complexation between the polyelectrolytes with different charges[155]. As the concentration, even the ionic strength has a maximum threshold over of the thickness is not modified, and it is due to the screening of the overall charge which limits the adsorption[156]. At the same time the structure of the multilayers could be modified by the swelling degree and their hydration, due to the ion effects to order or disorder the water around the molecules[157].

pH. pH has an important role during the LbL both at chemical and biochemical level. Firstly, pH affects the ionization degree of the molecules, and reducing the ionization it is possible to reduce the polyelectrolyte solubility increasing the ability of polyelectrolyte to deposit in more stable and homogenic way upon the substrate[158]. Secondly, at a biochemical level when biomolecules are used the pH has the role to lead the overall charge, this is mainly due to the presence of both carboxyl and amino group. With this molecule the thickness of the layers is affected by the pH which can increase, reduce, or invert the charge of the bio-polyelectrolytes exploited[158].

Temperature. Temperature has taken interest in its influence on the solubility of polyelectrolytes, especially the tuning of temperature is important to lead the growth to a non-linear way as well as a linear one affecting the interdiffusion of chains in similar way to contact time[159].

3.5 Layer-by-layer approaches

This group of techniques uses sequential immersion in different bath containing specific solutions in order to form the nanolayer upon the surface. These techniques are characterized by the sequential deposition of opposite charge polyelectrolytes with the requirement to always add a rinsing step to avoid the cross-interaction of opposite charge molecules.

During years, the LbL approach underwent different improvements. It started as laboratory method via manual dipping of the substrate until the achievement of more complex strategies such as the exploiting of automatic methods or microfluidic chamber for adapting to the specific requirements.

Manually. This specific method, as its name suggests, involves manual immersion in various solutions. This process can be executed on both flat surfaces and particulate substrates, although the latter requires some additional steps[160]. In the case of flat substrates (Figure 14.a), it entails immersing them in a polyelectrolyte solution followed by a washing solution, making it more efficient and quicker than the process for particulate substrates. The growth of the film can be controlled by adjusting parameters such as salt concentration, pH of the deposition solution, concentration of the layering material, immersion time, and washing conditions (3.4). In addition, the process can be further influenced by introducing a stirring and mixing step allowing to form a better covering or carefully control the thickness growth[161].

When working with particulate substrates, additional steps beyond simple immersion and washing are required (Figure 14.b). Typically, between deposition and rinsing steps NPs must be collected using centrifugation[162]. However, when scaling up LbL techniques for industrial applications, challenges arise mainly due to the tendency of particles to aggregate during centrifugation and the complexity of automating this procedure[163]. In laboratory settings, strategies such as employing sonication after centrifugation when the polymer becomes oversaturated or meticulously adding the precise amount of saturating polymer are implemented to ensure the firm attachment of all molecules to the substrate[164].

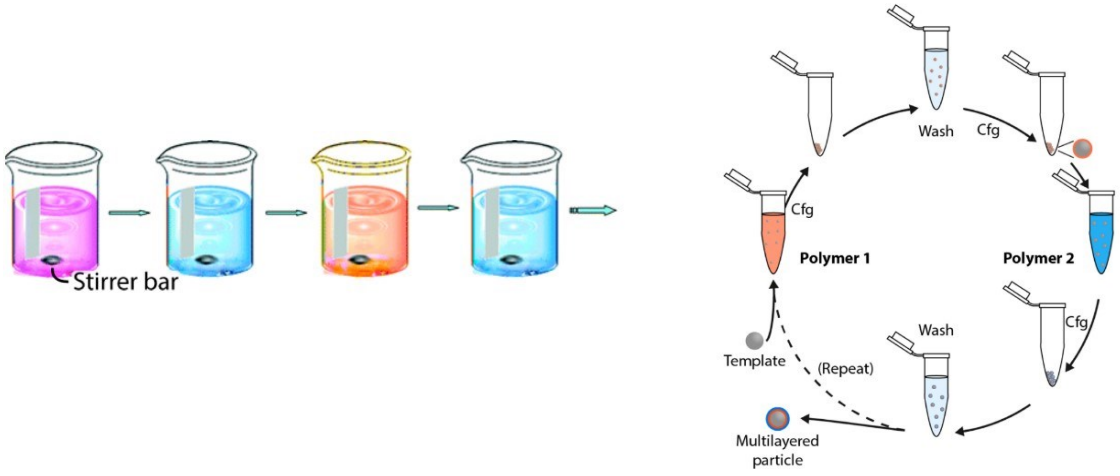

Figure 14 - Procedures to manually cover planar surfaces[179] (left) and spherical surfaces[161] (right)

Automated. This approach uses the same steps seen in the previous paragraph, but with the exploiting of automatic controls and arms to manage the solutions and substrates. In particular, some automated controls are used with the aim to know the exact time to wait after changing solution, but also to try optimizing the process. One of the most interesting and promising ways to control the process is the QCM method in which a specifically designed crystal allows to regulate the layering process by analysing the mass adsorbed[165]. On the other hand, among commercial devices, the most commons are the ones that check only the time to change solutions without any type of feedback control. Regarding nonplanar substrates, the achievement of automatic control is more difficult to reach. Until now it has only been possible to cover large particulates with diameter bigger than 100 µm (Figure 15)[166], while other approaches try to aggregate on a planar substrate the particles using for all intents and purposes the procedure seen before[167]. On of the last promising device developed is a microfluidic device specifically invented for spherical substrates. The original idea was to insert in the same microfluidic channel all the solutions required for the covering and then to let particles bouncing between the wells and thus entering in contact sequentially with the opposite charged solutions passing through the middle rinsing solvent (Figure 15)[168].

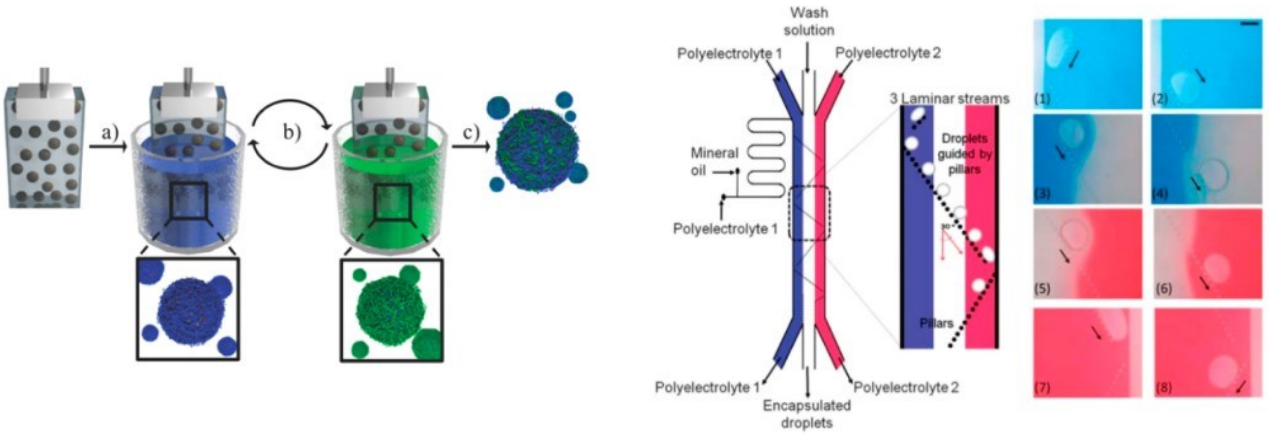

Figure 15 - Procedures to cover nanoparticles by exploiting the planar surface aggregator[167] (left) and a microfluidic device[168] (right)

4 AIM AND OBJECTIVES

Aim: The aim of the project is to propose and conceptually validate a novel theranostic formulation of nanocarriers in particle shape functionalized by different layers for the treatment and imaging of Prostate cancer (PCa) and Osteosarcoma (OSa). All the systema are characterized by an internal calcium phosphate (CaP) core covered by natural polyelectrolytes exploiting the layer-by-layer (LbL) assembly process. This technique allows to insert inside layers therapeutic agents, especially docetaxel (DTX) and enzalutamide (ENZ) or doxorubicin (DOXO), anti-inflammatory agent like resveratrol (RESV), active targeting molecules as PSMA-617 and hyaluronic acid (HA), and imaging probes exploiting carbon quantum dots (CQD). Therefore, the process had as target to produce and validate the specific group of therapies for the diseases with a controlled releasing of drugs in a designed time interval, the following objectives have been followed to design the pipeline and fulfil the thesis initial aim.

- **Objective 1:** to develop and optimise nanotheranostic systems with cores make up of CaP containing DOXO or RESV or being empty and to produce them via a pumping method stabilizing the compounds by PAH deposition.
- **Objective 2:** to exploit the LbL technique to coat the CaP cores with different molecules, using chitosan (CHI) and alginic acid (ALG) as polyelectrolytes, and inserting drugs to create a drug delivery system to specifically target PCa and OSa.
- **Objective 3:** to insert imaging probes to follow-up the nanoparticles (NPs) and allowing to diagnose the diseases through the internalization of them inside cells and fulfil the nanotheranostic initial aim.
- **Objective 4:** to conjugate agents such as hyaluronic acid and PSMA-617 to the outer layer of the system to promote active tumour targeting.
- **Objective 5**: to characterize NPs produced in their different formulations through chemical-physical and morphological analysis, with a focus on the layers ability to encapsulate and release drugs and anti-inflammatory agent as well as to emit fluorescence by CQDs.
- **Objective 6**: to assess the efficacy of the proposed treatment and the uptake of NPs by cancer cells, especially for this point different NPs were tested for cytotoxicity on prostatic cancer cells (LNCaP, Vcap) and OSa cells (SAOS, U2OS).

5 EXPERIMENTAL SECTION

5.1 Materials

In order to produce and cover calcium phosphate, the following materials have been exploited as main and auxiliary compounds. Calcium l-lactate hydrate (Mw = 218.22 Da, 21185), Dibasic ammonium phosphate (Mw = 132.06 Da, 09842), Doxorubicin hydrochloride (Mw = 579.99, PHR1789), Dulbecco's phosphate buffered saline(PBS, D8537), Dulbecco's modified eagle medium, high glucose(D5796), Dimethyl sulfoxide(DMSO, 276855), Chitosan (low molecular weight (around 150kDa), 448869), Alginic acid from brown algae (240kDa, A7003), Dialysis tubing cellulose membrane (D9527), Methyl cellulose (M0512), RPMI-1640 with L-Glutamine and Sodium bicarbonate (R8758) and Sodium chloride (S9888), Graphene quantum dots (900708) were bought from Sigma-Aldrich. Docetaxel (Mw = 807.879,BID2710), Resveratrol (Mw = 228.24 Da, BIK9013) were bought from Apollo Scientific. Dulbecco's Modified Eagle Medium, high glucose (DMEM-12-A) was also bought from Capricorn Scientific. Enzalutamide (Mw = 464.44 Da, MDV3100) was bought from Apexbio. Ethanol, absolute, 99.8% (E/0650DF/17) was bought from Fisher Scientific. Polyallylamine hydrochloride (PAH, Mw = 17 kDa 43092) was bought from Alfa Aesar. Hyaluronic acid (Mw > 500 kDa j66993.03) was bought from Thermos scientific. The PrestoBlue Cell Viability Reagent (A13261) and ReadyProbes Cell Viability Imaging Kit (Blue/Green R37609) was bought from Invitrogen. The Vipivotide tetraxetan (PSMA-617) (Mw=1042.14 Da), was purchased from MedChemExpress (MCE). Other materials used included Hydrochloric acid (HCl) (reagent grade 37%), (Sigma-Aldrich, UK), Sodium acetate (Mw=82.03 Da) and Glacial Acetic Acid (100%) (Mw=60.05 Da), deionized water (dH2O).

5.2 Methods

5.2.1 Synthesis of the core and the first charged layer

To fabricate the core of NPs, the methodology described by Urch et al. (2009)[169] and Elizarova et al. (2016)[170] were used with some modifications and the process is summarized in Figure 16. Four different formulations are prepared to test CaP NPs in treating both PCa and OSa. Main differences between formulations are the therapeutic agents encapsulated inside cores and the number of layers deposited with the LbL assembly. Moreover, in some formulations, RESV is inserted with the aim to give anti-inflammatory activity against the microenvironment of the tumour.

At the beginning, different 40 mL solutions of deionised water with calcium L-lactate (24mM, pH 10), dibasic ammonium phosphate (15mM, pH 10) are prepared separately, which will result in the formation of CaP nanocores, then others 40 mL solutions of deionised water with PAH polyelectrolyte (1 mg/ml, pH 10) are prepared for covering neo forming CaP cores. All the solutions are mixed on the stirrer at 1 g L^{-1} and conducted under ambient conditions.

For prostate cancer

For PCa the elicited type of drug is the DTX, the original protocol needed more modifications. Docetaxel could not be encapsulated inside CaP NPs for his strong lipophilic nature. However, formulations with and without antioxidant are tested. The PCa nanocores are produced with an empty capsule or containing RESV. For achieving this, an 88mM solution of RESV is prepared and tested for encapsulation in one of the two solutions of dibasic ammonium phosphate which have been prepared. The stock solution of RESV is prepared by dissolving it in DMSO, then, after homogenising on the stirrer, 134 μL of the solution is added into the respective solution of 40 mL dibasic ammonium phosphate.

The next step involves a P-3 peristaltic pump (Pharmacia Fine Chemicals). For each run all three different solutions of calcium l-lactate, dibasic ammonium phosphate and PAH are pumped with a flow rate of 10 mL/min through 3 different individual channels (comprised of silicon pipes) with different lengths, but with the same diameter of 3 mm. First, a 10-cm-long tube allows interaction between the calcium L-lactate and the dibasic ammonium phosphate solutions, forming CaP NPs encapsulating DTX or nothing. Then a second 100-cm-long tube allows adsorption of the PAH polyelectrolyte upon the surface of NPs.

For osteosarcoma

In the specific core designed for OSa the aim was to try increasing the amount of DOXO encapsulated. For doing this, a 10mM DOXO solution is prepared to test the encapsulation of 3 different volumes of DOXO in the nanoparticle cores. The stock solution of DOXO is dissolved in PBS:DMSO 1:1 and respectively 135, 270, 405 μL of the latter are added into 3 respective solutions of 40 mL dibasic ammonium phosphate. Thereafter, the three solutions are again mixed on the stirrer to homogenise the DOXO inside the solvent.

The next step involves a P-3 peristaltic pump (Pharmacia Fine Chemicals). For each run all three different solutions of calcium l-lactate, dibasic ammonium phosphate and PAH are pumped with a flow rate of 10 mL/min through 3 different individual channels (comprised of silicon pipes) with different lengths, but with the same diameter of 3 mm. First, a 10-cm-long tube allows interaction between the calcium L-lactate and the dibasic ammonium phosphate solutions, forming CaP NPs encapsulating DOXO. Then a second 100-cm-long tube allows adsorption of the PAH polyelectrolyte upon the surface of NPs.

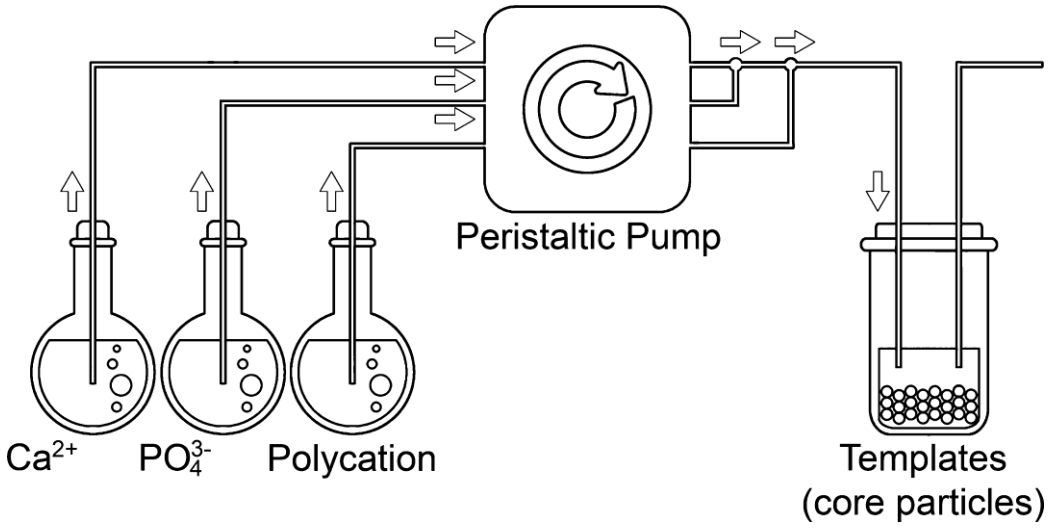

Figure 16 - Schematic illustration of the process to produce nanocores[170]

For each formulation, CaP NPs are collected in different beakers without filtering. The beakers with NPs are kept in stirring for 24 hours at 1-1.5 g L^{-1}. After that to dialyse solutions, the different batches are put in cellulose dialysis membranes stored inside a distilled water bath for 12 hours. When the solutions are ready to be collected, they are transferred into conical falcon tubes (of 50 mL or 15mL) and centrifuged at a speed of 4400 rpm for 20 mins in a Centrifuge 5702 (Eppendorf, Fisher scientific). After centrifugation, the supernatants are removed and the falcon tubes, containing NPs, are stored inside an incubator to fully dry the content for accurate weighing. The NPs are thus freeze-dried at 4 °C.

Therefore, after this step and its chemical and physical analysis only CaP core with 405 µL of DOXO, with 134 µL of RESV and empty are kept into account for the sequential process (Fig.17). From this moment on, the cores with different molecules inside are further processed by the LbL technique, so other samples have to prepared in the same way keeping always a multiply of 40mL for future experiments.

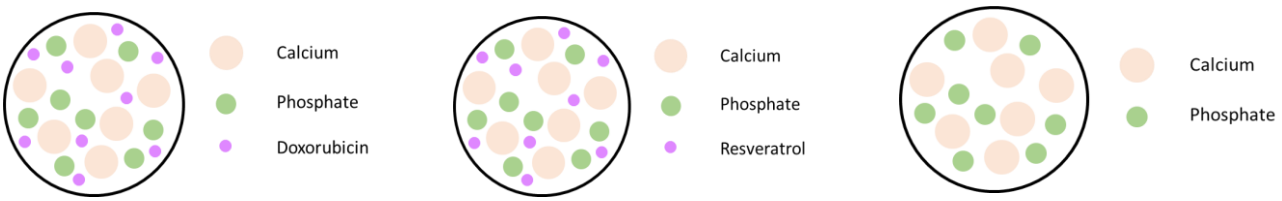

Figure 17 - Schematic diagram of the core formulation.
Osteosarcoma formulation (left), two formulation for prostate cancer (centre, right)

5.2.2 Layer-by-layer functionalization

Layer by layer deposition

The manufactured cores with the only presence of drugs require to add other specific properties and drugs to well treat and target the two tumour forms. So, to let NPs expressing specific superficial properties, LbL electrostatic assembly technique is performed. The scope of this step is to add specific chemical molecules upon the surface of NPs to acquire both therapeutic and diagnostic properties, these molecules are roughly for example peptides, drugs, diagnostic molecules, new materials.

Preparation and preliminary tests

The schematic procedure employed to perform LbL assembly is summarized in Figure 18. Firstly, the polyelectrolytes solutions are prepared, for this step it is worth remembering that 10 mL of each solution is used for each run. Therefore, 1 mg/mL CHI, 2 mg/mL CHI and 1 mg/mL ALG are dissolved inside deionised water, and in addition all solutions are titrated to pH 5.5 to obtain the best net charge. In first phase 4 layers were tested in two different formulations, in the first one 1 mg/mL CHI solution was used while and for the positive layers while in the second one 2 mg/mL. Using 2 mg/mL, nanolayers where more compact so that concentration was chosen for next experiments. A right volume of deionized water is prepared and titrated at pH 5.5 to complete all the rinsing steps between layers deposition. All samples are defrosted and 10 mg for each one is weighed and transferred in conical falcon tube (15 mL). It has to be taken into account that the process is described once, since it is equal in all steps for each sample, only therapeutic agents change. For adding layers, firstly, in accord with the initial design, the polyelectrolyte solutions are poured into the falcon tubes with NPs until they reach 10 mL, after that tubes are shacked at 93 rpm for 15 minutes on a mini orbital shaker, Stuart SSM1 and then are centrifuged at 4,400 rpm for 10 minutes in a Centrifuge 5702 (Eppendorf), Fisher Scientific. For the washing step supernatants are discarded and replaced with 10 mL of washing buffer, shacked for 10 minutes, and centrifuged for 10 minutes at same speed mentioned before, then another washing step is performed equal to the previous, but using only 5 minutes of shacking.

Figure 18 - Layer-by-layer deposition procedure

For prostate cancer

In this case two specific combinations of drugs and molecules have been chosen, with and without RESV as antioxidant, while in both ENZ and DTX are inserted into nanolayers as therapeutic agents. The aim was to understand the effects of combining drugs with other molecules which had a capability to target the cancer. These NPs are at last functionalized with 6 layers to achieve a gradient of the chosen drugs. For giving more clarity, the NPs with only drugs are named CaP-ENZ-DTX and with RESV CaP-R-ENZ-DTX.

CaP-ENZ-DTX. At the beginning 10mL of ALG solution with 34 μL of 600uM DTX solution are added, followed by an empty CHI layer. In the second negative layer ENZ and DTX are added together with a 34 μL volume, followed by an empty CHI layer. In the last negative layer only 34 μL of ENZ are added into ALG solution, followed by an empty CHI layer.

CaP-R-ENZ-DTX. For CaP-R-ENZ-DTX all steps as well as the order and quantity for therapeutic agents are the same. The difference is the presence of also RESV. For the first layer, in 10 mL of ALG solution within DTX also 34uL of the 88mM RESV solution is added, all other quantity were kept equal with CaP-ENZ-DTX. At the same time other 34 μL of RESV solution are added in the other anionic layer, so in the 3rd with ENZ and DTX and in the 5th only with ENZ.

In Figure 19 are reported the schematic diagrams of the two mentioned formulation, in addition CQD are already considered, although the process is described below (5.2.3).

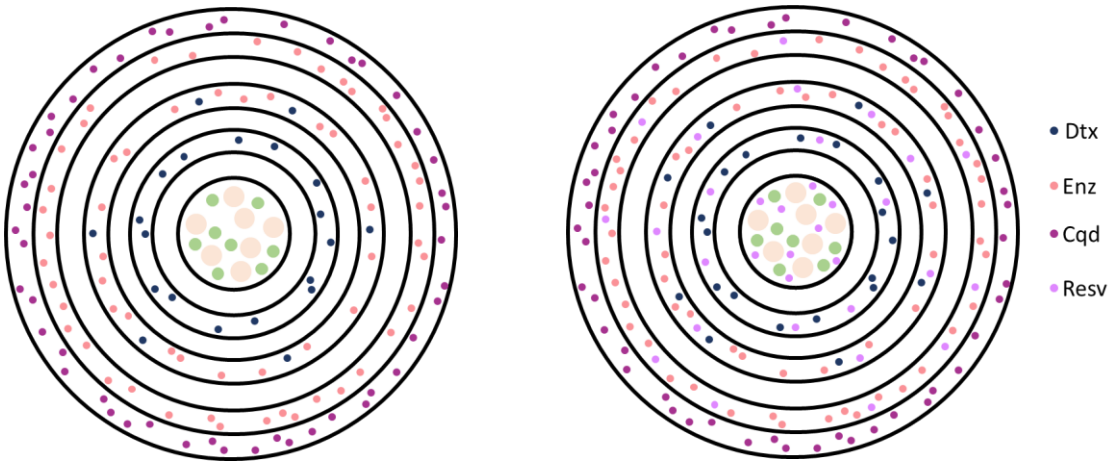

Figure 19 - Schematic diagram of the prostate cancer formulations.
CaP-DTX-ENZ (left) and CaP-R-DTX-ENZ (right)

For osteosarcoma

For targeting OSa, different formulations are designed and produced. In particular, the cores have been already produced containing DOXO, and in addition the drug is encapsulated in one of the layers, the first cationic layer. Also in this case, RESV is added but only in nanolayers to avoid cross-interactions with the release of DOXO. Therefore, 10 mg of DOXO-containing NPs is weighed and transferred in falcon tubes to proceed with the covering. In this specific case for the agents selected only 4 layers were enough to encapsulate all of them.

CaP-DOXO. This represents such a control for the second trial, in particular this formulation contains only DOXO. To achieve this, firstly ALG solution is poured to fill until 10mL into tubes. Secondly, the CHI solution is mixed with 101 µL of 10mM DOXO solution and then 10 mL of the new solution are added to tubes. It is worth noticing that 101 µL has been selecting to maintain the ratio used with the core, indeed, in that case 405 µL in 40mL has been added. At last other 2 layers of ALG and CHI respectively are added to be consistent with the second formulation for OSa.

CaP-R-DOXO. For CaP-R-DOXO all steps as well as the order and quantity for therapeutic agents are the same. The difference is with the antioxidant. As with the NPs designed against the PCa also in this case for the first layer 10mL of ALG is added with 34 µL of RESV from the 88mM solution prepared in DMSO. Then for the second layer of CHI 101 µL is transferred into 10mL that in turn are poured in the falcon tubes containing NPs. To have a good quantity of antioxidant, RESV is added with the same volume at before also in the 3rd layer of ALG and in the end a last CHI layer is deposited.

The schematic diagram in Figure 20 reports the structure of the mentioned formulations.

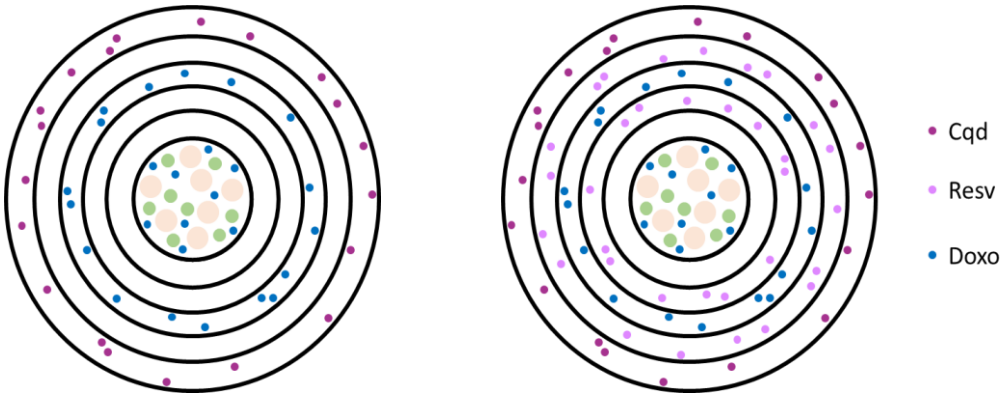

Figure 20 - Schematic diagram of osteosarcoma formulations. CaP-DOXO (left), CaP-R-DOXO (right)

5.2.3 Addition of carbon dots as imaging probes

Until this point cores and layers encapsulated only the selected drugs. Therefore, to acquire a theranostic approach it is still required to add imaging probes, thus CQD have been selected as imaging probes. The carbon quantum dots have been chosen due to sharing pros of quantum dots about the narrow emission and large etching spectrum in addition with a higher index of biocompatibility.
In order to add CQD, new cores of each formulation are produced, then they are covered until the second last layer of ALG. To encapsulate carbon dots, a new 2mg/ml CHI solution in deionized water solution is produced inserting, from a stock of 1mg/ml, graphene carbon dots solution that have a fluorescence in the blue spectra. The final chosen concentration of carbon dots is 250 μg/mL so it must be diluted directly in the falcon tubes to reach 10ml of CHI-carbon dots solution, adding an amount of CHI to reestablish the correct concentration of 2 mg/ml. The carbon dots charge was tested as well as the solution after the mixing with CHI solution. After the preparation of 10mL for each new nanoparticle solution the LbL technique process is continued.

5.2.4 Addition of targeting agents on the outer layer

For prostate cancer

The aim to add an active targeting ligand for PCa was reached considering PSMA which is a peptide that can interact with specific receptors upon the surface of tumour and that are overexpressed in the latter rather than normal cells. PSMA-617 is immobilized on the surface of the NPs using a reaction via carbodiimide between amino groups of CHI and carboxyl groups of PSMA. The protocol is designed starting from the one described by Chen et al. with some modifications[171], in addition the schematic procedure is reported in Figure 21. The amide bond is created using 1-Ethyl-3-(3-dimethylaminopropyl) carbodiimide (EDC) and N-hydroxysuccinimide (NHS) as coupling agents. After dissolving PSMA-617 (100 μg) in 0.1 M 2-(N-morpholino) ethanesulfonic acid (MES) buffer (5mL), EDC (22 μg) and NHS (6.63 μg) are added to the PSMA-617 solution (molar ratio of PSMA-617: EDC: NHS = 1: 1.2: 0.6). The solution is then incubated at room temperature for 30 min to activate the carboxyl groups of the PSMA-617. After 30 min of shaking at 80 rpm, the solution is added to the NPs solution dissolved in 0.1 M MES buffer (5 mL). The coupling reaction must be carried out for 24 h at room temperature.

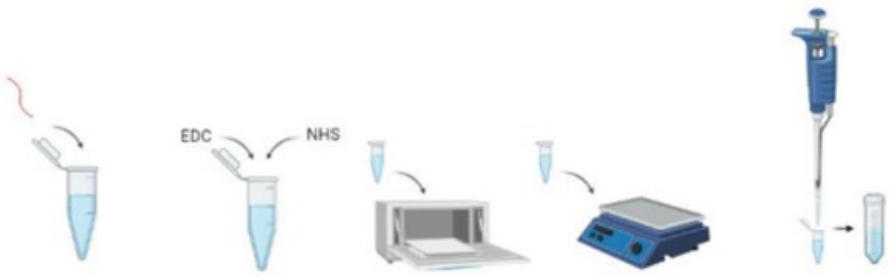

Figure 21 - Procedure to graft PSMA-617 upon CHI surface.

For osteosarcoma

In the specific case of OSa, HA has been chosen to interact with the CD44 receptors overexpressed on tumour cells. Following the same procedure seen for LbL deposition, a solution 1mg/ml of acid hyaluronic is produced and titrated at pH 5.5, similarly to the polyelectrolytes used for LbL. Hyaluronic acid is a negative polyelectrolyte and for this no other changes are required upon the last layer of CHI of NPs containing DOXO. After the solution is produced, the protocol for the LbL deposition is followed as for a new layer. Therefore, for adding layers, firstly, the HA solution is poured into the falcon tubes with NPs until it reaches 10 mL, after that tubes are shacked at 93 rpm for 15 minutes on a mini orbital shaker, Stuart SSM1 and then are centrifuged at 4,400 rpm for 10 minutes in a Centrifuge 5702 (Eppendorf), Fisher Scientific. For the washing step supernatants are discarded and replaced with 10 mL of washing buffer, shacked for 10 minutes, and centrifuged for 10 minutes at same speed mentioned before, then another washing step is performed equal to the previous, but using only 5 minutes of shacking.

5.3 Nanoparticles characterization methods

5.3.1 Morphological characterization

Size and shape of NPs - TEM

TEM analyses are performed in order to characterize the size and the shape of CaP NPs. For the Transmission Electron Microscopy (TEM) the device used was a Philips CM 100 Compustage (FEI) transmission electron microscope (Philips) at HV = 100.0 kV. The device was coupled with AMT CCD camera that allowed to capture digital images with a maximum magnification range of 130, 000×. For the analyses, NPs with and without layers are suspended in deionised water within an ultralow concentration and samples are transferred by drop-casting the solutions upon copper grids (Scientific Agar) and drying them under a heating lamp for 20s before inserting inside the microscopy device.

5.3.2 Physico-chemical characterization

Zeta potential

The ζ-potential of the different formulations of NPs is evaluated to assess the presence of the polyelectrolytes by the surface charge. The devices exploited was a Zetasizer Nano ZS Instrument (Malvern Panalytical, Ltd.) by a micro electrophoretic method. The device works using the Henry's equation (Eq. 1)[172] to find the value of the charge by several parameters.

$$\zeta = \frac{3\eta}{2\varepsilon F(\kappa\alpha)}\ \mu \quad \text{(Eq. 1)}$$

In the formula, η represents the dynamic viscosity, ε is the dielectric constant of the dispersant, F(κα) is the Henry function, and finally μ represents the electrophoretic mobility. To measure the ζ-potential, aliquots are saved after each washing step. Specifically, before discarding supernatants of the second washing step of each layer, 100 μL were saved and diluted 10 times with 900 μL of deionized water.

FTIR ATR

The Fourier Transform Infrared spectroscopy in ATR mode is performed to characterize chemical bonds of the surface and evaluate the deposition of layers, especially around 0.5 to 5 microns can be analysed. The spectra are useful to spot the occurrence of specific peaks that characterize the presence of layers compounds, in particular ALG, CHI, and the related therapeutic agents. Therefore, the FTIR spectroscopy is performed to characterize with cores alone and already functionalized with layers. The device was a Spectrum Two PE instrument equipped with a horizontal attenuated total reflectance (ATR) crystal (ZnSe) (PerkinElmer Inc., USA). For this analysis all NPs formulations were dried and analysed over a range of 4000 to 500 cm-1 with resolutions of 2 cm^{-1}.

XPS

X-ray photoelectron spectroscopy allows to characterize the surface in a depth of 2 to 10 nm. XPS can give a spectrum where results are directly correlated with the presence of specific atomic species. Therefore, the characterization is important to know if specific atoms are present upon the surface after the deposition of layers. XPS analyses of the different formulation of cores and NPs functionalized were carried out using the Kratos Axis UltraDLD XPS spectrometer, located at the EPSRC Harwell XPS Service facility in Cardiff, UK. This state-of-the-art spectrometer featured a precise monochromatic AlKα X-ray radiation source. Inside the analysis chamber, a controlled starting pressure of 10^-9 mbar was established. Subsequently, the samples kept in water underwent examination in High Power mode with an X-ray take-off angle set at 45°, resulting in a scanned area of roughly 1400 × 200 μm. Two distinct scan types were performed: survey scans in Fixed Analyser Transmission mode, covering a binding energy (BE) range of 0 to 1200 eV with a pass energy of 117.4 eV, and high-resolution spectra acquired in FAT mode with a pass energy of 29.35 eV. The high-resolution scans specifically targeted the C1s region for each specimen. Furthermore, the CasaXPS software package was used to determine the atomical percentage inside sample and to perform the peaks deconvolution.

Yield of the process

To evaluate the yield of the process, all NPs are weighed from each formulation and related to the weight of all initial compounds, especially calcium L-lactate, dibasic ammonium phosphate, PAH and relative therapeutic agents which were dissolved in initial solutions. The weights of calcium L-lactate, dibasic ammonium phosphate, PAH in each solution were the same between different formulations, therapeutic agent weights changed in accord to the different volumes mixed batches.

In order to measure the yield, the formulations have been completely dried and the values were used in the following equation (Eq.2):

$$Yield\ (\%) = \frac{weight\ of\ nanoparticles}{weight\ of\ all\ initial\ compounds\ (polymers + drugs + oder\ molecules)} \quad (Eq.2)$$

Entrapment efficiency (EE%)

The entrapment efficiency is calculated in the specific case of DOXO due to the optimisation performed in the cores designed for OSa. Zeta-potential confirmed that the higher concentration of DOXO did not affect the overall process of deposition. In more details, to value the encapsulated DOXO two different steps were performed sequentially. Firstly, 1 mg of NPs from each batch is weighed and dissolved within 3 mL of 1M HCL, the solutions are stirred at 120 °C until the acid is completely evaporated. A pellet with drug and polymers is obtained and that was due to the capability of strong acids to dissolve the chemical structure of CaP NPs. Secondly, a solvent that could solubilize only the drug is poured in the container, specifically a solution of ethanol and deionized water with a ratio of 3:1 is produced. The pellets obtained in the previous step are dispersed in the second solvent with volumes of 600 µL and the solutions are stirred for 5 hours at room temperature covering them to avoid evaporation. After the time expired, the solvent from the solutions is withdrawn and centrifuged at 13,000 rpm for 10 minutes. After that, 100 µL in triplicate for each sample is transferred into 96-well plates together with the triplicate of 100 µL ethanol-water solution as blank. The plates were read inside a FLUOstar Omega Microplate Reader, and the optical densities of solutions were measured at 480nm.

PBS release

To evaluate the ability of NPs to release their therapeutic effect, a in PBS releasing step is included[173]. A concentration 1 mg/mL of NPs in PBS was chosen, especially 3 mg is weighed and transferred in 3mL of PBS. After transferred, the solutions are incubated at 37 C°. Different time points have been used to saving aliquots, especially they were 10 min, 30 min, 60 min, 2 h, 4 h, 6 h, 24 h, 48 h and 7 days. In particular, the triplicate of 100uL is taken and transferred in small Eppendorf tubes (0.5 mL) and replaced by 300uL of fresh PBS, then solutions are again incubated at 37°. The device LC-MS_Agilent Infinity II 1260 UPLC-MSD-XT was used to perform the high-performance liquid chromatography (HPLC). Some parameters were tuned, especially the mass range was between 100 and 1200 Da, while the percentage of acetonitrile was set at 50% and 70% respectively for DOXO and DTX. Thereafter, after all time points are collected, they get transferred in small glass bottles specific for the HPLC tester. For doing so, a small syringe equipped with a 0.22 µm filter is exploited to dilute and transfer 100µL of the PBS solution within 900 µL of ultrapure water inside small glass bottles, and they are labelled with barcode to recognize them after the test. At the same time, the same procedure is exploited to prepare the calibration curve. In that case specific concentrations of DOXO and DTX are prepared for obtaining specific points to draw a releasing curve.

Carbon dots encapsulation

Initially, the solution of CHI containing QCD have been analysed by zeta-potential characterization. The aim was to understand if there were differences that could negatively interact with the overall charge. The encapsulation of graphene quantum dot is demonstrated in a qualitative way using a microscope with a DAPI filter. Dried NPs are transferred on a glass slide and analysed directly under the microscope. To compare the emission also the green and red channel have been used.

5.3.3 Cells preparation

Cells cultures

In order to perform in vitro tests, different cell lines from PCa and OSa have been exploited, especially Lncap and Vcap for PCa and Sao and U2os for OSa. To seed and grow them, the guidelines from the seller (ATCC) have been followed. Two kinds of medium were used, DMEM for and RPMI-1640 for Vcap and Lncap respectively, while Saos and U2os were cultured both with DMEM. Each medium bottle is filled with 50 mL of FBS and 5mL of Penicillin. At the beginning, the cells were stored in ice resistant Eppendorf tube at -80 °C in liquid Nitrogen and to seed them they had to be defrosted in a bath at 40 °C until the solvent started floating. After they were ready, 1 mL of cell solutions were diluted with 9 mL of their specific media into conical falcon tubes (15 mL) and centrifuged at 1,200 rpm for 5 minutes. After that, all 10 mL of solutions were transferred into T75 flasks and eventually a further volume of media was added to fill all their surfaces. After that cell flasks have been incubated at 37 °C. The cultures were left incubated until they reached the 80-90% of confluence and after they were split.

Spheroid formation.

Together with 2D cultures, spheroids have been chosen to mimic in a better way the real pathological tissue and acquire a better knowledge about the drug activity in organized 3D structures. Each cell line was chosen to produce spheroids in order to select the better ones for each disease. To create and culture spheroids the protocol reported in Figure 22 was employed. Firstly, the specific media are modified adding methylcellulose. The methylcellulose is able to let cells aggregate due to its chemical composition. Firstly, to prepare 0.25% w/v of media modified with methylcellulose, the polymer is weighed and left under UV light to sterilize. After 30 minutes of sterilizing, the methylcellulose is added to media, and they are mixed on a vortex. Lastly, the new media must be left for 24h in incubation at 4 C°. To form spheroids, different cell densities are used, in particular in this project 2.5k, 5k, 10k and 20k have been used for each cell line. After the counting of the cells, the right number of them is inserted into the u-bottom low-adherent 96-well plate with a volume of 150 µL in order to make cells aggregating in the following days. Moreover, images were taken at different time points, specifically 1, 3 ,7, 10 days after seeding and at the same time 2/3 of the media were substituted with fresh media.

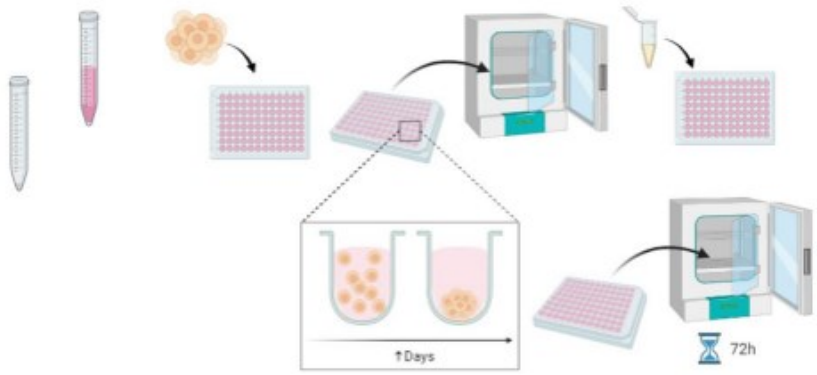

Figure 22 - Schematic picture about the method used for the formation of spheroids.

5.3.4 Cytotoxicity evaluation

Cell tests

Cell test have been performed to acquire information on in vitro behaviour of the formulation, both 2D and 3D cultures are exploited. In more details, CaP-ENZ-DTX and CaP -R-ENZ-DTX are tested on PCa cells Vcap and Lncap, while CaP-DOXO, Cap-R-DOXO on OSa cells Saos and U2os. To assess the cytotoxic activity of NPs the PrestoBlue and Live and Dead assays are performed.

The first one allows to obtain quantitative information about the availability of cells in an indirect way, while the second one allows to evaluate the number of cells alive in a qualitatively way by colouring them in green and comparing them with the dead cells in blue. To exploit these tests, 4 concentrations of nanoparticle from each sample have been tested: 1000, 500, 250, 100 µg/mL and the NPs are then inserted directly inside 150 µL containing 8k cells.

On the other hand, for 3D analysis, the concentration selected was the higher one, 1000 µg/mL, while the spheroids were formed with 10k cells inside the same volume of medium. It is worth noticing that for 2D cultures flat 96-well plates are exploited, while for the 3D cultures the spheroids are maintained inside the u-bottom plates.

For both assays the guidelines of the sellers have been followed and in addition the PrestoBlue procedure is schematically explained in Figure 23 , In both PrestoBlue and Live/Dead assays, cells are cultured using the media for 24 hours before nanoparticle treatment. NPs are dissolved in respective media, with a higher concentration being prepared initially and a lower concentration added during media transfer. For PrestoBlue, a 1:10 solution of PrestoBlue and media is prepared, added to wells, and incubated for 1 hour. Fluorescence readings are taken at 544 nm emission and 590 nm absorbance wavelengths and are compared to control. For Live/Dead, cells are incubated with assay solution (green for dead cells, blue for total cells) for 20 minutes, then analysed under a microscope. In 3D tests, spheroids are formed over 2 days before nanoparticle delivery. Cells are transferred to a flat plate for Live/Dead analysis due to well shape, and a fluorescence ratio is calculated.

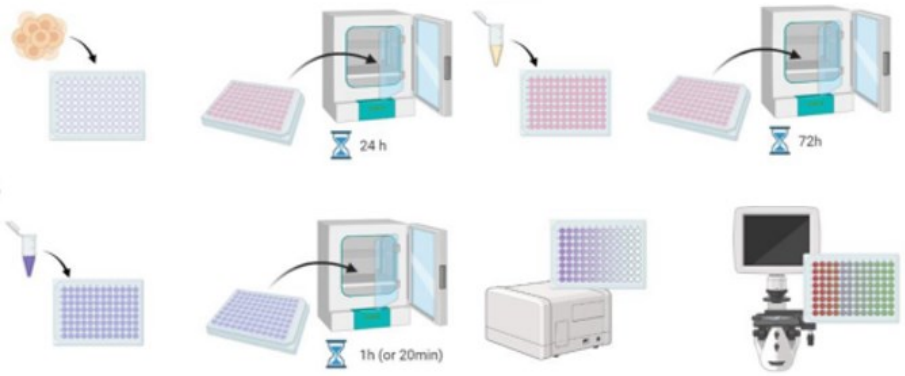

Figure 23 - Protocol for the evaluation of cellular viability

5.3.5 Statistical analysis

The results were presented as the mean ± standard deviation, based on data obtained from three independent experiments. Statistical analyses involved comparing the mean values of the samples. To determine statistical significance, a two-way ANOVA was performed, followed by Tukey's multiple comparison test, with significance levels set at * $p < 0.0332$, ** $p < 0.0021$, *** $p < 0.0002$, and **** $p < 0.0001$, as determined by the analysis tool. Data analysis was conducted using GraphPad software, and statistical significance was considered at the $p < 0.05$ level.

6 RESULT AND DISCUSSION

6.1 Calcium phosphate nanoparticles (CaP NPs) synthesis

6.1.1 Initial results

In this study calcium phosphate (CaP) nanoparticles (NPs) have been synthesized exploiting the peristaltic pump method. The device was able to control the flow rate of the solutions allowing the direct control of solution mixing and precipitation of NPs and thus regulate their size and morphology. The parallel link of pipes with their specific length allowed to precisely control the interaction between the calcium-containing solution and phosphate-containing solution which resulted in the precipitation of CaP particles. To be more specific, CaP NPs were created within a 5-second period of crystallization and then converted into a colloidal state by introducing PAH for 15 seconds. The timing for these steps was determined based on the flow rate of the pump and the diameter of the tubes and this process led to the precipitation of NPs[169].

The overall process leaded to a yield (Y (%)) of 13.82 ± 0.06% with minimal changes between empty, DOXO-encapsulating and RESV-encapsulating cores. A possible explanation of this percentage could be related to the dialysis step which removed from the dialysed solution most of the starting material together with secondary products that could have different chemical and stoichiometry structure, a reduction of the particle quantities

could be also due to the centrifuging step which use a low speed leaving some particles floating in the solvent. Therefore, using the process described, calcium and phosphate compound had been well combined in NPs through the pumping method and thus the templates for the sequential LbL approach were made. In the specific case of DOXO, in the following paragraph, it is reported the entrapment efficiency revealed.

6.1.2 Encapsulation efficiency (EE%)

In this project, for OSa and PCa different drugs have been chosen for the designed NPs. These drugs were: DOXO, DTX, ENZ, among them only DOXO have been added inside the core while the others were mainly inserted inside layers. After the analysis with the DLS to understand the zeta-potential of the DOXO-containing cores, 405 µL was chosen as standard volume since it was the highest value among the tested and that did not affect the overall manufacturing process. By a dissolution performed in two steps of the cores containing the chemotherapy the supernatant saved was analysed in absorbance, and the entrapment efficiency resulted to be above 90% and this might confirm the hypothesis that DOXO well interacts with CaP as explained for the size of cores (6.2).

6.1.3 Release in PBS

The extensive characterization of CaP NPs in a PBS solution was conducted using the HPLC device in order to investigate the release behaviour of the two chemotherapeutic agents, DTX and DOXO. In Figure 24 , the release profiles of these two molecules over a period of several days are presented. Notably distinct release patterns were observed for the two drugs, despite them exhibiting a similar overall trend. An initial burst release was observed for both compounds, with DTX releasing approximately 50% of its total payload within the first day, whereas DOXO released less than 30% during the same time frame. After 7 days, nearly 80% of DTX had been released, in contrast to slightly less than 40% of DOXO. This significant disparity in release behaviour can be attributed to the differing encapsulation mechanisms. Docetaxel was predominantly encapsulated within the nanolayers, facilitating a rapid and substantial release. Conversely, DOXO was primarily encapsulated within the nanoparticle cores, resulting in a slower release profile as it necessitated the dissolution of the cores to release the drug content.

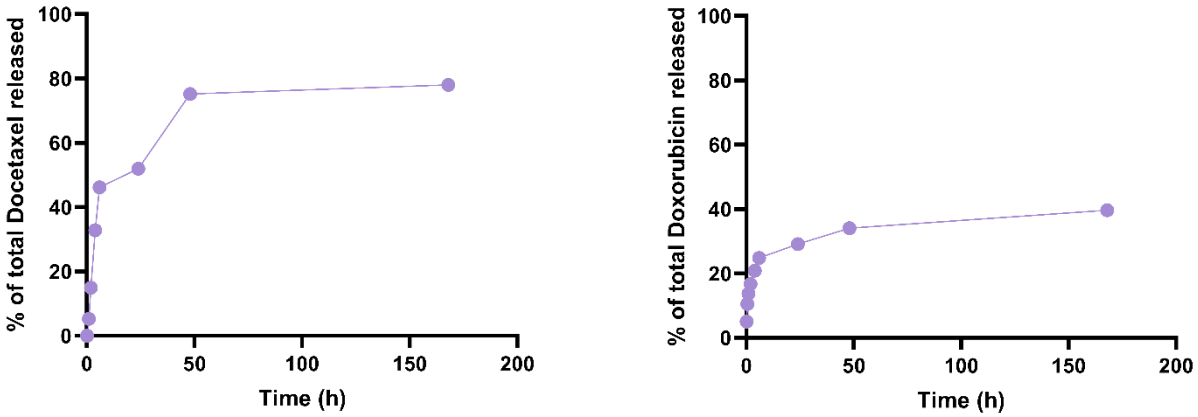

Figure 24 - Release of DTX and DOXO in PBS from functionalized nanoparticles

6.2 Chemical and physical analysis

6.2.1 TEM

TEM microscopy analysis was performed with the aim to characterize the shape and the size of NPs. In particular, all the formulations with and without layers were analysed, especially they were labelled as CaP (NL), CaP-DOXO (NL) and CaP-R (NL) in the case of cores, and CaP-R-DTX-ENZ, CaP-R-DOXO with layers and the values are reported in Figure 25. The dimension of the CaP particles strictly depends on the type and quantity of encapsulated drug. CaP particles with empty cores showed the higher size among cores with an average size of 86.4 ± 18 nm, while the others with RESV and DOXO had sizes of respectively 63.7 ± 11 nm and 48.7 ± 7.9 nm. On the other hand, after the deposition of layers the NPs grew in diameter and that confirmed the presence of molecules upon the surfaces. The shape after the deposition remained overall spherical, although some aggregates did not help to discern the real shape. In more details, the formulation designed for PCa functionalized with 6 layers in the formulations CaP-R-ENZ-DTX had an average size of 93.3 ± 25 nm, while the formulations with DOXO and 4 layers, CaP-R-DOXO, had a size of 112.8 ± 25.6 nm.

The behaviour of cores containing DOXO and RESV is notably distinctive due to their smaller size compared to empty cores. This peculiarity may be attributed to the characteristics of the drugs and the pH conditions during the process. In both cases, a consistent decreasing trend was observed, suggesting a potential adverse interaction between these drug molecules and the nucleation of the cores. It is possible that the presence of the drug and antioxidant had an influence on calcium and phosphate groups, hindering the growth process of the cores. At the same time, these molecules might play a role in stabilizing the compounds, preventing excessive growth of a CaP shell around the newly formed particles. However, the differences between DOXO-containing cores and RESV-containing cores may be linked to their electrostatic properties. The chemotherapeutic drug exhibits a cationic nature, which could facilitate interactions with negatively charged phosphate groups, resulting in greater constraint on the material and, consequently, smaller core sizes. In contrast, RESV, with its

slightly negative charge, might interact with calcium ions or poly (allylamine hydrochloride) (PAH), leading to a reduction in size, even lower than the one observed with DOXO.

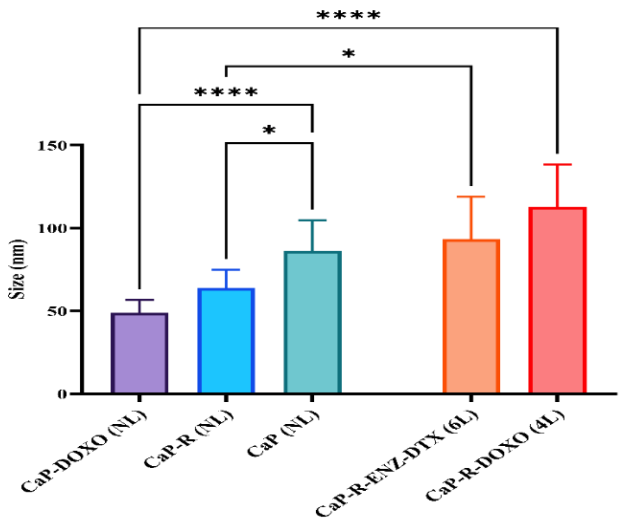

Figure 25 - Size of nanoparticles with and without layers

For the formulations comprising the whole combination of drugs as well as the multilayers shell, the sizes were higher than the cores alone, as expected (Figure 25). Therefore, the deposition of polyelectrolytes was confirmed by the increasing revealed by the TEM analysis. At the same time, the shape remained overall spherical, although some aggregates did not help to discern the real shape. Although NPs got large in both cases, an interesting thing was noticed comparing them. Nanoparticles with 6 layers for PCa expressed a lower size than NPs with 4 layers for OSa. A possible reason of this behaviour could be a better internalization and interaction of ENZ and DTX with the surrounding layers allowing a higher restriction of materials and thus a reduction in the size. However, it is important to take into account that the difference was not statistical relevant.

As it is possible to notice from Figure 26, the NPs showed up aggregates which were higher of ordines of magnitudes than the single NPs, meanwhile it is possible to notice the singular NPs which make up the big cluster. A consideration about this behaviour may be that during the stirring, NPs nucleated and grown, probability in that step some NPs were able to grow alone, while others merge at early stages and remained encapsulated in the new formed cluster.

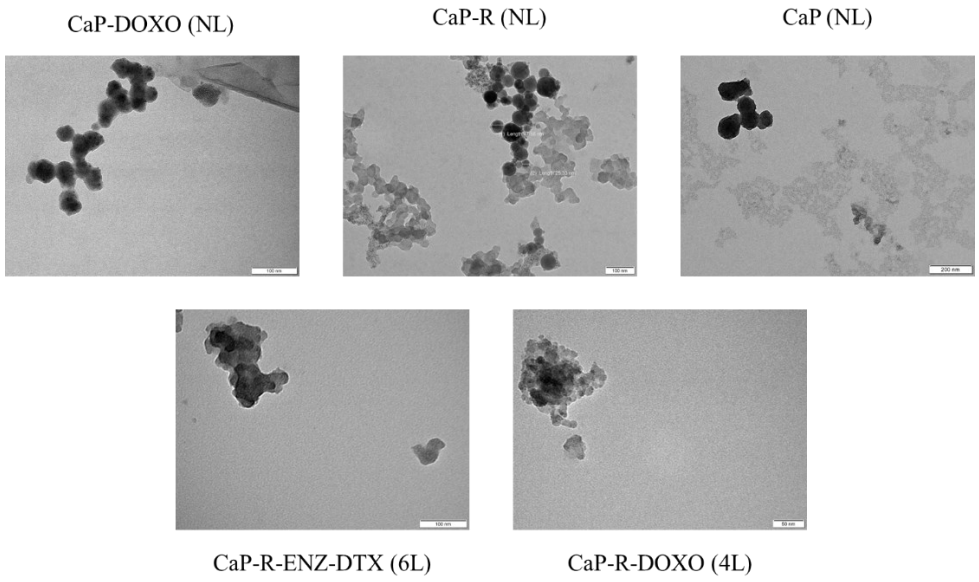

Figure 26 - TEM pictures of different nanoparticles formulation

6.2.2 Zeta-potential

Through a dynamic laser scattering device, it was possible to perform analysis on the surficial charge of NPs, especially the zeta-potential allows to understand the charge considering the water shell that form upon NPs surface inside aqueous solution. In the case of this project the zeta-potential was a crucial characterization to firstly assess the right manufacturing workflow for nanocores, expecting a positive surface for the PAH deposition, that was confirmed by the data below. Secondly, the analysis of the charge was a procedure to decide the best concentration of DOXO which did not affect the overall fabrication of the cores and the outer layer of PAH. Lastly, the value of zeta-potential signed after each deposition confirmed the presence of the polyelectrolytes upon the surface. Furthermore, the analysis was useful to understand the well interaction between drugs and other molecules that expressed a good combination in the formulation designed.

The zeta-potential of the positive layer (0th) composed by PAH was lowly affected by the agent inside. In the specific case of DOXO, the average was 11.9 ± 0.95 mV, in contrast with the formulation containing RESV that had a zeta-potential of 16.1 ± 3.6 mV. The difference may be caused by the increased size of RESV-containing NPs that could graft a higher amount of PAH. At the same time, a modification in the composition could have fairly changed the superficial charge of the formulation affecting the overall charge of the PAH layer.

For the second analysis it has been tested the zeta potential of the formulations with different content of DOXO. Figure 27 shows the result obtained form that analysis, especially in the first two layers there were not statistical differences and that indicated that the highest selected amount of DOXO could not affect the overall process. Therefore, the experiments on OSa formulation proceeded with 405 µL of 10mM DOXO solution inserted inside cores, confirmed by zeta-potential evaluation.

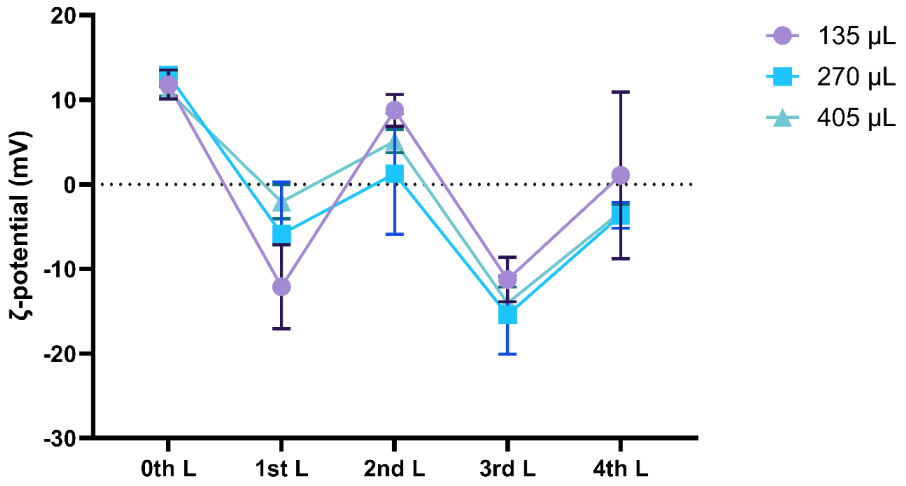

Figure 27 - Zeta-potential values of DOXO-containing cores with different concentrations of the drug.

Lastly, the zeta potential has been exploited for characterizing the deposition of layers of each formulation. To maintain consistency the NPs containing DOXO were tested again in comparison with the NPs thought for PCa in order to have the same experimental parameters from the start.

Figure 28 reveals a very similar trend between the formulations designed for PCa, nevertheless the main difference between them is the presence of RESV in cores and layers.
In the specific case of PCa formulations, the first two layers showed an increased distance between mean values, and this could be for the presence of RESV. It was inside the core and in the anionic layers in contrast with the second formulation not containing RESV anywhere. The lack of the antioxidant could affect the superficial charge and the distribution of PAH with the consequence of the initial differences. Nevertheless, first layers had some differences, from the 3rd layer until the last one, the trends of zeta-potential are analogous, even so small imbalance on the average may be caused by the presence of RESV. Therefore, this data confirm that the presence can influence the whole charge of the layer in which it is inserted, even so the deposition was not hindered by that allowing a good functionalization with the antioxidant.

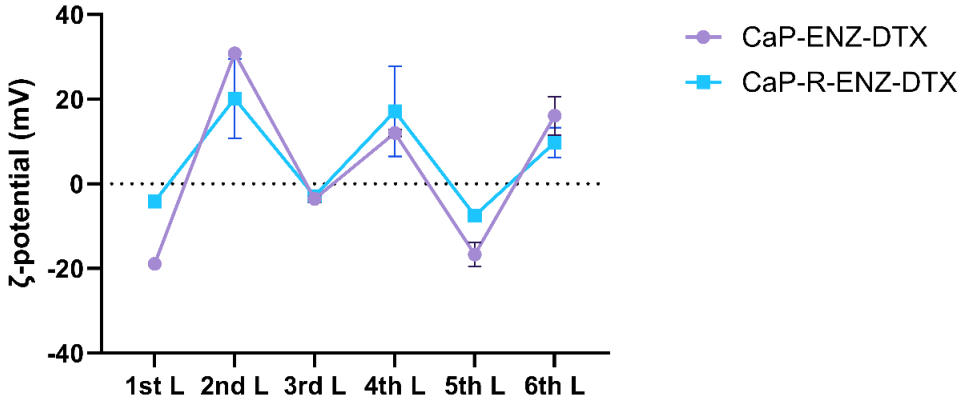

Figure 28 - Zeta-potential values of CaP-ENZ-DTX and CaP-R-ENZ-DTX for prostate cancer.

Focusing on the OSa formulations, Figure 29 shows a clear overlap in the mean values of the 3rd and 4th layers. In contrast, as it was seen for PCa, the first two layers have been affected by the presence of RESV, although the trend remained the same. Therefore, this formulation confirmed the behaviour of RESV and its ability to influence the charge without spoiling the overall deposition process.

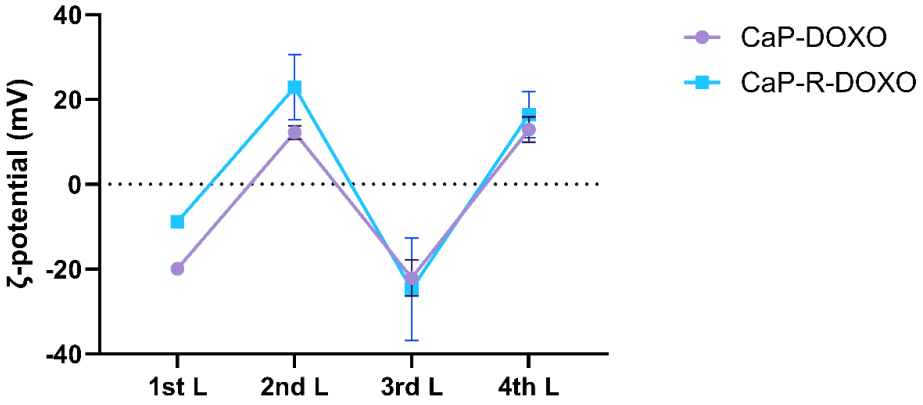

Figure 29 - Zeta-potential values of CaP-DOXO and CaP-R-DOXO for osteosarcoma.

6.2.3 FTIR-ATR

This analysis was performed with the aim to understand the materials present in NPs as well as to confirm the deposition of layers and the right functionalization with active targeting agents.

FTIR technique in ATR mode was useful to analyse a depth of 1-2 um, it means that it could characterize the overall surface of the NPs allowing to determinate the chemical bonds of polyelectrolytes which make up the covering layers. The technique was employed with 3 main objectives, the first one was to analyse differences between the cores formulations that contained different drugs or no drugs.

Secondly, the shell had been tested with the aim to evaluate the presence of chemical species inside layers which represent the therapeutic agents.
Lastly, FTIR analysis was exploited to check the right interactions between the surfaces and the active targeting agents designed both for PCa and OSa (described below 6.4).

The three different formulations of cores have been tested. From Figure 30, it is possible to indagate the materials of particles as well as the presence of the different drugs in comparison with the empty core. Specific regions have been highlighted to indicate all the bonds present in each formulation and thus likely to be part of CaP particles and/or PAH. Therefore, the two peaks at 550 and 600 cm^{-1} indicate a bending vibration of the phosphate group. Instead, the next large peak between 900-1150 cm^{-1} could represent the phosphate group but in a stretching vibration. The peaks appeared between 2820 and 3050 cm^{-1} can reveal the presence of O-H and C-H bonds that can be both from the phosphate group, drugs, and the polyelectrolytes. Furthermore, the deposition of PAH is confirmed by different regions, firstly the peak around 1250 cm^{-1} indicates the presence of an amide III bound, with a prevalence of C-N stretching and N-H bending vibration, while at 1650 cm^{-1} it is highlighted the appearance of an amide I group indicating a high proportion of C=O stretching. The FTIR peaks have been also confirmed by a study in the current field[174]. Lastly, the region between 3200 and 3420 cm^{-1} is likely to represent a stretching of the N-H group.

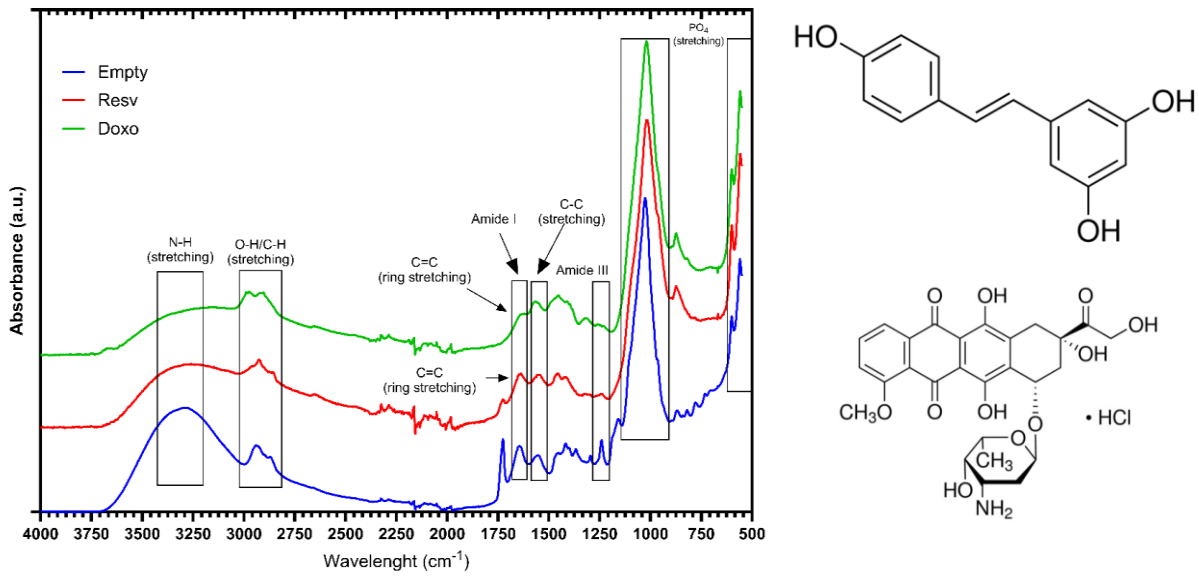

Figure 30 - FTIR spectra of CaP (NL), CaP-DOXO (NL) and CaP-R (NL) (left) and chemical structure of RESV (right-top) and DOXO (right-bottom).

Focusing on the specific peaks signed individually on Figure 30, the curve related to DOXO shows a tiny peak at 800 cm^{-1} that indicates a C=C bending of the aromatic rings, in addition a similar peak is overlapped with amide I group at 1650 cm^{-1}. Moreover, the peak at 1550 cm^{-1} can be from the stretching of the DOXO structure, but it is more likely to be from the stretching of the PAH carbon because it is expressed in all three curves. On

the other hand, the chart about RESV-containing cores have peak similar to the DOXO curve due to the presence of aromatic rings in both molecules and in addition this was confirmed by recent study that used that kind of drugs[175,176].

After the analysis of cores, FTIR was still employed to characterize NPs covered with layers and containing therapeutic agents. It is worth mentioning that the peaks of formulations with and without RESV were superimposable and due to this only the complete formulations have been reported.

In Figure 31 a comparison between the polyelectrolytes and CaP-R-ENZ-DTX spectra is reported. In the region between 2800 and 3500 cm^{-1} the appearance of N-H, C-H and O-H stretching is still confirmed and that could be from both polyelectrolytes, the shorter peak of the sample in comparison with the ones of polyelectrolytes may be due to an interaction between CHI and alginate after deposition reducing the stretching of the group. Focusing on lower regions, the large peaks between 900 cm-1 and 1100 cm-1 can reveal the stretching of both C-C and C-O group. Furthermore, at 1600 cm-1 starts the peak belonging to the C=O stretching, it is likely to be the group of CHI even so the alginate can contribute to the overall number of such group. Lastly, the C-C stretching and C-H stretching are likely to be part of the two drugs used since in the polyelectrolytes spectra they did not appear.

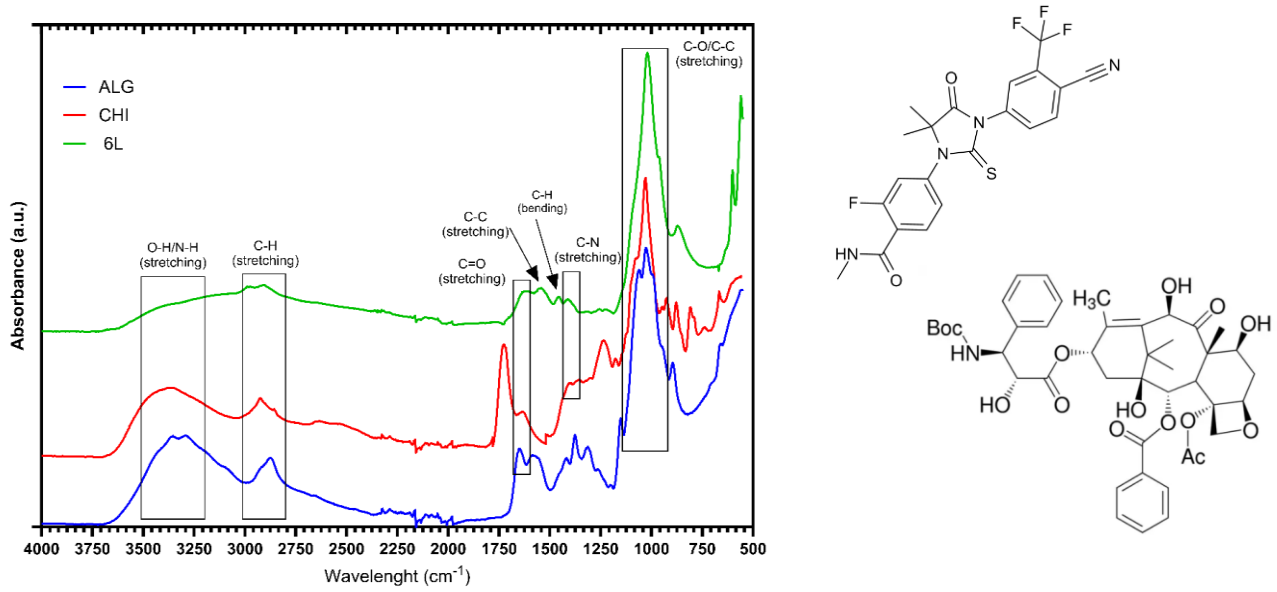

Figure 31 - FTIR spectra of ALG, CHI and CaP-R-ENZ-DTX (left) and chemical structure of ENZ (right-top) and DTX (right-bottom).

In Figure 32 is reported the spectrum of the complete formulation designed for OSa. The same peaks revealed from the previous picture are present, indicating that polyelectrolytes have been correctly deposited upon the surface of DOXO-containing cores. In more details, the highest peak between 900 and 1100 cm^{-1} as well as C-N and C=O stretching are present in the same position of before. Moreover, in the last part of the chart O-H and C-H stretching appeared with a few differences, especially the peak of C-H group was higher in comparison with the trend of CaP-R-ENZ-DTX which may indicate a higher amount due to the DOXO.

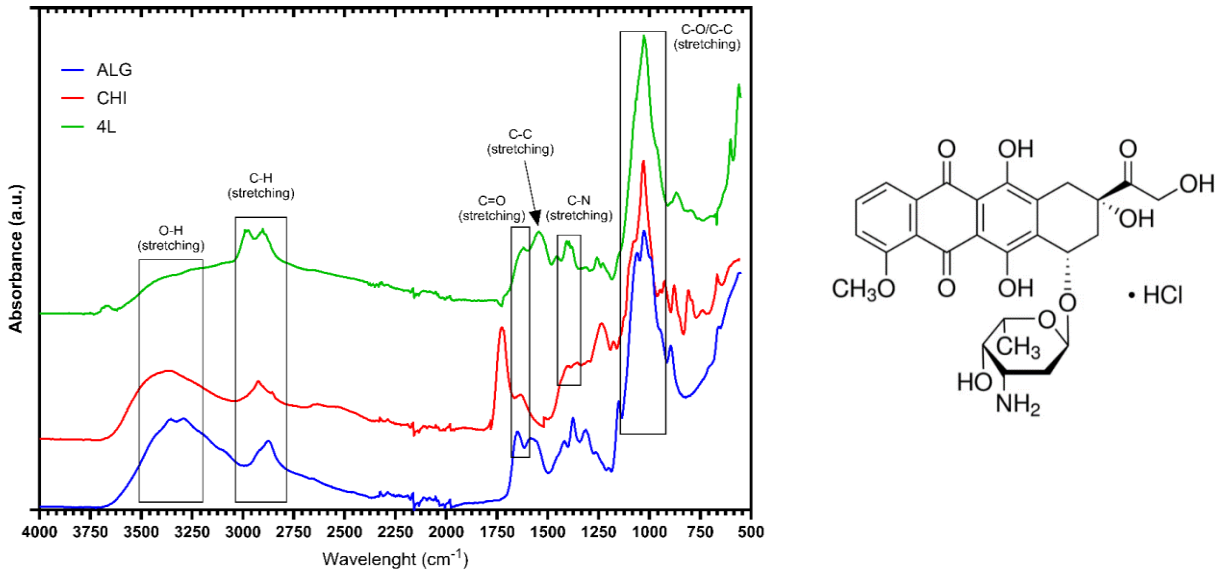

Figure 32 - FTIR spectra of ALG, CHI and CaP-R-DOXO (left) and chemical structure of DOXO (right).

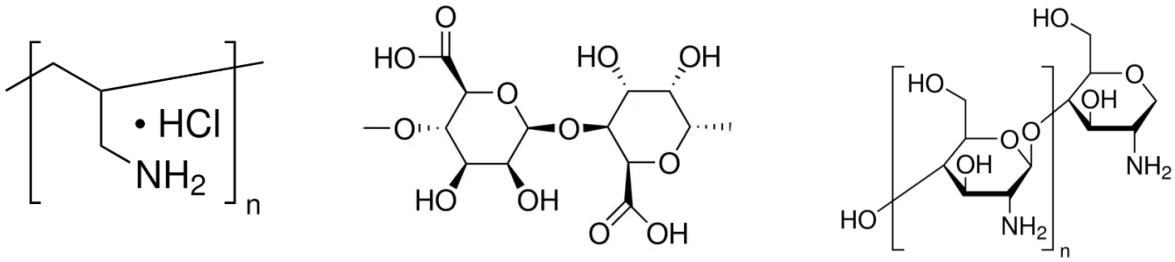

Figure 33 - Chemical structure of polyelectrolytes, PAH (left), ALG (centre), CHI (right).

6.2.4 XPS

The XPS was another technique performed to analyse the surface of NPs. This characterization in contrast with FTIR was employed to reveal the presence of specific atomic species of the substrate analysed. For this reason, this technique was performed to characterize the nanolayers reducing the noise from the surrounding materials. As well each characterization, all the formulation were tested before and after the LbL functionalization to compare the appearance of specific peaks after the deposition of new materials.

The XPS spectrum showed in Figure 34.a regards a formulation without layers and drugs. The spectrum of the empty NPs confirms the presence of PAH, as evidenced by the O1s peak at 531 eV and the appearance of a C1s peak at 285 eV. Additionally, a peak at 400 eV in the N1s region could be attributed to PAH, along with a residual compound from dibasic ammonium phosphate.

Furthermore, distinct peaks at 347 eV and 133 eV manifest the presence of Ca2p and P2p, respectively, signifying the utilization of calcium and phosphate materials in the formation of CaP NPs, thus confirming their presence in the sample. Furthermore, other peaks represent undoubtedly the presence of unwanted compounds or secondary products or artifacts form the analysis which must be not taken into account.

Throughout an in-depth analysis of C1s and O1s is possible to appreciate the presence of secondary peaks mainly related to phosphate group. In particular, for the C1s spectrum (Figure 34.b) in addition to the common peak of C-C bond there is a specific peak that reveals the interaction between carbon and phosphate group at 286 eV. The same data could be noticed by the deconvolution of the O1s spectrum that at 531 eV there is the peak about the oxygen inside the phosphate group. The analysis has been confirmed also by a compulsory study about CaP products[177]. Furthermore, an essential analysis concerns the ratio between calcium and phosphate content. Initially, the CaP NPs exhibited a ratio of 1.6, while natural hydroxyapatite, from which the nanoparticle composition was derived, possesses a ratio of 1.667. However, a calculation about the percentage of calcium and phosphate suggests a ratio of approximately 1.17. The deviation from the initial and natural ratios may be attributed to various purification steps and the presence of initial compounds such as PAH.

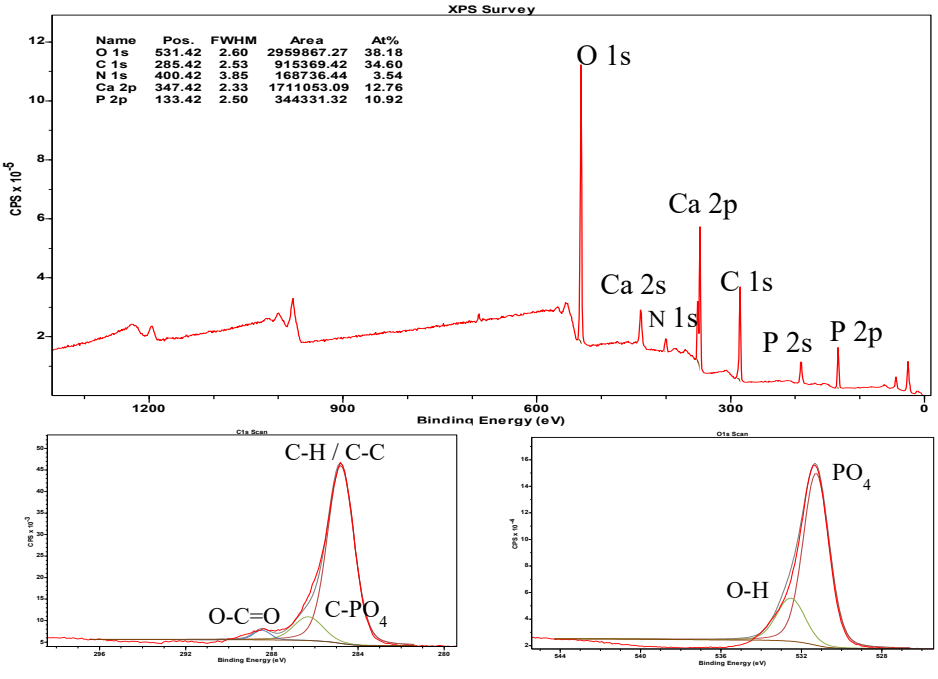

Figure 34 - XPS spectra of empty calcium phosphate cores.
High-resolution spectrum (top, a), C1s spectrum (bottom-left, a), O1s (bottom-right, c).

The XPS analysis was also performed with the aim to give a strong confirm about the deposition of layers. Figure 35 shows peaks in the XPS spectrum after the deposition of layers. It is immediately clear that carbon and nitrogen amount widely increased due to the presence of CHI and ALG in comparison with the previous chart. Those peaks highlight the presence of the layers, especially the CHI contains a high concentration of amino groups, while the ALG gives a contribute to the amount of C and O. The little quantity of Sodium (Na) at 1070 eV could be explained by the addition of sodium chloride inside polyelectrolyte solution to stabilize them which might remain entrapped inside layers. From the C1s and O1s there were not differences excepted for a higher peak at 286 eV representing C-O which could be related to the polyelectrolytes chemical structure.

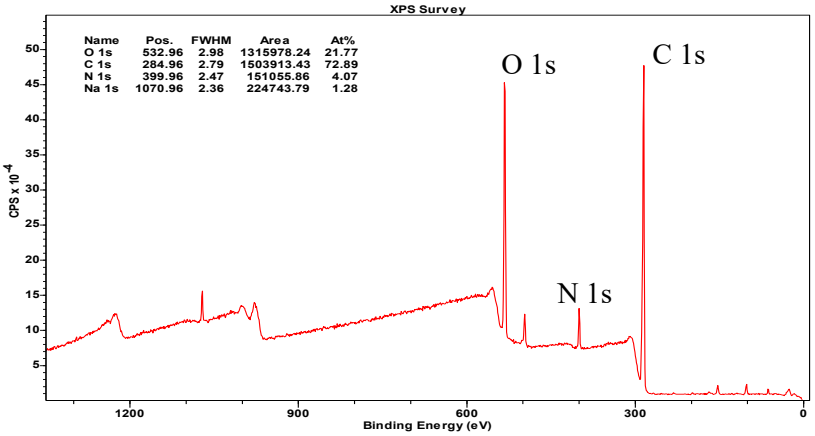

Figure 35 - XPS spectra of formulation with layers.

6.3 Carbon dots

The initial objective of this project was to create a nanotheranostic approach to treat PCa and OSa. For the part of diagnose, CQD have been chosen as probe to follow up the disease and at the same time to confirm the right accumulation inside the specific location. Carbon dots have been encapsulated in the last layer of CHI, due to the mandatory positioning inside the last layer to enhance the fluorescent emission of the latter. Carbon dots solution was transferred and diluted inside the CHI solution. However, before starting, the CQD-containing solution was analysed and although the stock solution of carbon dots was negative, the interaction with the CHI increases the positive charge of the polyelectrolyte, increasing the value 14.4+-2.46 mV to 19.67+-1.72 mV. It was unexpected, even so it represented a better solution for the cationic layer. A possible explanation was the dilution of a x4 factor and the possibility that carbon dots mimicked a core around which CHI deposited due to the electrostatic force. Indeed, the overall zeta-potential value of NPs covered by this new solution remained the same of the NPs covered with alone CHI.

Secondly, the presence of carbon dots was confirmed by a microscope used for detecting the blue emission report by the seller of CQD. In each formulation was passible to notice the presence of blue crystals both alone and aggregated (Figure 36).

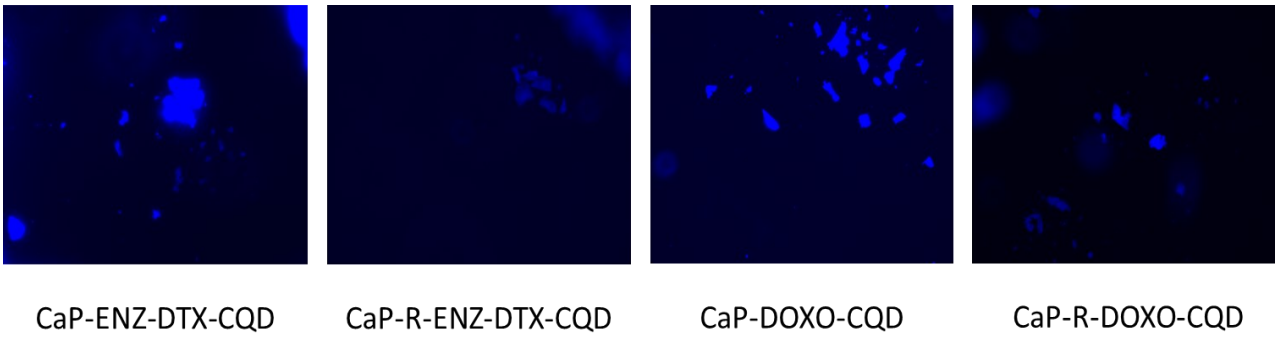

Figure 36 - Fluorescence of CQD-containing formulations.

6.4 Active targeting agents

Active targeting agents are one of the most exploited group of molecules in combination with NPs, especially they give the ability to reach, interact and/or penetrate inside specific cells, whether they are physiological or pathological. In particular, for a nanotheranostic approach is almost mandatory having molecules for that aim. In this specific project, two different strategies of active targeting have been developed to specifically target either PCa or OSa.

For prostate cancer

The PSMA-617 ligand has been attached at the surface using the carbodiimide chemistry. The FTIR-ATR device was used to assess the presence upon the surface of the ligand. From Figure 37, it is immediately clear that specific peaks increased in high and could confirm the presence of the active targeting molecule. In the region between 1300 and 1700 cm-1 two peaks were prominent, a first one at around 1620 cm^{-1} related to the C=O stretching and a second one associated to C-N stretching at about 1350.

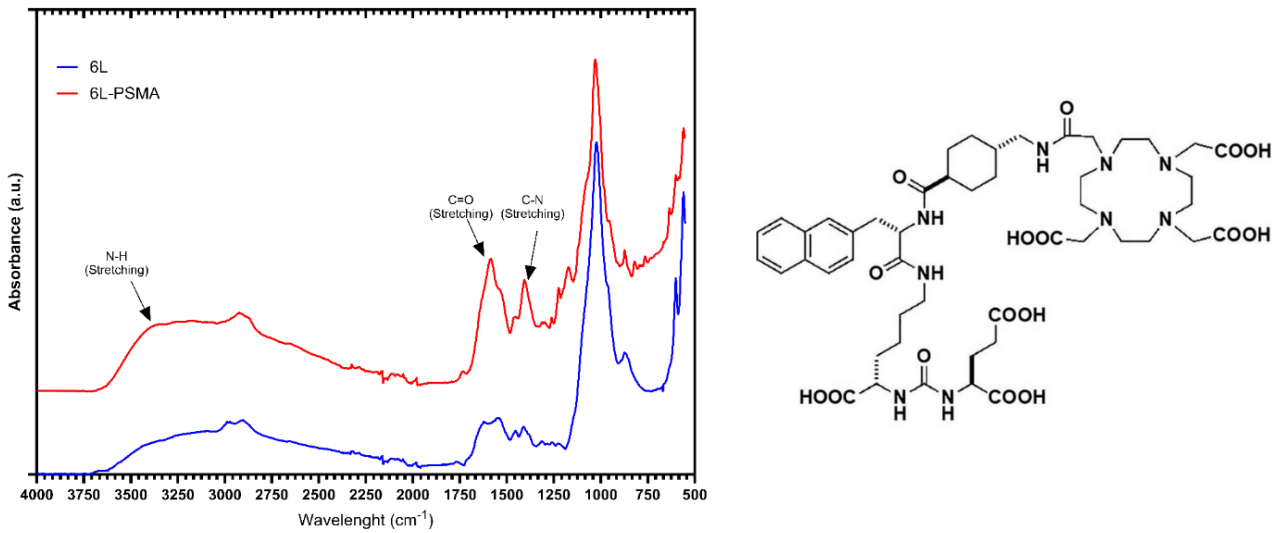

Figure 37 - FTIR spectrum of formulation functionalized with PSMA-617 (left) and chemical structure of PSMA-617.

For osteosarcoma

In the specific formulation designed for OSa, CHI layer was covered by a further layer of HA using the same procedure seen for LbL technique. For this particular reason, there were not influences by the covalent bonds formed with carbodiimide. The positions of the peaks were comparable with the previous curve and they found confirm in a study which employed HA[178]. Therefore, the stretching of C=O and C-N were located around 1600 and 1350 cm^{-1}. Lastly, the higher region between 3000 and 3500 cm-1 may indicate an increased value of amino group and this confirm the deposition of the HA layer (Figure 38).

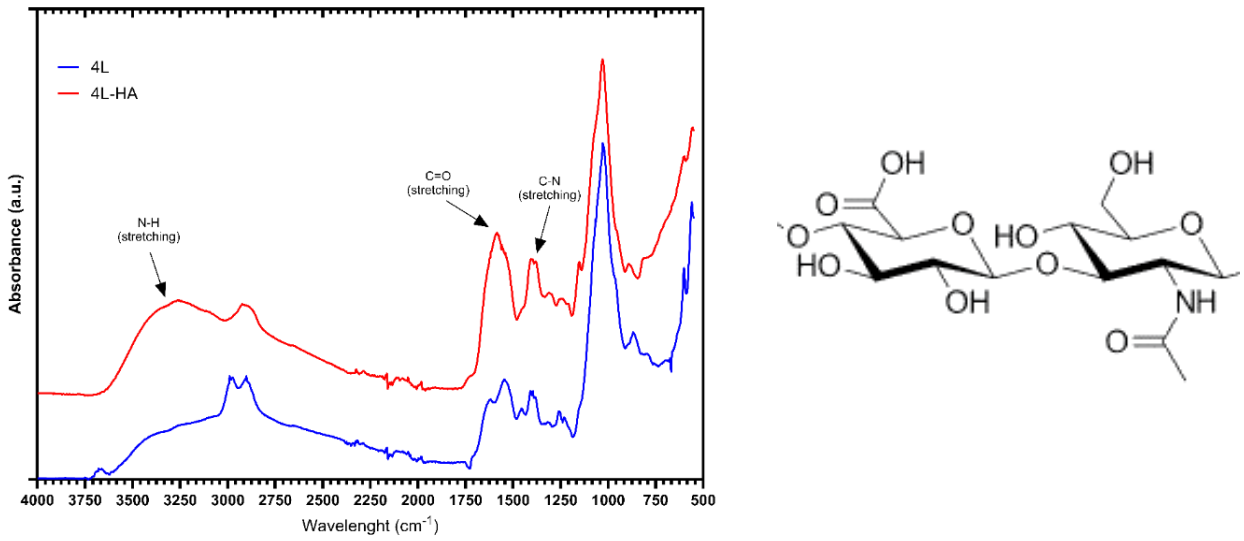

Figure 38 - FTIR spectrum of formulation functionalized with HA (left) and chemical structure of HA.

6.5 Spheroid formation

After the seeding inside the u-bottom-wells plate cells have been followed up to check the growth for 10 days, especially the parameters taken into account were the size and the homogeneity of the spheroid structure. The test was mandatory to decide the cell line to use for 3D tests in addition with the right time point. Therefore, the information acquired lead to choose Vcap and U2os as lines for 3D models and the NPs were inserted after 2 and 4 days on culture containing 10k cells.

For prostate cancer

Overall, for the PCa the Lncap cells expressed the higher size but with a lower organization of their spheroid structures plenty of fenestration in comparison with Vcap spheroids that were smaller but better organized (Figure 40). In the first time point, both cell lines expressed a similar diameter with a linear growth in dependence with the density, especially no statistical differences could be discerned. However, Lncap in the sequential time points increased in the size in a bigger way than Vcap (Figure 39). Although with the same size, the dispositions of the structures were pretty much different. The shape of Vcap remained much spherical

and it was simple to distinguish the different cells, in contrast Lncap seemed to be more cohesive with a higher number of cells in the centre of the sphere. In the consecutive time points the difference enhanced, the Lncap spheroid size increased more than Vcap, so much so that the 3d model of Lncap could be noticed by naked eye. Instead, spheroid made up by Vcap remained with a smaller size and had a liner growth, with a characteristic shape and discernible cells from others. In this case, Vcap have been chosen as cells for 3d cytotoxicity tests, mainly due to their structure without lacks and a more linear growth that was thought to better mimic the real behaviour inside the body. At the end 10k cells were seeded again for cytotoxicity test and treated with 2 and 4 days as time points.

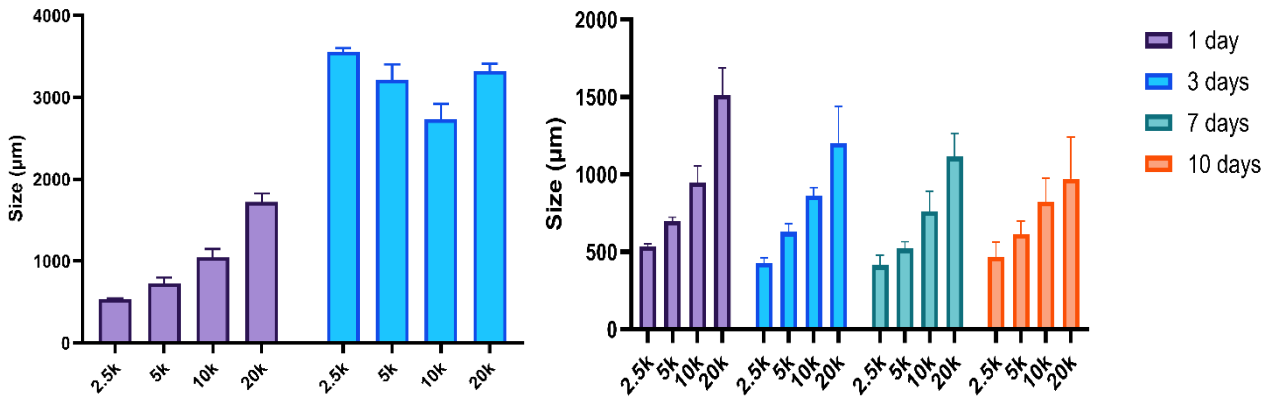

Figure 39 - Comparison between Lncap (left) and Vcap (right) spheroids with 2.5k, 5k, 10k, 20k cells and after 1, 3, 7, 10 days.

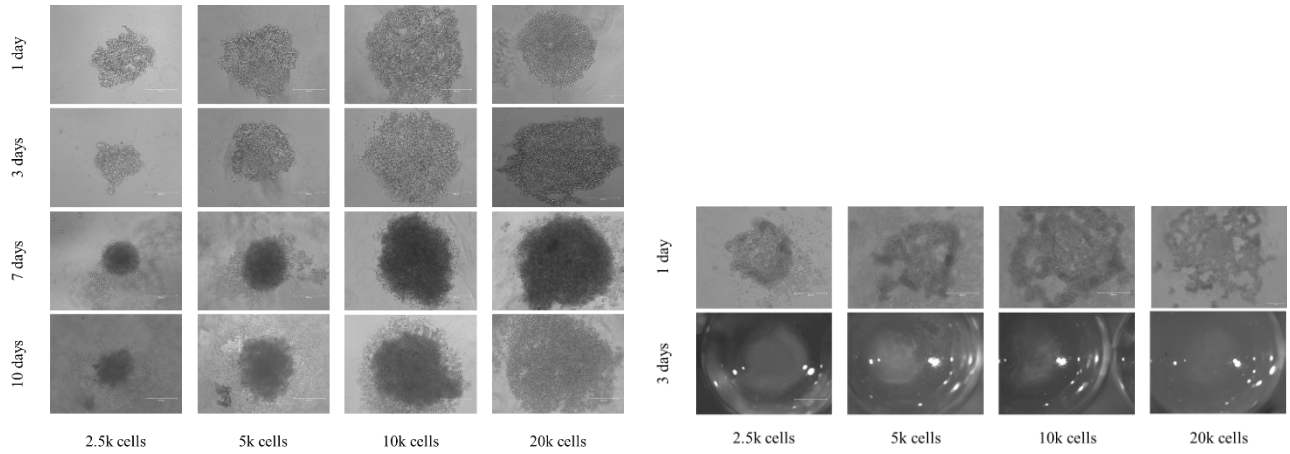

Figure 40 - Pictures of Vcap (left) and Lncap (right) spheroids.

For osteosarcoma

In the specific case of OSa, Figure 41 shows that both Saos and U2os shared the same behaviour. The first day the pair of lines had an initial size dependent on an initial aggregation, that in U2os was higher than Saos. After the first day, cells started to aggregate in order to organize their structure and start growing. Moreover, as expected, the size increase with higher densities. The trend of cells growth was thus linear and then positive, if the experiment was proceeded over 10 days it would have seen an increase that would indicate proliferation of cells, and it is confirmed by the slightly increasing of the diameter at 10 days. Regarding the cell line selected for cytotoxicity tests, U2os line has been chosen due to higher organized structure and the size that was thought to better mimic the real disease (Figure 42). For the time point, 3 days were enough to acquire a good structure without fenestration and to limit a further reduction of the diameter. Furthermore, over 3 days cells started undergoing death with the origin of a necrotic core.

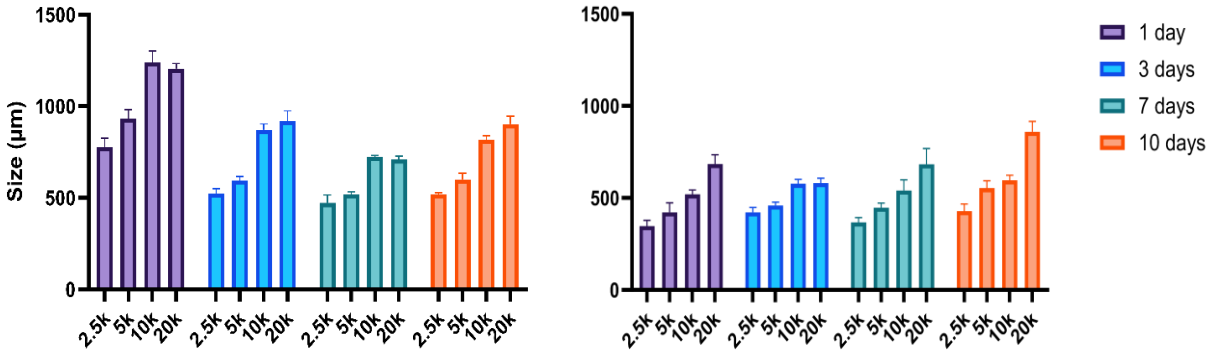

Figure 41 - Pictures of U2os (left) and Saos (right) spheroids.

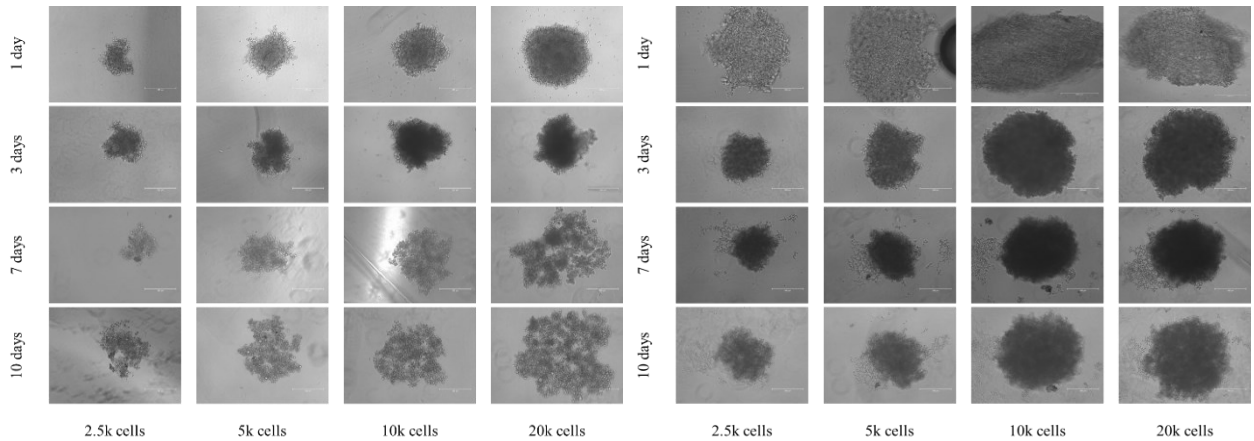

Figure 42 - Comparison between Saos(left) and U2os (right) spheroids with 2.5k, 5k, 10k, 20k cells and after 1, 3, 7, 10 days.

6.6 Cytotoxicity evaluation

After nanoparticle have been extensively studied throughout physicochemical analyses, the efficiency of them was evaluated by cytotoxicity tests on cell cultures. The cytotoxicity has been tested both for PCa and OSa cells, directly on 2D models or 3D models. The tests relied on PrestoBlue and Live/Dead assays.

PrestoBlue. The PrestoBlue is a quantitative assay that evaluate the fluorescence emitted in the blue spectrum and related it to the viability of cells in an indirect way. In this specific project it has been employed to understand the viability of cell lines after the delivery of drugs from the NPs created. For each run two time points have been chosen, sometimes the first one was enough to kill a remarkable part of cells, while in others only the second time point expressed meaningful values.
Live/Dead. The PrestoBlue is a qualitative assay that evaluate by coloration the viability of cells. In this specific project it has been employed to understand the viability of cells after the delivery of drugs from the NPs created. In particular, the colours exploited were green for dead cells and blue for live cells.

Prostate cancer – 2D

Lncap and Vcap have been treated using the formulation CaP-R-ENZ-DTX and CaP-ENZ-DTX and data have been recorded at 24 hours and 5 days.

Figure 43 below shows the cytotoxicity profile on Lncap cells, and immediately it is possible to notice differences in having RESV inside particles or not. Overall, comparing the formulation grouped by time points, the RESV was able to reduce the viability of cells, especially statistical relevance has been recorded between the lowest concentrations with and without RESV.

Focusing on CaP-ENZ-DTX, the viability of cells which received 1000 μg/mL was lower than the others, and this confirm that the systems were able to deliver the chemotherapeutic molecules affecting the cells in a directly proportional way. On the other hand, the RESV-containing NPs (CaP-R-ENZ.DTX) worked better using 100 μg/mL on tumour cells. A possible explanation of this peculiar behaviour could firstly confirm that RESV enhances the efficacy of selected drugs in a long-term way due to the encapsulation strategy exploited, and secondly it lets hypothesize that the antioxidant is better released when NPs are highly diluted avoiding agglomerate that can hind the releasing. Indeed, in the specific case of this project the behaviour might be due to the presence of aggregates that prevent the RESV from being fairly released. Nevertheless, the overall values indicated that after 5 days the viability of cells was reduced, also confirming the discovered by the release in PBS (6.1.3).

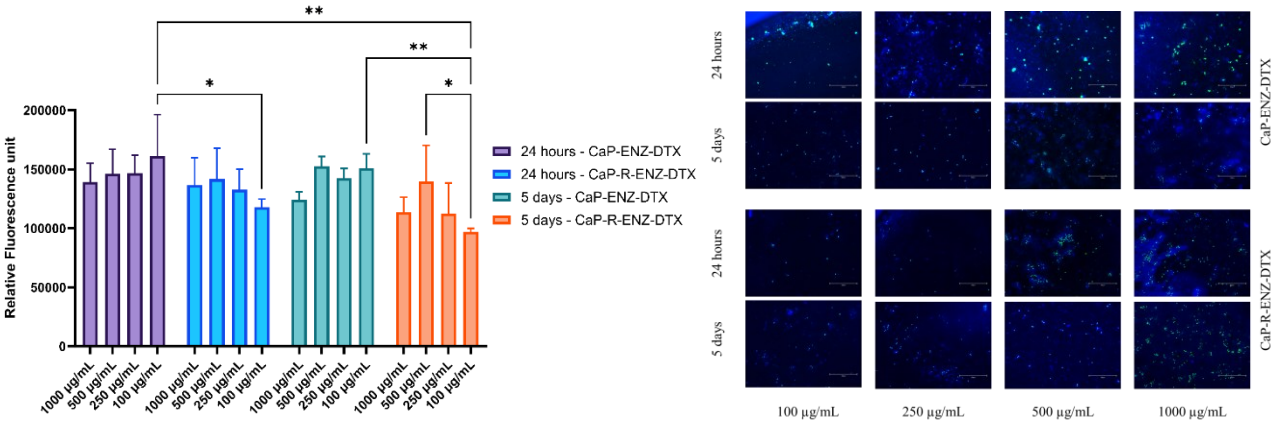

Figure 43 - PrestoBlue values and Live/Dead pictures of Lncap 2D model.

The behaviour described for Lncap has been confirmed also by Vcap. The results exposed in Figure 44 reveals promising response after the uptake of NPs, and one of the first interesting outcome was the wide decreasing of viability after the second time point. All the concentrations were able to significantly kill cells, reducing their number of a percentage around 40%, as highlighted by the statistical differences. Moreover, as seen before for Lncap, CaP-ENZ-DTX followed a trend in which higher concentrations were more deleterious for cells in an expected way, the RESV-containing formulation, CaP-R-ENZ-DTX, worked better with the lowest concentration.

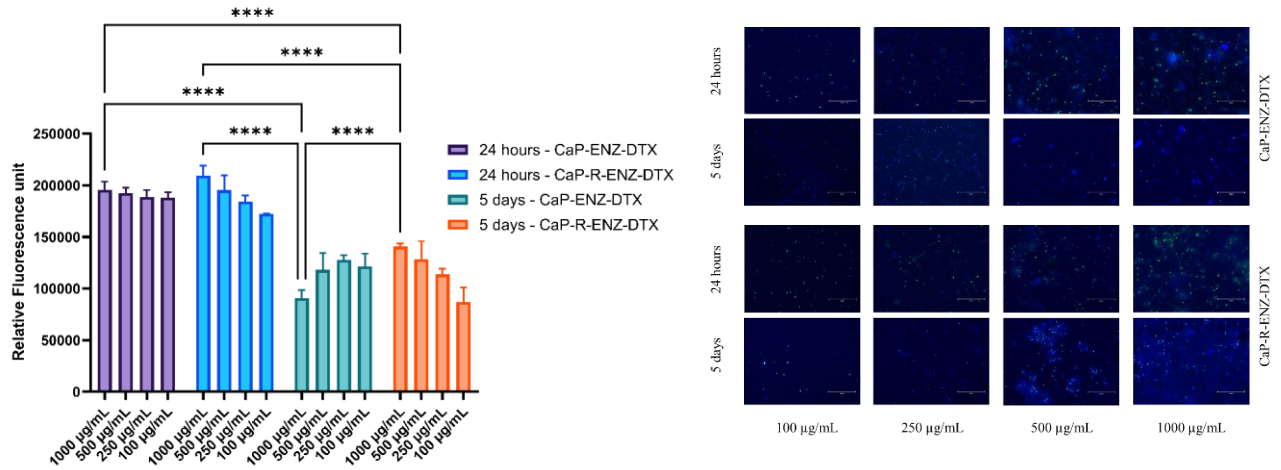

Figure 44 - PrestoBlue values and Live/Dead pictures of Vcap 2D model.

Prostate cancer – 3D

The 3D tests for PCa relied only on Vcap since, as reported above (Figure 45, Figure 46), the spheroid properties of the latter were better than Lncap (6.5). From , it is immediately clear that the viability of cells was highly affected during the two time points. Focusing on the first time point, CaP-ENZ-DTX NPs had a better cytotoxic profile with 500 µg/mL rather than 1000 µg/mL, especially in the first case only around the 10% of cells have been killed while in the second more than the 20%. In contrast, CaP-R-ENZ-DTX NPs had statistical differences and with the highest concentration they were able to reduce the cell number of 30% and of 35% with the lowest. The cytotoxicity had a reversed profile regarding the expectation, the lowest concentration could work better in the first time point due to a higher dilution of NPs that not aggregated can better penetrate inside the organized structure of spheroids. Nevertheless, in the second time point the overall viability was lower than the first and in addition the trend was in line with a directly proportional relationship between concentration and viability. In particular, CaP-ENZ-DTX recorded the higher cytotoxicity activity killing almost the 40% of cells. The opposite trend could be related to the higher quantity of drugs released inside the microenvironment of the spheroids that were able to better penetrate inside the cells. Overall, the second time point indicates that for an initial period the cells died, although for the lower concentration cells were able to rearrange and restart to proliferate, instead higher concentrations have higher amount of drug and can prolong their releasing.

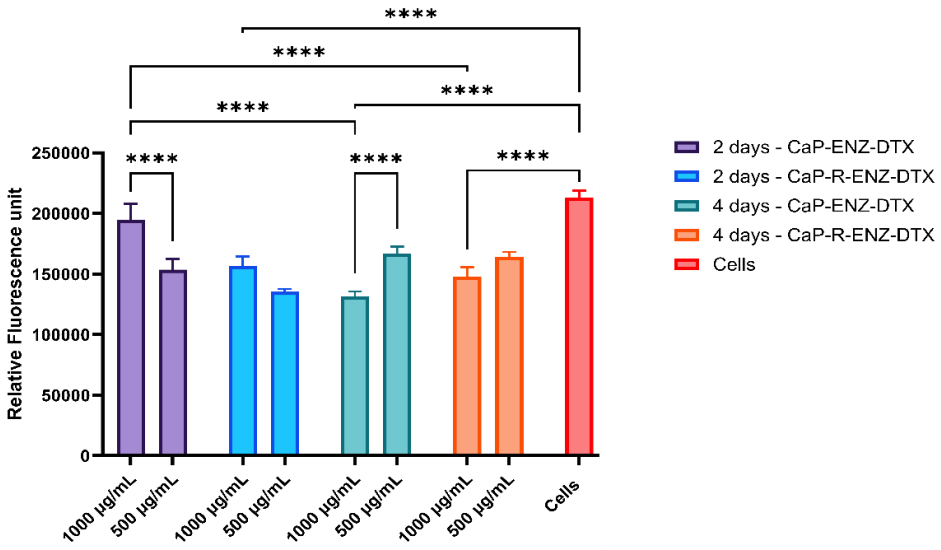

Figure 45 - PrestoBlue values of Vcap 3D model.

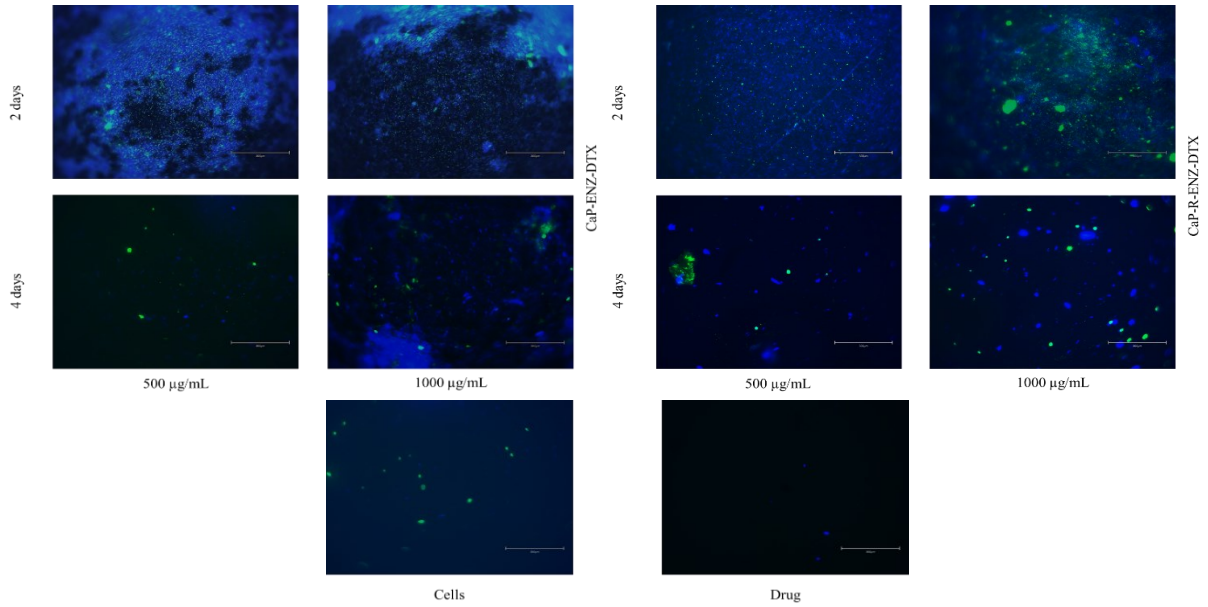

Figure 46 - Live/Dead pictures of Vcap cells in the 3D model.

Osteosarcoma – 2D

Saos and U2os have been treated using the formulation CaP-R-DOXO and CaP-DOXO and data have been recorded at 24 hours and 5 days. From Figure 47, it is immediately clear that in case of DOXO the trend followed the expectation for each time point and formulation, therefore, 1000 µg/ml leaded to the lowest viability of cells. Focusing on CaP-DOXO, the formulation more affected cells in the first 24 hours, while after 5 days the number of cells increased, and in addition the behaviour was enhanced for lower concentrations. It may indicate that the amount of DOXO was not enough, and cells proliferate even with the presence of the drug. In contrast, CaP-R-DOXO expressed a higher cytotoxic activity, resulting in a good combination of RESV with the chemotherapeutic molecule. In this case, RESV could act in a predictable way, and this could be due to the lower number of layers in comparison with the CaP-R-ENZ-DTX and CaP-ENZ-DTX.

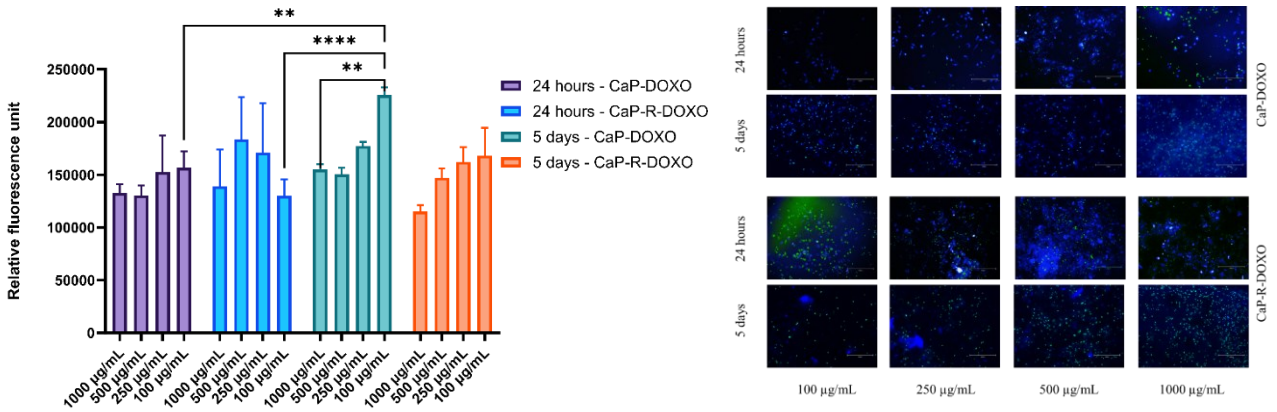

Figure 47 - PrestoBlue values and Live/Dead pictures of Saos 2D model.

U2os behaviour is reported in Figure 48. The values express that the time played an important role in treating this kind of cells. Indeed, both formulations had an increased cytotoxicity activity after 5 days, 3-fold higher than the one recorded at 24 hours. Nevertheless that, in comparison with Saos behaviour, the trend is nearly different, not statistically differences have been observed between different concentrations of the same formulation. It is worth noticing that DOXO, in addition to nanolayers, was also encapsulated inside the cores increasing the quantity of available drug and this could have slowed down the delivery of the latter. Furthermore, no relevance has been observed with RESV, indicating that the quantity of DOXO, higher than the amount of RESV, leaded the process.

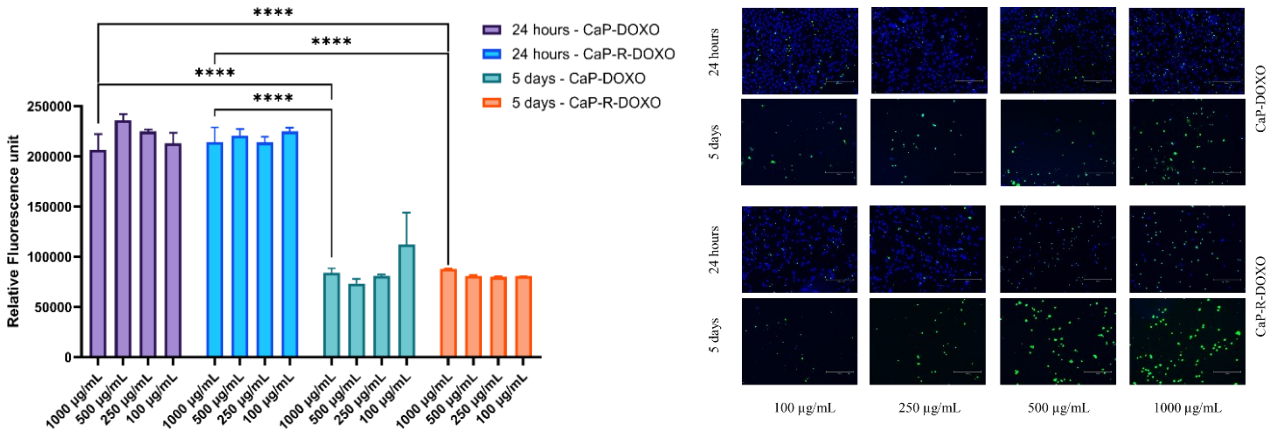

Figure 48 - PrestoBlue values and Live/Dead pictures of U2os 2D model.

Osteosarcoma – 3D

Osteosarcoma cultures have been modelized also in 3D to better mimic the real disease.

In the case of OSa, U2os have been employed to produce and test spheroids. From both Figure 49 and Figure 50, it can be understood that after 4 days spheroids have been highly affected by DOXO and RESV. The trend of U2os in 3D structure is comparable with the one seen for 2D models. In particular, no meaningful differences have been reported between CaP-R-DOXO and CaP-DOXO confirming that the DOXO overcomes RESV action as seen for 2D tests. Moreover, both of them reduce in the same percentage the number of cells. Focusing on the second time point, the releasing of therapy is well confirmed and the number cells decrease to the 20%. Overall, the cytotoxic profile revealed by this results reinforces the hypothesis that DOXO is fairly released in the tumour microenvironment penetrating in a high quantity inside cells.

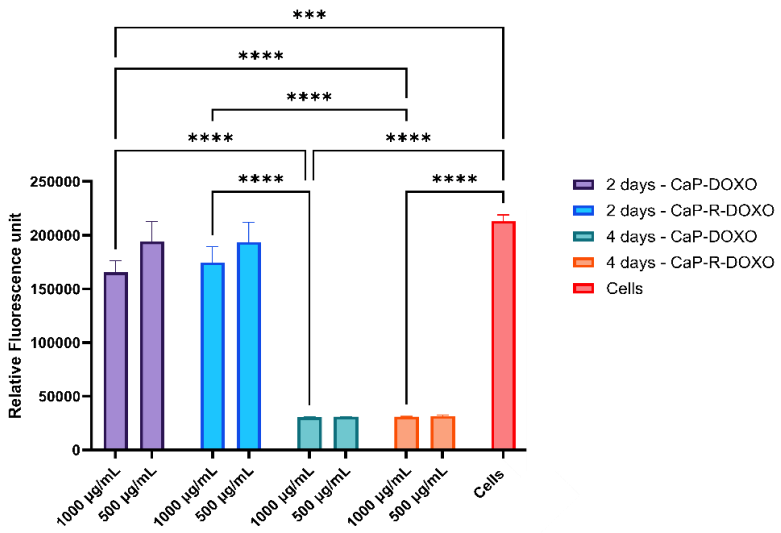

Figure 49 - PrestoBlue values of U2os 3D model.

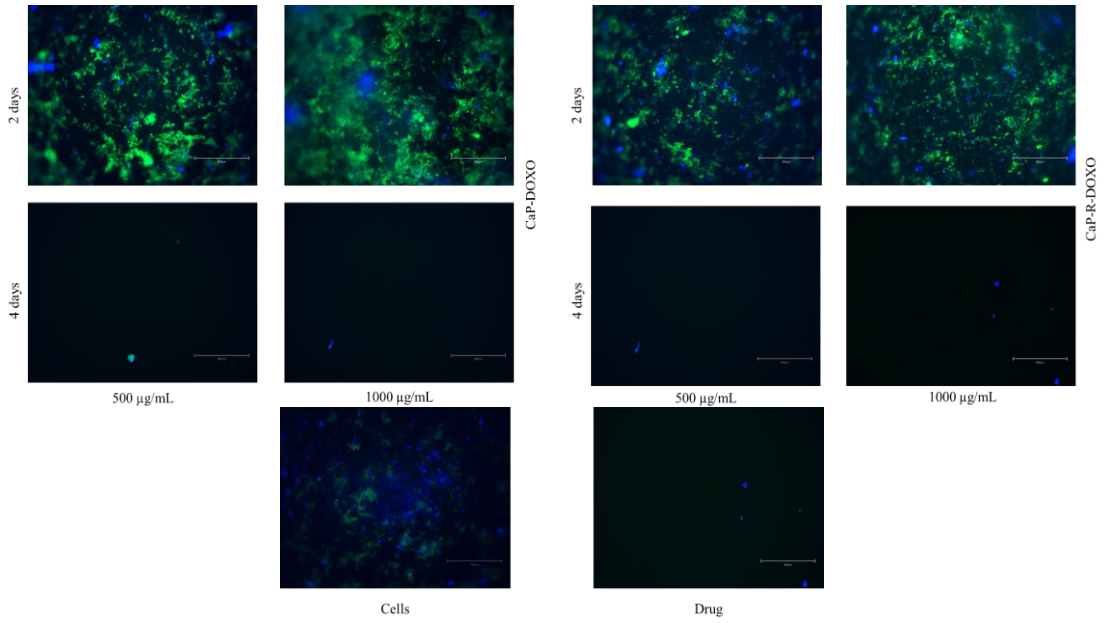

Figure 50 - Live/Dead pictures of U2os cells in the 3D model.

CONCLUSIONS

In this study, calcium phosphate (CaP) nanoparticles (NPs) have been used to develop a nanotheranostic approach to treat two forms of tumours, prostate cancer (PCa) and osteosarcoma (OSa). The CaP NPs showed a highly versatility allowing to encapsulate a wide spectrum of drugs without affecting the overall stability of the cores.

In the specific case of PCa, the cores of the inorganic materials constituted the template for a formulation loading docetaxel (DTX) and enzalutamide (ENZ) with a specific gradient, while in addition resveratrol (RESV) and PSMA ligand are respectively thought to reduce the inflammation in the microenvironment tumour and to specifically bind prostate cancer cells due to higher affinity. On the other hand, CaP NPs showed promising ability to encapsulate doxorubicin (DOXO) and interact with more affinity with cells by hyaluronic acid (HA). All the formulations have been tested in term of their physicochemical and morphological properties. Moreover, formulations have been used to demonstrate as well as possible their therapeutic effect testing their cytotoxicity in in vitro cultures of Lncap and Vcap for PCa and Saos and U2os for OSa.

The designed particles were characterized by containing different molecules, and in addition they were stabilized by the presence of PAH that was also useful in its ability to give an initial positive charge upon the surface. In the specific case of DOXO, an optimizing step was performed for trying to insert a high amount of drug without affecting stability, the overall result was a high encapsulation assessed by entrapment efficiency formula and in addition confirmed by a reduction of the DOXO-containing cores size due to electrostatic affinity between materials and the drug.

The project continued with the further modification of the surface of cores, it is worth considering that CaP surface is less suitable for chemical addition than other types of NPs, instead they are highly suitable for physical modification due to their electrostatic nature, and due to this, layer-by-layer was selected to improve the drug loading and the addition of specific molecules for imaging and targeting. The core was functionalized with 6 layers and 4 layers respectively for PCa and OSa with alginic acid (ALG) and chitosan (CHI) as polyelectrolytes. Alginic acid and CHI are two natural polymers that express interesting and promising qualities for biomedical applications, in particular they are natural compound with a high biocompatibility also due to their biodegradability inside human body, in addition at specific conditions they have net charges, especially a positive charge for CHI and negative in the case of ALG. The layers in each formulation worked as containers for the drugs, especially for ENZ and DTX, ALG was the selected polymer to encapsulate them, while in the case of DOXO the CHI was the more affine type of layer, moreover, RESV was inserted with good results in the negative layers of each formulation which encapsulated it. After initial test on the described layered cores, the targeting and imaging molecules were designed to be added. For allowing the theranostic models to be completed, carbon quantum dots (CQD) were exploited and inserted in the outermost layer of CHI to avoid artifacts due to their depth. In particular, the CQD were chosen for their lower toxicity in

comparison with the semi-metallic quantum dots, and in addition for their more similar chemistry to human body molecules. On the other hand, it has been designed a way for allowing NPs to reach and stay in the right site of tumour, avoiding a permanent circulation around the body due to their stability at neutral and alkaline pH or the releasing in the wrong location for the presence of a physiological acid environment. Therefore, for PCa, PSMA-617 ligand was properly grafted upon the last layer of CHI connecting amino groups of the polymer with the carboxyl groups of the ligand through the carbodiimide chemistry. On the other hand, for OSa, HA, that is a glycosaminoglycan with a negative charge, was added as a new layer upon the last layer of CHI and it was thought to interact more times with osteosarcoma due to the overexpression of CD44 receptors highly affine with the molecule chosen.

All the formulation after the manufacturing process have been characterized by morphological and physicochemical analysis. In particular, TEM analyses have shown differences between sizes of cores and after the deposition of layer and around 60 nm were added for the formulations with DOXO and around 40 nm for the formulations designed for PCa with some differences starting from the empty cores or RESV containing. However, the deposition of layers was confirmed by the zeta-potential evaluation, in particular the inversion of the charge after the deposition of each polyelectrolyte upon the surfaces demonstrated a well covering not affected by the presence of drugs. At the same time FTIR and XPS analyses were performed with the aim to spot from their spectra the presence of specific chemical groups as well as atoms upon the surfaces characterized. It is worth noticing that FTIR confirmed the presence of specific bonds and their vibration and thus to assess the presence of CHI and ALG as well drugs, in contrast XPS showed the same results but analysing the atomical content of the surfaces. In the specific case of FTIR, some runs have been performed to detect the presence of the targeting compounds and thus confirm the right addition of HA and PSMA-617 ligand.

Subsequentially, the cytotoxicity of the formulations was tested by exploiting 2D and 3D models of 4 different cell lines. Among the cell lines for prostate cancer were Lncap and Vcap, while for osteosarcoma were chosen Saos and U2os. For all 2D tests, 2 time points have been chosen, 24 hours and 5 days, and 4 concentrations have been selected, 100 ug/mL, 250ug/mL, 500 ug/mL and 1000 ug/mL. The availability of cells was evaluated by the PrestoBlue and Live/Dead assays.
Lastly, considering tests in 2D cultures to perform comparison, also 3D models have been tested in this project to better mimic the real structure of in vivo and real tumours. A first set of experiments was performed to understand the forming process of spheroid of each cell line. A first result was acquired for prostate cancer, after 10 days Lncap grew in higher size in comparison with Vcap, even so they were less structured and with holes, and thus Vcap were chosen to follow with 3D tests. On the other hand, for osteosarcoma only U2os were chosen because the size of Saos spheroids was drastically lower and in addition the structure had too many fenestrations. After the cell lines for spheroids were chosen, the cytotoxicity effect of NPs was tested again on spheroids using only the highest concentration.

FUTURE PROSPECTIVE

The formulations exposed in this project have expressed promising ability to loading different type of drugs and release them to treat cancer cells. Although promising, the system could be furtherly improved. In particular DOXO has been tested with only 3 different concentrations while DTX was not optimized at all, and so other optimising steps may be performed. This is true also for the therapeutic agents added in layers that could be increased in their amount verifying not to affecting the overall process. In this specific project drugs have been inserting in the solutions with the same charge, for adding further analysis it could be interesting to understand if inserting them in the opposite charged layer could increase the uptake without affecting the structure of the latter. Moreover, the specific disposition used may be changed to confirm or not if it was the best kinetics to release drugs and at the same time avoiding cross-interaction limiting the therapeutic effects. Regarding cytotoxicity models, the 3D models were made up by spheroids, although the structure was better than 2D tests, it was missing several parts to increase the mimicking level, as for examples other cellular components as well as specific conditions and agents. Therefore, 3D models require to add other components to verify the ability of NPs to treat a realer model. Lastly, the imaging and targeting agents should be tested in more complex models, as for example in vivo, to realistically confirm their ability to emit fluorescence and be detected and to interact with the specific tumour environment without affecting wrong location with unwanted side effects.

BIBLIOGRAPHY

1. *How does prostate work?* vol. InformedHealth.org (2006).
2. McNeal, J. E. Normal Histology of the Prostate. *Am J Surg Pathol* **12**, 619–633 (1988).
3. Di Sant'Agnese, P. A. Neuroendocrine cells of the prostate and neuroendocrine differentiation in prostatic carcinoma: a review of morphologic aspects. *Urology* **51**, 121–124 (1998).
4. Isaacs, J. T. Prostatic structure and function in relation to the etiology of prostatic cancer. *Prostate* **4**, 351–366 (1983).
5. Chung, L. W. The role of stromal-epithelial interaction in normal and malignant growth. *Cancer Surv* **23**, 33–42 (1995).
6. Carbajal-García, A., Reyes-García, J. & Montaño, L. M. Androgen Effects on the Adrenergic System of the Vascular, Airway, and Cardiac Myocytes and Their Relevance in Pathological Processes. *Int J Endocrinol* **2020**, 1–25 (2020).
7. Webb, S. J., Geoghegan, T. E., Prough, R. A. & Michael Miller, K. K. The Biological Actions of Dehydroepiandrosterone Involves Multiple Receptors. *Drug Metab Rev* **38**, 89–116 (2006).
8. Tang, J., Chen, L.-R. & Chen, K.-H. The Utilization of Dehydroepiandrosterone as a Sexual Hormone Precursor in Premenopausal and Postmenopausal Women: An Overview. *Pharmaceuticals* **15**, 46 (2021).
9. Nassar, G. N. & Leslie, S. W. *Physiology, Testosterone*. (2023).
10. Morley, J. The benefits and risks of testosterone replacement therapy: a review. *Ther Clin Risk Manag* 427 (2009) doi:10.2147/TCRM.S3025.
11. Wolfe, R., Ferrando, A., Sheffield-Moore, M. & Urban, R. Testosterone and Muscle Protein Metabolism. *Mayo Clin Proc* **75**, S55–S60 (2000).
12. Marchetti, P. M. & Barth, J. H. Clinical biochemistry of dihydrotestosterone. *Annals of Clinical Biochemistry: International Journal of Laboratory Medicine* **50**, 95–107 (2013).
13. Wilson, J. D., George, F. W. & Griffin, J. E. The Hormonal Control of Sexual Development. *Science (1979)* **211**, 1278–1284 (1981).
14. Kaipainen, A. *et al.* Testosterone accumulation in prostate cancer cells is enhanced by facilitated diffusion. *Prostate* **79**, 1530–1542 (2019).
15. Anthony, P. & Sant'agnese, D. I. *NEUROENDOCRINE CELLS OF THE PROSTATE AND NEUROENDOCRINE DIFFERENTIATION IN PROSTATIC CARCINOMA: A REVIEW OF MORPHOLOGIC ASPECTS*. (1998).
16. Davey, R. A. & Grossmann, M. *Androgen Receptor Structure, Function and Biology: From Bench to Bedside*. *Androgen Receptor Biology Clin Biochem Rev* vol. 37 (2016).
17. Heinlein, C. A. & Chang, C. Androgen Receptor (AR) Coregulators: An Overview. *Endocr Rev* **23**, 175–200 (2002).
18. Leek, J. *et al.* Prostate-specific membrane antigen: evidence for the existence of a second related human gene. *Br J Cancer* **72**, 583–588 (1995).

19. Su, S. L., Huang, I. P., Fair, W. R., Powell, C. T. & Heston, W. D. Alternatively spliced variants of prostate-specific membrane antigen RNA: ratio of expression as a potential measurement of progression. *Cancer Res* **55**, 1441–3 (1995).

20. Bostwick, D. G., Pacelli, A., Blute, M., Roche, P. & Murphy, G. P. Prostate specific membrane antigen expression in prostatic intraepithelial neoplasia and adenocarcinoma. *Cancer* **82**, 2256–2261 (1998).

21. Thompson, I. M. *et al.* Prevalence of Prostate Cancer among Men with a Prostate-Specific Antigen Level ≤4.0 ng per Milliliter. *New England Journal of Medicine* **350**, 2239–2246 (2004).

22. Ferlay, J. *et al.* Cancer statistics for the year 2020: An overview. *Int J Cancer* **149**, 778–789 (2021).

23. Bergengren, O. *et al.* 2022 Update on Prostate Cancer Epidemiology and Risk Factors—A Systematic Review. *European Urology* Preprint at https://doi.org/10.1016/j.eururo.2023.04.021 (2023).

24. Lim Ng, K. The Etiology of Prostate Cancer. in *Prostate Cancer* 17–28 (Exon Publications, 2021). doi:10.36255/exonpublications.prostatecancer.etiology.2021.

25. Jarvis, T., Chughtai, B. & Kaplan, S. Testosterone and benign prostatic hyperplasia. *Asian J Androl* **17**, 212 (2015).

26. Isaacs, J. T. Prostate stem cells and benign prostatic hyperplasia. *Prostate* **68**, 1025–1034 (2008).

27. Berry, S. J., Coffey, D. S., Walsh, P. C. & Ewing, L. L. The Development of Human Benign Prostatic Hyperplasia with Age. *Journal of Urology* **132**, 474–479 (1984).

28. McNeal, J. E. The zonal anatomy of the prostate. *Prostate* **2**, 35–49 (1981).

29. Isaacs, J. T. & Coffey, D. S. Etiology and disease process of benign prostatic hyperplasia. *Prostate* **15**, 33–50 (1989).

30. Schaeffer, A. J. Chronic Prostatitis and the Chronic Pelvic Pain Syndrome. *New England Journal of Medicine* **355**, 1690–1698 (2006).

31. Krieger, J. N. NIH Consensus Definition and Classification of Prostatitis. *JAMA: The Journal of the American Medical Association* **282**, 236–237 (1999).

32. Brunner, H., Weidner, W. & Schiefer, H.-G. Studies on the Role of Ureaplasma urealyticum and Mycoplasma hominis in Prostatitis. *Journal of Infectious Diseases* **147**, 807–813 (1983).

33. Alexander, R. B. & Trissel, D. Chronic prostatitis: Results ofan internet survey. *Urology* **48**, 568–574 (1996).

34. Weidner, W. Relevance of male accessory gland infection for subsequent fertility with special focus on prostatitis. *Hum Reprod Update* **5**, 421–432 (1999).

35. Ruska, K. M., Sauvageot, J. & Epstein, J. I. Histology and Cellular Kinetics of Prostatic Atrophy. *Am J Surg Pathol* **22**, (1998).

36. van Leenders, G. J. L. H. *et al.* Intermediate Cells in Human Prostate Epithelium Are Enriched in Proliferative Inflammatory Atrophy. *Am J Pathol* **162**, 1529–1537 (2003).

37. Woenckhaus, J. & Fenic, I. Proliferative inflammatory atrophy: A background lesion of prostate cancer? in *Andrologia* vol. 40 134–137 (2008).

38. Kim, H. L. & Yang, X. J. *PREVALENCE OF HIGH-GRADE PROSTATIC INTRAEPITHELIAL NEOPLASIA AND ITS RELATIONSHIP TO SERUM PROSTATE SPECIFIC ANTIGEN*. *Clinical Urology International Braz J Urol Official Journal of the Brazilian Society of Urology* vol. 28.

39. Cheville, J. C., Reznicek, M. J. & Bostwick, D. G. The Focus of "Atypical Glands, Suspicious for Malignancy" in Prostatic Needle Biopsy Specimens: *Incidence, Histologic Features, and Clinical Follow-Up of Cases Diagnosed in a Community Practice*. *Am J Clin Pathol* **108**, 633–640 (1997).

40. Epstein, J. I. Precursor lesions to prostatic adenocarcinoma. *Virchows Archiv* vol. 454 1–16 Preprint at https://doi.org/10.1007/s00428-008-0707-5 (2009).

41. Goeman, L. *et al.* Is low-grade prostatic intraepithelial neoplasia a risk factor for cancer? *Prostate Cancer Prostatic Dis* **6**, 305–310 (2003).

42. De Marzo, A. M., Haffner, M. C., Lotan, T. L., Yegnasubramanian, S. & Nelson, W. G. Premalignancy in Prostate Cancer: Rethinking What We Know. *Cancer Prevention Research* **9**, 648–656 (2016).

43. Herawi, M., Kahane, H., Cavallo, C. & Epstein, J. I. Risk of Prostate Cancer on First Re-Biopsy Within 1 Year Following a Diagnosis of High Grade Prostatic Intraepithelial Neoplasia is Related to the Number of Cores Sampled. *Journal of Urology* **175**, 121–124 (2006).

44. Humphrey, P. A. Histological variants of prostatic carcinoma and their significance. *Histopathology* **60**, 59–74 (2012).

45. Grignon, D. J. Unusual subtypes of prostate cancer. *Modern Pathology* **17**, 316–327 (2004).

46. Huang, H. & Chen, F. Prostatic Ductal Adenocarcinoma Exhibits More Advanced Histopathological Features than Acinar Adenocarcinoma. *American Chinese Journal of Medicine and Science* **5**, 208 (2012).

47. Cheville, J. C. Urothelial carcinoma of the prostate: an immunohistochemical comparison with high grade prostatic adenocarcinoma and review of the literature. *JOURNAL OF UROLOGIC PATHOLOGY* **9**, 141–154 (1998).

48. Wang, W. & Epstein, J. I. Small Cell Carcinoma of the Prostate. *American Journal of Surgical Pathology* **32**, 65–71 (2008).

49. Aggarwal, S., Mitra, S., Dewan, A. & Durga, G. Carcinosarcoma prostate with osteosarcomatous differentiation: A rare de novo presentation. *BMJ Case Rep* **12**, (2019).

50. Shannon, R. L. *et al.* Sarcomatoid carcinoma of the prostate a clinicopathologic study of 12 patients. *Cancer* **69**, 2676–2682 (1992).

51. Hawlina, S., Chowdhury, H. H., Smrkolj, T. & Zorec, R. Dendritic cell-based vaccine prolongs survival and time to next therapy independently of the vaccine cell number. *Biol Direct* **17**, 5 (2022).

52. Qiu, Z.-Y., Cui, Y. & Wang, X.-M. Chapter 1 - Natural Bone Tissue and Its Biomimetic. in *Mineralized Collagen Bone Graft Substitutes* (eds. Wang, X.-M., Qiu, Z.-Y. & Cui, H.) 1–22 (Woodhead Publishing, 2019). doi:https://doi.org/10.1016/B978-0-08-102717-2.00001-1.

53. Florencio-Silva, R., Sasso, G. R. da S., Sasso-Cerri, E., Simões, M. J. & Cerri, P. S. Biology of Bone Tissue: Structure, Function, and Factors That Influence Bone Cells. *Biomed Res Int* **2015**, 1–17 (2015).

54. Knothe Tate, M. L. "Whither flows the fluid in bone?" An osteocyte's perspective. *J Biomech* **36**, 1409–1424 (2003).

55. Parvizi, J. & Kim, G. K. Osteoclasts. in *High Yield Orthopaedics* 337–339 (Elsevier, 2010). doi:10.1016/B978-1-4160-0236-9.00174-7.

56. Prater, S. & McKeon, B. *Osteosarcoma*. (2023).

57. Bielack, S. S. *et al.* Prognostic Factors in High-Grade Osteosarcoma of the Extremities or Trunk: An Analysis of 1,702 Patients Treated on Neoadjuvant Cooperative Osteosarcoma Study Group Protocols. *Journal of Clinical Oncology* **20**, 776–790 (2002).

58. Klein, M. J. & Siegal, G. P. Osteosarcoma. *Am J Clin Pathol* **125**, 555–581 (2006).

59. Piperdi, S. *et al.* β -Catenin Does Not Confer Tumorigenicity When Introduced into Partially Transformed Human Mesenchymal Stem Cells. *Sarcoma* **2012**, 1–10 (2012).

60. Rojas, G. A., Hubbard, A. K., Diessner, B. J., Ribeiro, K. B. & Spector, L. G. International trends in incidence of osteosarcoma (1988-2012). *Int J Cancer* **149**, 1044–1053 (2021).

61. Sadykova, L. R. *et al.* Epidemiology and Risk Factors of Osteosarcoma. *Cancer Investigation* vol. 38 259–269 Preprint at https://doi.org/10.1080/07357907.2020.1768401 (2020).

62. Ottaviani, G. & Jaffe, N. The etiology of osteosarcoma. in *Cancer Treatment and Research* vol. 152 15–32 (Kluwer Academic Publishers, 2009).

63. Horvai, A. & Unni, K. K. Premalignant conditions of bone. in *Journal of Orthopaedic Science* vol. 11 412–423 (Springer Tokyo, 2006).

64. Greditzer, H. G., McLeod, R. A., Unni, K. K. & Beabout, J. W. Bone sarcomas in Paget disease. *Radiology* **146**, 327–333 (1983).

65. Bertoni, F., Bacchini, P. & Staals, E. L. Malignancy in giant cell tumor of bone. *Cancer* **97**, 2520–2529 (2003).

66. Tafti, D. & Cecava, N. D. *Fibrous Dysplasia*. (2023).

67. Bertoni, F. *et al.* Osteosarcoma. Low-grade intraosseous-type osteosarcoma, histologically resembling parosteal osteosarcoma, fibrous dysplasia, and desmoplastic fibroma. *Cancer* **71**, 338–345 (1993).

68. WG, C. Sarcoma arising in irradiated bone: report of eleven cases. 1948. *Cancer* **82**, 8–34 (1998).

69. Inoue, Y. Z. *et al.* Clinicopathologic features and treatment of postirradiation sarcoma of bone and soft tissue. *J Surg Oncol* **75**, 42–50 (2000).

70. Klein, M. J. & Siegal, G. P. Osteosarcoma. *Am J Clin Pathol* **125**, 555–581 (2006).

71. Goorin, A. M. *et al.* Phase II/III Trial of Etoposide and High-Dose Ifosfamide in Newly Diagnosed Metastatic Osteosarcoma: A Pediatric Oncology Group Trial. *Journal of Clinical Oncology* **20**, 426–433 (2002).

72. Sundaram, M. Introduction. in *Tumors and Tumorlike Lesions of Bone* 1–27 (Springer Berlin Heidelberg, 1994). doi:10.1007/978-3-642-49954-8_1.

73. Fletcher, C. D. M., Unni, K. K. & Mertens, F. *Pathology and genetics of tumours of soft tissue and bone*. vol. 4 (Iarc, 2002).

74. Murphey, M. D. *et al.* Telangiectatic Osteosarcoma: Radiologic-Pathologic Comparison. *Radiology* **229**, 545–553 (2003).

75. Nakajima, H., Sim, F. H., Bond, J. R. & Unni, K. K. Small cell osteosarcoma of bone. *Cancer* **79**, 2095–2106 (1997).

76. Unni, K. K., Dahlin, D. C., McLeod, R. A. & Pritchard, D. J. Intraosseous well-differentiated osteosarcoma. *Cancer* **40**, 1337–1347 (1977).

77. Okada, K. *et al.* Parosteal osteosarcoma. A clinicopathological study. *JBJS* **76**, 366–378 (1994).

78. Unni, K. K., Dahlin, D. C. & Beabout, J. W. Periosteal osteogenic sarcoma. *Cancer* **37**, 2476–2485 (1976).

79. Zhang, C. *et al.* Progress, challenges, and future of nanomedicine. *Nano Today* **35**, 101008 (2020).

80. Silva, C. O. *et al.* Current Trends in Cancer Nanotheranostics: Metallic, Polymeric, and Lipid-Based Systems. *Pharmaceutics* **11**, 22 (2019).

81. Riedinger, A. *et al.* Subnanometer Local Temperature Probing and Remotely Controlled Drug Release Based on Azo-Functionalized Iron Oxide Nanoparticles. *Nano Lett* **13**, 2399–2406 (2013).

82. Henderson, N. L. Chapter 28. Recent Advances in Drug Delivery System Technology. in 275–284 (1983). doi:10.1016/S0065-7743(08)60783-6.

83. Yagublu, V. *et al.* Overview of Physicochemical Properties of Nanoparticles as Drug Carriers for Targeted Cancer Therapy. *Journal of Functional Biomaterials* vol. 13 Preprint at https://doi.org/10.3390/jfb13040196 (2022).

84. Rodríguez-Nogales, C., González-Fernández, Y., Aldaz, A., Couvreur, P. & Blanco-Prieto, M. J. Nanomedicines for Pediatric Cancers. *ACS Nano* **12**, 7482–7496 (2018).

85. Iyer, A. K., Khaled, G., Fang, J. & Maeda, H. Exploiting the enhanced permeability and retention effect for tumor targeting. *Drug Discov Today* **11**, 812–818 (2006).

86. Yang, Z. *et al.* Opportunities and Challenges of Nanoparticles in Digestive Tumours as Anti-Angiogenic Therapies. *Front Oncol* **11**, (2022).

87. Ovais, M., Guo, M. & Chen, C. Tailoring Nanomaterials for Targeting Tumor-Associated Macrophages. *Advanced Materials* **31**, (2019).

88. Wang, Y., Shang, W., Niu, M., Tian, J. & Xu, K. Hypoxia-active nanoparticles used in tumor theranostic . *Int J Nanomedicine* **Volume 14**, 3705–3722 (2019).

89. Ovais, M. *et al.* Designing Stimuli-Responsive Upconversion Nanoparticles that Exploit the Tumor Microenvironment. *Advanced Materials* **32**, (2020).

90. Nag, O. K. & Delehanty, J. B. Active Cellular and Subcellular Targeting of Nanoparticles for Drug Delivery. *Pharmaceutics* **11**, 543 (2019).

91. Srinivasa-Gopalan, S. & Yarema, K. J. Nanotechnologies for the life sciences: dendrimers in cancer treatment and diagnosis. *Nanotechnologies for the Life Sci* **7**, (2007).

92. Stiriba, S.-E., Frey, H. & Haag, R. Dendritic Polymers in Biomedical Applications: From Potential to Clinical Use in Diagnostics and Therapy. *Angewandte Chemie International Edition* **41**, 1329–1334 (2002).

93. Atanase, L. I. Micellar Drug Delivery Systems Based on Natural Biopolymers. *Polymers (Basel)* **13**, 477 (2021).

94. Apolinário, A. C., Hauschke, L., Nunes, J. R. & Lopes, L. B. Lipid nanovesicles for biomedical applications: 'What is in a name'? *Prog Lipid Res* **82**, 101096 (2021).

95. Karlsson, J., Vaughan, H. J. & Green, J. J. Biodegradable Polymeric Nanoparticles for Therapeutic Cancer Treatments. *Annu Rev Chem Biomol Eng* **9**, 105–127 (2018).

96. Zhang, L. *et al.* Co-delivery of Docetaxel and Resveratrol by liposomes synergistically boosts antitumor efficiency against prostate cancer. *European Journal of Pharmaceutical Sciences* **174**, 106199 (2022).

97. Gazzano, E. *et al.* Hyaluronated liposomes containing H2S-releasing doxorubicin are effective against P-glycoprotein-positive/doxorubicin-resistant osteosarcoma cells and xenografts. *Cancer Lett* **456**, 29–39 (2019).

98. Shitole, A. A. *et al.* LHRH-conjugated, PEGylated, poly-lactide-co-glycolide nanocapsules for targeted delivery of combinational chemotherapeutic drugs Docetaxel and Quercetin for prostate cancer. *Materials Science and Engineering: C* **114**, 111035 (2020).

99. Li, X. *et al.* Overcoming therapeutic failure in osteosarcoma *via* Apatinib-encapsulated hydrophobic poly(ester amide) nanoparticles. *Biomater Sci* **8**, 5888–5899 (2020).

100. Barve, A., Jain, A., Liu, H., Zhao, Z. & Cheng, K. Enzyme-responsive polymeric micelles of cabazitaxel for prostate cancer targeted therapy. *Acta Biomater* **113**, 501–511 (2020).

101. Xi, Y. *et al.* Dual targeting curcumin loaded alendronate-hyaluronan- octadecanoic acid micelles for improving osteosarcoma therapy . *Int J Nanomedicine* **Volume 14**, 6425–6437 (2019).

102. Lesniak, W. G. *et al.* Evaluation of PSMA-Targeted PAMAM Dendrimer Nanoparticles in a Murine Model of Prostate Cancer. *Mol Pharm* **16**, 2590–2604 (2019).

103. Yu, W. *et al.* Zinc phthalocyanine encapsulated in polymer micelles as a potent photosensitizer for the photodynamic therapy of osteosarcoma. *Nanomedicine* **14**, 1099–1110 (2018).

104. Kuang, Y. *et al.* Geometrical Confinement of Gadolinium Oxide Nanoparticles in Poly(ethylene glycol)/Arginylglycylaspartic Acid-Modified Mesoporous Carbon Nanospheres as an Enhanced T_1 Magnetic Resonance Imaging Contrast Agent. *ACS Appl Mater Interfaces* **10**, 26099–26107 (2018).

105. Cole, A. J., Yang, V. C. & David, A. E. Cancer theranostics: the rise of targeted magnetic nanoparticles. *Trends Biotechnol* **29**, 323–332 (2011).

106. Mohamed Isa, E. D., Ahmad, H. & Abdul Rahman, M. B. Optimization of Synthesis Parameters of Mesoporous Silica Nanoparticles Based on Ionic Liquid by Experimental Design and Its Application as a Drug Delivery Agent. *J Nanomater* **2019**, 1–8 (2019).

107. Ngen, E. J. *et al.* MRI Assessment of Prostate-Specific Membrane Antigen (PSMA) Targeting by a PSMA-Targeted Magnetic Nanoparticle: Potential for Image-Guided Therapy. *Mol Pharm* **16**, 2060–2068 (2019).

108. Ai, J., Liu, B. & Liu, W. Folic acid-tagged titanium dioxide nanoparticles for enhanced anticancer effect in osteosarcoma cells. *Materials Science and Engineering: C* **76**, 1181–1187 (2017).

109. Luo, D. *et al.* Targeted Radiosensitizers for MR-Guided Radiation Therapy of Prostate Cancer. *Nano Lett* **20**, 7159–7167 (2020).

110. Lupusoru, R. V. *et al.* Effect of TAT-DOX-PEG irradiated gold nanoparticles conjugates on human osteosarcoma cells. *Sci Rep* **10**, 6591 (2020).

111. Du, D., Fu, H.-J., Ren, W., Li, X.-L. & Guo, L.-H. PSA targeted dual-modality manganese oxide–mesoporous silica nanoparticles for prostate cancer imaging. *Biomedicine & Pharmacotherapy* **121**, 109614 (2020).

112. Martínez-Carmona, M., Lozano, D., Colilla, M. & Vallet-Regí, M. Lectin-conjugated pH-responsive mesoporous silica nanoparticles for targeted bone cancer treatment. *Acta Biomater* **65**, 393–404 (2018).

113. Sokolova, V. & Epple, M. Biological and Medical Applications of Calcium Phosphate Nanoparticles. *Chemistry - A European Journal* vol. 27 7471–7488 Preprint at https://doi.org/10.1002/chem.202005257 (2021).

114. Bose, S., Tarafder, S., Edgington, J. & Bandyopadhyay, A. Calcium phosphate ceramics in drug delivery. *JOM* **63**, 93–98 (2011).

115. Sokolova, V., Knuschke, T., Buer, J., Westendorf, A. M. & Epple, M. Quantitative determination of the composition of multi-shell calcium phosphate–oligonucleotide nanoparticles and their application for the activation of dendritic cells. *Acta Biomater* **7**, 4029–4036 (2011).

116. Degli Esposti, L. *et al.* Calcium Phosphate Nanoparticle Precipitation by a Continuous Flow Process: A Design of Experiment Approach. *Crystals (Basel)* **10**, 953 (2020).

117. Mahl, D., Diendorf, J., Meyer-Zaika, W. & Epple, M. Possibilities and limitations of different analytical methods for the size determination of a bimodal dispersion of metallic nanoparticles. *Colloids Surf A Physicochem Eng Asp* **377**, 386–392 (2011).

118. Decher, G. Fuzzy Nanoassemblies: Toward Layered Polymeric Multicomposites. *Science (1979)* **277**, 1232–1237 (1997).

119. Ruesing, J., Rotan, O., Gross-Heitfeld, C., Mayer, C. & Epple, M. Nanocapsules of a cationic polyelectrolyte and nucleic acid for efficient cellular uptake and gene transfer. *J Mater Chem B* **2**, 4625–4630 (2014).

120. Epple, M. Review of potential health risks associated with nanoscopic calcium phosphate. *Acta Biomater* **77**, 1–14 (2018).

121. Zhao, J. & Stenzel, M. H. Entry of nanoparticles into cells: the importance of nanoparticle properties. *Polym Chem* **9**, 259–272 (2018).

122. Kumari, S., MG, S. & Mayor, S. Endocytosis unplugged: multiple ways to enter the cell. *Cell Res* **20**, 256–275 (2010).

123. Kollenda, S. *et al.* A pH-sensitive fluorescent protein sensor to follow the pathway of calcium phosphate nanoparticles into cells. *Acta Biomater* **111**, 406–417 (2020).

124. Müller, K. H. *et al.* The effect of particle agglomeration on the formation of a surface-connected compartment induced by hydroxyapatite nanoparticles in human monocyte-derived macrophages. *Biomaterials* **35**, 1074–1088 (2014).

125. Alivisatos, A. P. Perspectives on the Physical Chemistry of Semiconductor Nanocrystals. *J Phys Chem* **100**, 13226–13239 (1996).

126. Ashoori, R. C. Electrons in artificial atoms. *Nature* **379**, 413–419 (1996).

127. Kubendhiran, S., Bao, Z., Dave, K. & Liu, R.-S. Microfluidic Synthesis of Semiconducting Colloidal Quantum Dots and Their Applications. *ACS Appl Nano Mater* **2**, 1773–1790 (2019).

128. Alivisatos, A. P. Semiconductor Clusters, Nanocrystals, and Quantum Dots. *Science (1979)* **271**, 933–937 (1996).

129. Yoffe, A. D. Semiconductor quantum dots and related systems: Electronic, optical, luminescence and related properties of low dimensional systems. *Adv Phys* **50**, 1–208 (2001).

130. Amaral, P. E. M. *et al.* Fibrous Phosphorus Quantum Dots for Cell Imaging. *ACS Appl Nano Mater* **3**, 752–759 (2020).

131. Gidwani, B. *et al.* Quantum dots: Prospectives, toxicity, advances and applications. *J Drug Deliv Sci Technol* **61**, 102308 (2021).

132. Liang, Y., Zhang, T. & Tang, M. Toxicity of quantum dots on target organs and immune system. *Journal of Applied Toxicology* **42**, 17–40 (2022).

133. Kang, Z. & Lee, S. T. Carbon dots: Advances in nanocarbon applications. *Nanoscale* vol. 11 19214–19224 Preprint at https://doi.org/10.1039/c9nr05647e (2019).

134. Kim, T. H. *et al.* Selective toxicity of hydroxyl-rich carbon nanodots for cancer research. *Nano Res* **11**, 2204–2216 (2018).

135. Xia, C., Zhu, S., Feng, T., Yang, M. & Yang, B. Evolution and Synthesis of Carbon Dots: From Carbon Dots to Carbonized Polymer Dots. *Advanced Science* vol. 6 Preprint at https://doi.org/10.1002/advs.201901316 (2019).

136. Allakhverdiev, S. I. Photosynthetic and biomimetic hydrogen production. *Int J Hydrogen Energy* **37**, 8744–8752 (2012).

137. Tian, C., Li, B., Liu, Z., Zhang, Y. & Lu, H. Hydrothermal liquefaction for algal biorefinery: A critical review. *Renewable and Sustainable Energy Reviews* **38**, 933–950 (2014).

138. Mehrabadi, A., Craggs, R. & Farid, M. M. Pyrolysis of wastewater treatment high rate algal pond (WWT HRAP) biomass. *Algal Res* **24**, 509–519 (2017).

139. Simão, B. L., Santana Júnior, J. A., Chagas, B. M. E., Cardoso, C. R. & Ataíde, C. H. Pyrolysis of Spirulina maxima: Kinetic modeling and selectivity for aromatic hydrocarbons. *Algal Res* **32**, 221–232 (2018).

140. Mohan, D., Pittman, C. U. & Steele, P. H. Pyrolysis of Wood/Biomass for Bio-oil: A Critical Review. *Energy & Fuels* **20**, 848–889 (2006).

141. Kudaibergenov, S., Tatykhanova, G., Bakranov, N. & Tursunova, R. Layer-by-Layer Thin Films and Coatings Containing Metal Nanoparticles in Catalysis. in *Thin Film Processes - Artifacts on Surface Phenomena and Technological Facets* (InTech, 2017). doi:10.5772/67215.

142. Guzmán, E., Rubio, R. G. & Ortega, F. A closer physico-chemical look to the Layer-by-Layer electrostatic self-assembly of polyelectrolyte multilayers. *Advances in Colloid and Interface Science* vol. 282 Preprint at https://doi.org/10.1016/j.cis.2020.102197 (2020).

143. Wang, D. Y. *Novel Fire Retardant Polymers and Composite Materials*. (Elsevier Science, 2016).

144. Díez-Pascual, A. & Shuttleworth, P. Layer-by-Layer Assembly of Biopolyelectrolytes onto Thermo/pH-Responsive Micro/Nano-Gels. *Materials* **7**, 7472–7512 (2014).

145. Guzmán, E., Ritacco, H. A., Ortega, F. & Rubio, R. G. Growth of Polyelectrolyte Layers Formed by Poly(4-styrenesulfonate sodium salt) and Two Different Polycations: New Insights from Study of Adsorption Kinetics. *The Journal of Physical Chemistry C* **116**, 15474–15483 (2012).

146. Shen, L., Chaudouet, P., Ji, J. & Picart, C. pH-Amplified Multilayer Films Based on Hyaluronan: Influence of HA Molecular Weight and Concentration on Film Growth and Stability. *Biomacromolecules* **12**, 1322–1331 (2011).

147. Burke, S. E. & Barrett, C. J. Swelling Behavior of Hyaluronic Acid/Polyallylamine Hydrochloride Multilayer Films. *Biomacromolecules* **6**, 1419–1428 (2005).

148. Guzmán, E. *et al.* Adsorption of Conditioning Polymers on Solid Substrates with Different Charge Density. *ACS Appl Mater Interfaces* **3**, 3181–3188 (2011).

149. Lingström, R. & Wågberg, L. Polyelectrolyte multilayers on wood fibers: Influence of molecular weight on layer properties and mechanical properties of papers from treated fibers. *J Colloid Interface Sci* **328**, 233–242 (2008).

150. Panchagnula, V., Jeon, J. & Dobrynin, A. V. Molecular Dynamics Simulations of Electrostatic Layer-by-Layer Self-Assembly. *Phys Rev Lett* **93**, 037801 (2004).

151. Guzmán, E. *et al.* Self-Consistent Mean Field Calculations of Polyelectrolyte-Surfactant Mixtures in Solution and upon Adsorption onto Negatively Charged Surfaces. *Polymers (Basel)* **12**, 624 (2020).

152. Izquierdo, A., Ono, S. S., Voegel, J.-C., Schaaf, P. & Decher, G. Dipping versus Spraying: Exploring the Deposition Conditions for Speeding Up Layer-by-Layer Assembly. *Langmuir* **21**, 7558–7567 (2005).

153. Decher, G. & Schlenoff, J. B. *Multilayer Thin Films: Sequential Assembly of Nanocomposite Materials*. (Wiley, 2006).

154. Poptoshev, E., Schoeler, B. & Caruso, F. Influence of Solvent Quality on the Growth of Polyelectrolyte Multilayers. *Langmuir* **20**, 829–834 (2004).

155. Farhat, T., Yassin, G., Dubas, S. T. & Schlenoff, J. B. Water and Ion Pairing in Polyelectrolyte Multilayers. *Langmuir* **15**, 6621–6623 (1999).

156. Buron, C. C. *et al.* Surface morphology and thickness of a multilayer film composed of strong and weak polyelectrolytes: Effect of the number of adsorbed layers, concentration and type of salts. *Thin Solid Films* **517**, 2611–2617 (2009).

157. Record, M. T., Guinn, E., Pegram, L. & Capp, M. Introductory Lecture: Interpreting and predicting Hofmeister salt ion and solute effects on biopolymer and model processes using the solute partitioning model. *Faraday Discuss.* **160**, 9–44 (2013).

158. Guzmán, E. *et al.* pH-Induced Changes in the Fabrication of Multilayers of Poly(acrylic acid) and Chitosan: Fabrication, Properties, and Tests as a Drug Storage and Delivery System. *Langmuir* **27**, 6836–6845 (2011).

159. Salomäki, M., Vinokurov, I. A. & Kankare, J. Effect of Temperature on the Buildup of Polyelectrolyte Multilayers. *Langmuir* **21**, 11232–11240 (2005).

160. Donath, E. *et al.* Nonlinear Hairy Layer Theory of Electrophoretic Fingerprinting Applied to Consecutive Layer by Layer Polyelectrolyte Adsorption onto Charged Polystyrene Latex Particles. *Langmuir* **13**, 5294–5305 (1997).

161. Fu, Y. *et al.* Facile and Efficient Approach to Speed up Layer-by-Layer Assembly: Dipping in Agitated Solutions. *Langmuir* **27**, 672–677 (2011).

162. Caruso, F., Caruso, R. A. & Möhwald, H. Nanoengineering of Inorganic and Hybrid Hollow Spheres by Colloidal Templating. *Science (1979)* **282**, 1111–1114 (1998).

163. Nagaraja, A. T. *et al.* Layer-by-layer modification of high surface curvature nanoparticles with weak polyelectrolytes using a multiphase solvent precipitation process. *J Colloid Interface Sci* **466**, 432–441 (2016).

164. Hong, J., Char, K. & Kim, B.-S. Hollow Capsules of Reduced Graphene Oxide Nanosheets Assembled on a Sacrificial Colloidal Particle. *J Phys Chem Lett* **1**, 3442–3445 (2010).

165. Shiratori, S. S. & Yamada, M. Nano-scale control of composite polymer films by mass-controlled layer-by-layer sequential adsorption of polyelectrolytes. *Polym Adv Technol* **11**, 810–814 (2000).

166. Peiffre, D. G., Corley, T. J., Halpern, G. M. & Brinker, B. A. Utilization of polymeric materials in laser fusion target fabrication. *Polymer (Guildf)* **22**, 450–460 (1981).

167. Richardson, J. J. *et al.* Immersive Polymer Assembly on Immobilized Particles for Automated Capsule Preparation. *Advanced Materials* **25**, 6874–6878 (2013).

168. Kantak, C., Beyer, S., Yobas, L., Bansal, T. & Trau, D. A 'microfluidic pinball' for on-chip generation of Layer-by-Layer polyelectrolyte microcapsules. *Lab Chip* **11**, 1030–1035 (2011).

169. Urch, H., Vallet-Regi, M., Ruiz, L., Gonzalez-Calbet, J. M. & Epple, M. Calcium phosphate nanoparticles with adjustable dispersability and crystallinity. *J Mater Chem* **19**, 2166 (2009).

170. Elizarova, I. S. & Luckham, P. F. Fabrication of polyelectrolyte multilayered nano-capsules using a continuous layer-by-layer approach. *J Colloid Interface Sci* **470**, 92–99 (2016).

171. Chen, W. *et al.* Human Embryonic Stem Cell-Derived Mesenchymal Stem Cell Seeding on Calcium Phosphate Cement-Chitosan-RGD Scaffold for Bone Repair. *Tissue Eng Part A* **19**, 915–927 (2013).

172. Kaszuba, M., Corbett, J., Watson, F. M. & Jones, A. High-concentration zeta potential measurements using light-scattering techniques. *Philosophical Transactions of the Royal Society A: Mathematical, Physical and Engineering Sciences* **368**, 4439–4451 (2010).

173. Lian, H., Sun, J. & Zhang, T. A rapid and sensitive determination of paclitaxel in rat plasma by UPLC-MS/MS method: Application to a pharmacokinetic study. *Asian J Pharm Sci* **8**, 199–205 (2013).

174. Elahi, M., Guan, G., Wang, L. & King, M. Influence of Layer-by-Layer Polyelectrolyte Deposition and EDC/NHS Activated Heparin Immobilization onto Silk Fibroin Fabric. *Materials* **7**, 2956–2977 (2014).

175. Bansal, R., Singh, R. & Kaur, K. Quantitative analysis of doxorubicin hydrochloride and arterolane maleate by mid IR spectroscopy using transmission and reflectance modes. *BMC Chem* **15**, 27 (2021).

176. Lin, Y.-C., Hu, S. C.-S., Huang, P.-H., Lin, T.-C. & Yen, F.-L. Electrospun Resveratrol-Loaded Polyvinylpyrrolidone/Cyclodextrin Nanofibers and Their Biomedical Applications. *Pharmaceutics* **12**, 552 (2020).

177. Shin, H.-Y., Jung, J.-Y., Kim, S.-W. & Lee, W.-K. XPS analysis on chemical properties of calcium phosphate thin films and osteoblastic HOS cell responses. *Journal of Industrial and Engineering Chemistry* **12**, 476–483 (2006).

178. Mohammed, A. A. & Niamah, A. K. Identification and antioxidant activity of hyaluronic acid extracted from local isolates of Streptococcus thermophilus. *Mater Today Proc* **60**, 1523–1529 (2022).

179. Yan, Y., Björnmalm, M. & Caruso, F. Assembly of Layer-by-Layer Particles and Their Interactions with Biological Systems. *Chemistry of Materials* **26**, 452–460 (2014).